Microglia specific transcriptional regulation of the Translocator protein (18 kDa) (TSPO)

Inaugural-Dissertation

zur
Erlangung des Doktorgrades
der Mathematisch-Naturwissenschaftlichen Fakultät
der Universität zu Köln

vorgelegt von

Khalid Rashid
aus Nakuru, Kenya

Köln 2019

Berichterstatter:	Prof. Dr. Ulrich Baumann
	Prof. Dr. Peter Nürnberg
Tag der mündlichen Prüfung:	Februar 19, 2019

Dedicated to the three most important women in my life; my dear mother Dekah Yusuf, sister Asha Anab and wife Halima Sonny Juma

"***The scientist is not a person who gives the right answers, he is one who asks the right questions"***

Claude Lévi-Strauss

Summary

Various stimuli that perturb neuronal homeostasis and cause neurodegeneration trigger microglia reactivity. The microglia reaction and the increased production of pro-inflammatory mediators is intended to protect the central nervous system, including the retina, from noxious insults and facilitate a rapid return to normal homeostasis. However, sustained and dysregulated microglia inflammatory responses can lead to robust neuropathological changes that contribute to the severity and progression of neurodegenerative diseases. In the retina, pathologically activated microglia have been shown to not only contribute to neurodegenerative processes indirectly via the release of neurotoxic substances, but also directly via the indiscriminate phagocytosis of stressed but living photoreceptors. Consistently, innumerous studies have demonstrated that microglial modulation represents an attractive therapeutic avenue to alleviate or delay neurodegenerative diseases of the retina. Translocator protein (18kDa) (TSPO) located in the outer mitochondrial membrane is acutely and specifically expressed in activated microglia during retinal pathology. Importantly, specific TSPO ligands have been shown to potently modulate microglia inflammatory responses and ameliorate light-induced photoreceptor degeneration in mice. However, understanding the regulation of TSPO expression in microglia during health and disease is paramount prior to any utilization of this protein as a therapeutic target to modulate chronic microglia inflammatory responses and alleviate retinal degeneration. The aim of the current study therefore was to carry out a detailed functional characterization of the TSPO promoter and identify genetic elements and transcription factors responsible for maintaining basal and mediating induced TSPO expression in microglia.

To this end, a 2.812Kb murine Tspo promoter sequence was amplified by PCR and cloned into the promoterless pGL4.10-Basic luciferase reporter vector. Plasmids containing 5’ unidirectional deletions of the promoter were then generated by PCR. BV-2 microglia cells were transfected with the generated reporter plasmids for 24 h, and an additional 6 h in the case of lipopolysaccharide (LPS) stimulation before measuring luciferase activity. Sequence analysis was performed using Matinspector software and site-directed substitution

mutagenesis was used to confirm the functional status of the putative transcription factor binding sites. Chromatin immunoprecipitation (ChIP) was used to investigate binding of transcription factors to the endogenous promoter. The effect of transcription factor knockdown on Tspo promoter activity was assessed using RNAi mediated gene silencing followed by transfection with the reporter constructs and measurement of luciferase activity 24 h later. Additionally, effects of RNAi mediated gene silencing on endogenous Tspo protein levels were determined using western blot analysis.

Deletion mutagenesis indicated that −845 bp upstream of the transcription initiation site was sufficient to reconstitute near maximal promoter activity in BV-2 microglia cells. Deletion of sequences extending -593 to -520, which harbour an Ap-1, Ets.2 and Nkx3.1 site which also serves as a non-canonical binding site for Sp1-family transcription factors, led to a dramatic decrease in both basal as well as LPS induced promoter activity. Further deletion of sequences extending -168 to -39, which contains four GC boxes, also significantly decreased Tspo promoter activity. Site-directed mutagenesis of Ap-1, Ets.2, Nkx3.1/Sp1/3/4 and the proximal GC boxes led to significant decreases in promoter activity. ChIP-qPCR revealed that Pu.1, Ap-1(cJun/cFos), Stat3, Sp1, Sp3 and Sp4 bind the endogenous Tspo promoter. Notably, upon LPS stimulation, the binding of these factors, with the exception of Stat3, was significantly enhanced. RNAi mediated silencing of Pu.1, cJun, cFos, Stat3, Sp1, Sp3 and Sp4 gene expression significantly diminished Tspo promoter activity while Ap1(cJun/cFos) silencing effectively blocked LPS-induced increase in Tspo protein levels. Taken together, these findings demonstrate that the consensus binding sequences for Ap-1, Ets.2, distal as well as proximal Sp1/3/4 sites must be intact for maximal basal and LPS induced Tspo promoter activity in microglia. Furthermore, the current findings indicate that LPS-mediated increase in Tspo expression is mediated, at least in part, at the transcriptional level and is accompanied by an enhanced recruitment of Pu.1, Ap-1(cJun/cFos), Sp1, Sp3, and Sp4 factors to the Tspo promoter.

Zusammenfassung

Verschiedenste Stimuli, welche die neuronale Homöostase stören und neurodegenerative Erkrankungen verursachen, führen zur inflammatorischen Aktivierung von Mikrogliazellen. Mikrogliaaktivierung und die erhöhte Freisetzung von pro-inflammatorischen Signalmolekülen dienen ursprünglich dem Schutz des zentralen Nervensystems, inklusive der Netzhaut, vor schädlichen Einflüssen und ermöglichen ein rasches Wiederherstellen der gesunden Homöostase. Dauerhafte und fehlregulierte inflammatorische Reaktivität von Mikrogliazellen führt hingegen zu auffälligen neuropathologischen Veränderungen, welche die Schwere und den Verlauf neurodegenerativer Erkrankungen negativ verstärken können. In der Netzhaut tragen pathologisch aktivierte Mikroglia nicht nur indirekt, durch die Ausschüttung neurotoxischer Substanzen, sondern auch direkt, durch die fehlgesteuerte Phagozytose von geschädigten aber noch lebenden Photorezeptorzellen, zum verschlechterten Krankheitsverlauf bei. Auf diesen Beobachtungen basierend, demonstrierten bereits zahlreiche Studien die Modulation der Mikrogliaaktivität als vielversprechenden therapeutischen Weg um neurodegenerative Erkrankungen der Netzhaut zu mildern oder zu verzögern. Das Translokatorprotein (18 kDa) (TSPO) befindet sich in der äusseren Mitochondrienmembran und ist selektiv in reaktiven Mikrogliazellen während verschiedenen Netzhautdegenerationen verstärkt exprimiert. Interessanterweise konnte bereits nachgewiesen werden, dass spezifische TSPO Liganden in der Lage sind die pro-inflammatorische Mikrogliaaktivierung zu modulieren und dadurch die lichtinduzierte Photorezeptordegeneration im Mausmodell zu reduzieren. Das klare Verständnis der Regulation der TSPO Expression in Mikrogliazellen während Homöostase und Krankheit stellt eine Grundvoraussetzung für die Nutzung des Proteins als therapeutisches target im Kontext der Mikrogliaaktivierung und Netzhautdegeneration dar. Daher war das Ziel der vorliegenden Studie eine detaillierte funktionelle Charakterisierung des TSPO Promotors sowie die Identifikation von genetischen Elementen und Transkriptionsfaktoren, welche für die basale sowie induzierbare TSPO Expression in Mikrogliazellen verantwortlich sind. Zu diesem Zwecke wurde eine 2,812 kb grosse murine Tspo Promotorsequenz mittels PCR amplifiziert und in

den promotorlosen pGL4.10-Basic Luciferase Reporter Vektor kloniert. Als nächstes wurden durch PCR einzelne Plasmide mit 5` Deletionen verschiedener Längen generiert. BV-2 Mikrogliazellen wurden mit den so erhaltenen Reporterplasmiden für 24 h transfiziert und nach weiterer sechsstündiger Inkubation mit Lipopolysaccharid (LPS) die Luciferaseaktivität gemessen. Sequenzanalyse wurde mittels der Software MatInspector ausgeführt und zielgerichtete Mutagenese PCR wurde angewandt um die Funktionalität der putativen Transkriptionsfaktorbindestellen nachzuweisen. Die tatsächliche Bindung verschiedener Transkriptionsfaktoren an den endogenen Promotor wurde mittels Chromatin Immunpräzipitation (ChIP) experimentell belegt. RNAi-vermittelte Gen-Silencing Experimente wurden zur Untersuchung des Effekts von Transkriptionsfaktor Knock-Down auf die Luziferaseaktivität der Reporterkonstrukte durchgeführt. Zusätzlich wurde die endogene Tspo Protein Menge nach diesen RNAi Gen-Silencing Experimenten mittels Western Blot analysiert. Unsere Mutageneseexperimente belegten, dass ein Abschnitt von -845 bp upstream der Transkriptionsinitiationsstelle für nahezu maximale Promotoraktivität in BV-2 Mikrogliazellen ausreichend ist. Die Deletion des Sequenzbereichs zwischen -593 und -520, welcher sowohl eine Ap-1, Ets.2 als auch Nkx3.1 Bindestelle - die auch als Bindestelle für Transkriptionsfaktoren der Sp1-Familie fungiert – enthält, führte zu einem drastischen Verlust sowohl der basalen als auch LPS induzierten Promotoraktivität. Des Weiteren führte die Deletion des Sequenzbereichs von -168 bis -39, welcher vier GC Boxen enthält, ebenfalls zu einem signifikanten Abfall der Tspo Promotoraktivität. Analog dazu führte die zielgerichtete Mutagenese der AP-1, Ets.2, Nkx3.1/Sp1/3/4 und proximalen GC Boxen ebenfalls zu starken Abschwächungen der Promotoraktivität. ChiP-qPCR Experimente belegten anschliessend die tatsächliche physikalische Bindung der Faktoren Pu.1, Ap-1(cJun/cFos), Stat3, Sp1, Sp3 und Sp4 am endogenen Tspo Promotor. Bemerkenswerterweise war die Bindung aller dieser Faktoren (mit Ausnahme von Stat3) nach LPS-Stimulation siginifikant verstärkt. RNAi-vermitteltes Gen-Silencing von Pu.1, cJun, cFos, Stat3, Sp1, Sp3 und Sp4 reduzierte die Tspo Promotoraktivität signifikant, wohingegen ein Silencing von Ap1(cJun/cFos) effektiv die LPS vermittelte Tspo Induktion blockierte. Zusammenfassend demonstrieren unsere

Ergebnisse, dass die Konsensusbindesequenzen für Ap-1, Ets.2 und der distalen wie proximalen Sp1/3/4 Bindestellen für maximale basale und LPS induzierte Tspo Promotor Aktivität in Mikrogliazellen vorhanden und intakt sein müssen. Zusätzlich deuten unsere Ergebnisse darauf hin, dass der LPS induzierte Anstieg der Tspo Expression zumindest teilweise auf dem transkriptionellen Weg vermittelt wird und mit einer erhöhten Rekrutierung der Transkriptionsfaktoren Pu.1, Ap-1(cJun/cFos), Sp1, Sp3, und Sp4 zum Tspo Promotor einhergeht.

Contents

List of Tables

List of Figures

List of abbreviations and acronyms

AMD	Age-related macular degeneration
ANOVA	Analysis of variance
AP-1	Activator protein-1
BAC	Bacteria artificial chromosome
BDNF	Brain derived neurotrophic factor
bFGF	Basic fibroblast growth factor
BM	Bone marrow
BRB	Blood retinal barrier
ChIP	Chromatin immunoprecipitation
CSF1R	Colony stimulating factor-1 receptor
CTNF	Ciliary neurotrophic factor
DBI	Diazepam Binding Inhibitor protein
DMEM	Dulbecco's modified eagle's medium
DR	Diabetic retinopathy
EAE	Experimental autoimmune encephalomyelitis
eGFP	Enhanced green fluorescent protein
GCL	Ganglion cell layer
GDNF	Glial cell-line derived neurotrophic factor
Iba1	Ionized calcium-binding adapter molecule 1
INL	Inner nuclear layer
IPL	Inner plexiform layer
IRF8	Interferon regulatory factor 8
IS	Inner segments
JAK	Janus kinase
LDTF	Lineage determining transcription factor
LIF	Leukemia Inhibitory factor
LPS	Lipopolysaccharide
NEMO	NF-κB essential modulator
NF-κB	Nuclear factor kappa-light-chain-enhancer of B cells
ONL	Outer nuclear layer
OPL	Outer plexiform layer

OS	Outer segments
PU.1	PU box binding-1
RGCs	Retinal ganglion cells
RNAi	Ribonucleic acid interference
RONS	Reactive oxygen and nitrogen species
RPE	Retinal pigment epithelium
RPMI	Roswell Park Memorial Institute
RUNX1	Runt-related transcription factor 1
SDTF	Signal dependent transcription factor
siRNA	Small interfering ribonucleic acid
SOCS	Suppressor of cytokine signaling
SP	Specificity protein
STAT	Signal transducer and activator of transcription
TFBS	Transcription factor binding site
TNF-α	Tumor necrosis factor-α
TSA	Trichostatin A
TSPO	Translocator protein (18 kDa)
TSS	Transcription start site

1.0 Introduction

1.1 The Retina

The sensory retina is a subtle, 200 µM thick central nervous tissue lining the back of the eye and whose structure is evolutionary conserved (Masland, 2012). It consists of more than 60 different functional cell types that come in a wide collection of shapes and sizes (Masland, 2001). Retinal cells are highly ordered into anatomical layers where cellular nuclei and neuronal processes are distinctly segregated (Forrester et al., 2015). The innermost layer of the retina near the vitreous is the ganglion cell layer (GCL) which contains the cell bodies of the retinal ganglion cells (RGCs). Electrical signals are transmitted from photoreceptors to RGCs via bipolar cells in the inner plexiform layer (IPL) (Wässle, 2004). However, some bipolar cells do not transmit signals directly to RGCs, but rather form synapses with amacrine cells which subsequently transmit these visual signals to dendrites of RGCs within the IPL (Masland, 2012). Amacrine cells which are inhibitory interneurons function to modulate signals reaching ganglion cells (Forrester et al., 2015). RGCs then relay the collected visual signals from bipolar and amacrine cells to the brain via their axons which bundle together to form the optic nerve (Tian and Copenhagen, 2003). Thus, the RGCs make up the primary output units of the retina and inform the brain everything it knows about the content of the visual world (Dhande and Huberman, 2014).

Adjacent to the GCL is the IPL, one of the two major synaptic layers found in the vertebrate retina (Koontz and Hendrickson, 1987). This layer is composed of multiple strata where intricate synaptic connections between processes of different types of bipolar cells, RGCs and amacrine cells can be found (Wässle, 2004). The IPL is also broadly subdivided into two functionally discrete sublaminae termed as sublamina “a” and “b” (Wässle, 2004). The axons of “OFF” bipolar cells terminate in sublamina “a” (outer half) of the IPL where they make contact with “OFF” retinal ganglion cell arbors, whereas “ON” bipolar cells

terminate in sublamina “b” (inner half) and make contact with “ON” ganglion cells (Wässle, 2004). This bisublaminar organization of the IPL is designed to separate “ON” and “OFF” channels in retinal ganglion cells (Kolb and Famiglietti, 1974). The next layer is the inner nuclear layer (INL), composed of nuclei from bipolar, amacrine and horizontal cells. The nuclei are oriented such that those of horizontal cells are located next to the outer plexiform layer (OPL) whereas those of the amacrine cells are located next to the inner plexiform layer (Forrester et al., 2015). Such an organization allows amacrine and horizontal cells to make synaptic contacts with RGCs and photoreceptors respectively with ease (Forrester et al., 2015). The bipolar cells in the INL pass their dendrites outwards to synapse with the rod spherules and cone pedicles in the OPL and relay their signals to the RGCs and amacrine cells in the IPL (Masland, 2012). Similarly, the horizontal cells in the INL, which are second order neurons in the retina, extend wide spreading lateral processes to the OPL where they make synaptic connections with the axon terminals of cone and rod photoreceptors (Strettoi and Masland, 1995). These horizontal cells in most vertebrate retinas can be categorized into two morphological forms; a Type A which is a large axon-less cell with stout dendritic processes that makes contact exclusively with cones, and a Type B which is smaller in size and bears, in addition to dendritic ends that contact cones, an extensive 300 μM axon that contacts exclusively rods (Boije et al., 2016). Horizontal cells, like amacrine cells, function as inhibitory neurons to modulate synaptic transmission between photoreceptors and bipolar cells (Chaya et al., 2017). Therefore, the outer plexiform layer can be termed as a as a layer of synapses where glutamatergic neurotransmission occurs between photoreceptors and bipolar cells, with the horizontal cells playing an integrative role in photoreceptor signal processing via the release of the inhibitory neurotransmitter γ-aminobutyric acid (GABA) (Wu, 2010).

The photoreceptor layer lies in the outermost part of the retina. The two types of photoreceptor cells, rods and cones, have a basic structure composed of four morphologically distinguishable compartments namely outer segment, inner segment, a nucleus and a synaptic terminal that contacts bipolar and horizontal

cells in the OPL (Sung and Chuang, 2010). The outer segment (OS) lies adjacent to the retinal pigment epithelium (RPE) and is composed of cylindrically shaped membranous disks that are synthesized at the base of the OS (Forrester et al., 2015). Once synthesized, the disks travel over a course of around 10 days to the OS tips where they are enclosed by microvilli present on the apical side of the RPE (Forrester et al., 2015; Wright et al., 2010). Older disks are continuously shed from the OS tips in a circadian fashion and phagocytosed by the RPE (Forrester et al., 2015; Wright et al., 2010). The inner segment (IS), connected to the OS via a modified cilium, contains the major metabolic and biosynthetic machinery of the cell including the mitochondria, endoplasmic reticulum, Golgi complex and lysosomes (Molday and Moritz, 2015). The OS are incapable of synthesizing membrane proteins required for phototransduction, and therefore once produced in the IS, these proteins have to be trafficked to the OS via a connecting cilium (Molday and Moritz, 2015). Failure of connecting cilium function has been implicated in many retinal diseases including retinitis pigmentosa and Leber congenital amaurosis (Adams et al., 2007). The nuclei of the photoreceptors are tightly stacked in the ONL, with cone nuclei forming just a single row beneath the outer limiting membrane and rod nuclei making up the remainder (Molday and Moritz, 2015; Mustafi et al., 2009). Of note is that out of the different photoreceptor compartments, the light-sensitive photopigments are contained in the outer segments which lie furthest from the path of incoming light (Figure 1) (Masland, 2001). Rods, responsible for scotopic vision, contain rhodopsin in their OS as the light sensitive pigment whereas cones posses one of three different types of cone opsins in their OS to mediate photopic vision (Mustafi et al., 2009). Light must pass through vitreous humor and the different layers of the retina before it can be captured and converted into chemical signals by the photoreceptors (Masland, 2001, 2012).

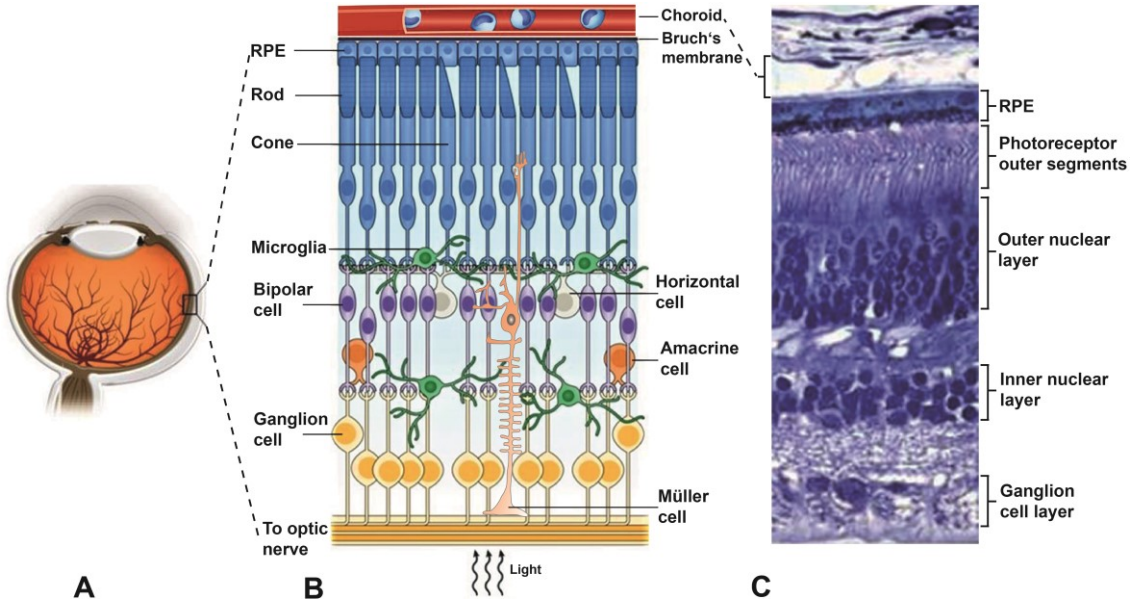

Figure 1: Cellular organization of the mammalian retina. **A)** Schematic representation of the human eye showing the posterior location of the retina. **B)** Simple schematic diagram of the cellular and synaptic organization of the vertebrate retina **C)** Representative cross-section of the human neural retina, the retinal pigment epithelium and the choroidal vessels showing the highly ordered arrangement of retinal layers. **A)** modified from (Rajala and Gardner, 2016), (**B)** schematic representation of the retina modified from (Reyes et al., 2017)**,** choroid adopted from (Akhtar-Schäfer et al., 2018) **(C)** modified from (Wright et al., 2010).

In addition, and similar to other parts of the nervous system, neuronal cells in the retina are found in intimate apposition to glia cells (Reichenbach and Robinson, 1995). Three morphologically distinct glia cells types can be identified in the mammalian retina including Müller cells, astrocytes and microglia (Vecino et al., 2016). Müller cells, first described by Heinrich Müller in 1851 as radial fibres, are the predominant glial cells in the retina representing approximately 90% of the retinal glia population (Forrester et al., 2015; Vecino et al., 2016). They are the only cells that span the entire depth of the neural retina, radiating from the outer limiting membrane where they form adherens junctions with photoreceptor inner segments to the inner limiting membrane where their expanded end-foot terminate (Forrester et al., 2015; Newman and Reichenbach, 1996). They are seen to wrap neuronal somata and axons in an insulating sheath, helping maintain neuronal function by providing neuronal termini with nutrients and neurotransmitter precursors (Vecino et al., 2016). Moreover, Müller cells support

neuronal survival and function by releasing trophic factors, recycling neurotransmitters and controlling ionic balance in the extracellular space (Bringmann et al., 2009; Goldman, 2014; Pow and Crook, 1996). Retinal astrocytes on the other hand are predominantly located in the nerve fibre layer where their processes join to form a honeycomb structure (Ramírez et al., 1998). They perform similar functions to Müller cells including extracellular ion balance and neurotrophic, metabolic and mechanical support of neurons (Vecino et al., 2016). They also constitute a key functional component of the blood-retina barrier, which is essential in maintaining retinal homeostasis (Ramírez et al., 1998; Vecino et al., 2016). The third group of retinal glial cells, microglia, constitute the primary immune cell type in the retina and morphologically resemble those found throughout the CNS with their highly branched and dynamic protrusions (Langmann, 2007; Silverman and Wong, 2018). They are regarded as immunological watchdogs in the healthy retina, where they fulfil diverse tasks of surveillance (Karlstetter et al., 2015).

1.2 Retinal microglia

Microglial cells, distributed in the GCL, IPL and OPL layers, form an integral part of the innate immune defense system in the retina (Chen and Xu, 2015). They are equipped with a host of surface receptors and filopodia-like processes that constantly extend and retract to allow them efficiently monitor the surrounding microenvironment (Karlstetter et al., 2015). In addition, microglia housekeeping activities such as phagocytic removal of cellular corpses and debris and sculpting of synaptic circuits helps maintain a conducive retinal environment for the healthy functioning and survival of neurons (Linnartz and Neumann, 2013; Schafer et al., 2012; Wong, 2013). In the presence of tissue damaging stimuli, microglia cells respond by undergoing rapid proliferation and migration to the site of injury where they release a host of proinflammatory mediators aimed at neutralizing the noxious insult (Rashid et al., 2018c; Scholz et al., 2015c). However, while much is known about the major pathways involved in microglia activation and proinflammatory responses, it was not until recently when the expansion and

renewal mechanisms of microglial cells in the retina were uncovered (Elmore et al., 2014; Huang et al., 2018).

1.2.1 Origin and maintenance of microglia in the retina

Over several decades, questions lingered as to whether myeloid cell populations in the CNS including retina were renewed by *in-situ* proliferation of resident microglia or whether bone marrow (BM) derived macrophages could also migrate to the healthy CNS tissue and readily differentiate into functional microglia (Simard and Rivest, 2004). To address this question, earlier studies used bone marrow (BM) chimeras obtained by transplantation of labelled BM derived cells from a transgenic donor animal to a recipient that has been lethally irradiated to ablate BM cells (Ransohoff, 2007). Xu and colleagues used this protocol to adoptively transfer BM derived cells expressing enhanced green fluorescent protein (eGFP) from eGFP-transgenic mice into lethally irradiated normal adult mice and waited for 8, 14- and 26-weeks prior to sacrificing the animals (Xu et al., 2007). Retinal flatmounts from the recipient mice revealed that BM derived $eGFP^+$ cells could be detected in the retina as early as 8-weeks post transplantation, and by the 6^{th} month, the entire retinal myeloid cell population was $eGFP^+$ (Xu et al., 2007). A separate study using *Cx3cr1-gfp/+* knock-in mice as BM donors, where eGFP protein expression is restricted to cells of the monocyte lineage, observed recruitment of $eGFP^+$ monocyte-derived cells into recipient retinas just 4 weeks post-transplantation (Kezic and McMenamin, 2008). The authors attributed the earlier appearance of $eGFP^+$ donor cells observed in their study, as opposed to that of Xu *et al.*, to differences in chimera models (global eGFP mice vs. *Cx3cr1-gfp/+*) and blood retinal barrier (BRB) integrity between the mouse strains (Kezic and McMenamin, 2008). Of note is that both studies observed very little *in-situ* proliferation of the resident microglia under steady state conditions and therefore concluded that a majority of the microglia/macrophages in the retinal tissue were replenished from BM derived monocyte precursor cells (Kezic and McMenamin, 2008; Xu et al., 2007). In contrast, findings from a different study where irradiated mice were injected with

eGFP$^+$ BM derived cells showed that a very small number of eGFP$^+$ cells accessed the uninjured healthy retina up to 12 months post transplantation, despite a large number of them accumulating in surrounding ocular tissues such as the ciliary body, RPE, choroid and the optic nerve head (ONH) (Kaneko et al., 2008). However, in response to the neurotoxic agent N-methyl-N-nitrosourea that induces retinal degeneration, numerous eGFP$^+$ BM derived cells could be detected in the retina, implying that the recruitment of BM-derived microglia in the retina occurs almost exclusively under retinal damage (Kaneko et al., 2008). Interestingly, the authors argued that the enhanced migration of BM-derived cells to the retina observed in the previous studies might have been prompted by an unintentional damage of retinal neurons and vasculature as a result of not shielding the eyes and heads of experimental animals during irradiation (Kaneko et al., 2008). This line of thought was in fact consistent with previous findings which had demonstrated that rats exposed to X-ray doses between 200-500 cGy (compared to 800-1000 cGy used in the aforementioned studies) exhibited structural abnormalities in the retina characterized by damaged rod photoreceptor outer segment membranes and swollen or ruptured mitochondria in the RPE (Amoaku et al., 1989). Nonetheless, while the arguments from Kaneko et al. were accurate, they were somehow understated and failed to capture other flaws of the irradiation experimental protocol that might have biased the system towards a non-physiological transmigration of eGFP+ cells to the CNS: Firstly, irradiation induced bone marrow ablation is associated with enormous fluxes of cytokines through circulation and in tissue which subsequently cause disruptive changes to the blood brain barrier (BBB) (Ransohoff, 2007; Varatharaj and Galea, 2017); Secondly, irradiation of the CNS induces vascular perturbations that affect the competence of the BBB (Figure 2) (Greene-Schloesser et al., 2012; Ransohoff, 2007).

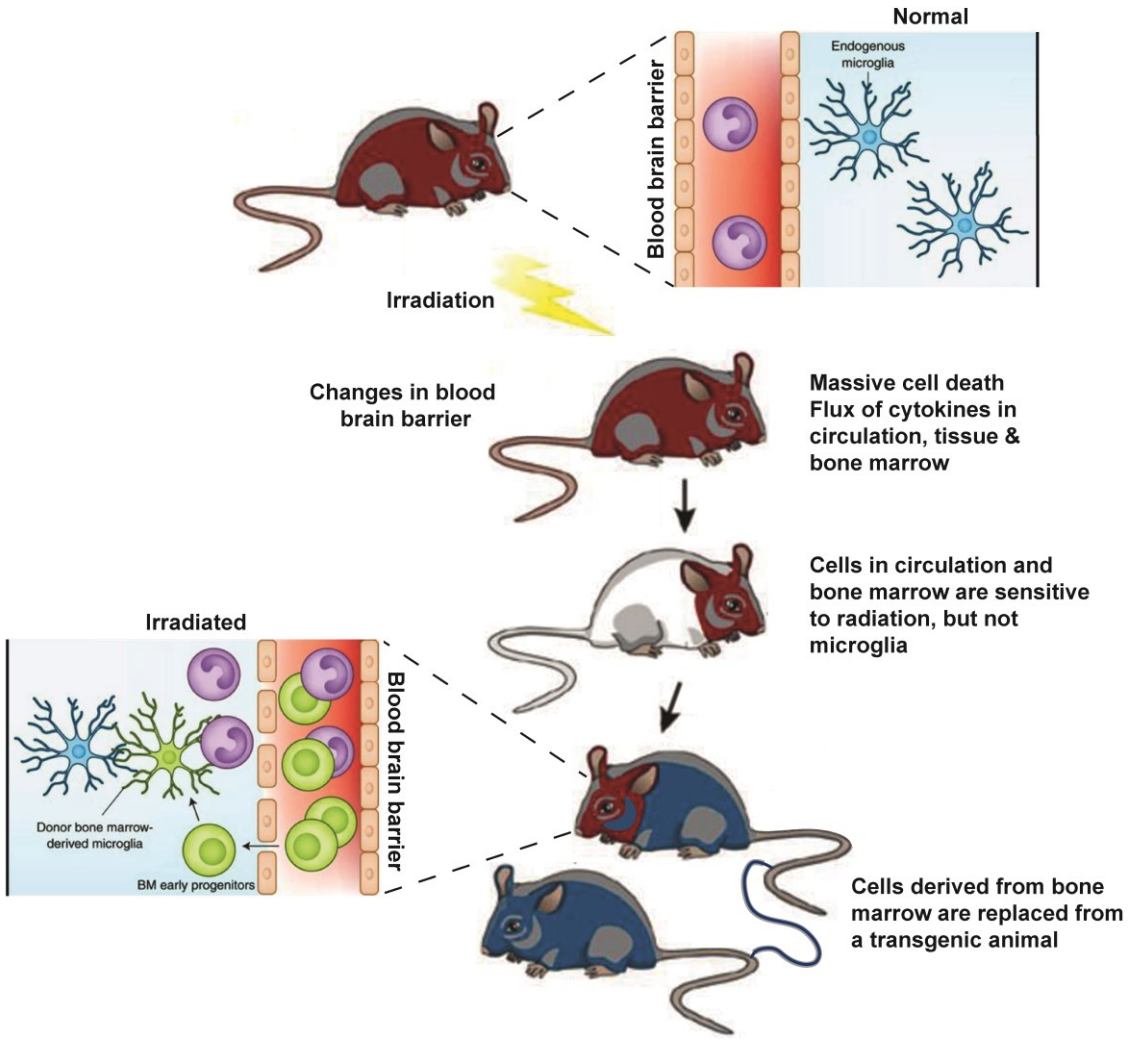

Figure 2: Irradiation weakens the integrity of the blood brain barrier. To investigate whether bone marrow (BM) derived microglia precursors are recruited to the healthy CNS, animals are exposed to irradiation to kill their bone-marrow cells. These are then replaced with labeled ones derived from a transgenic animal. Irradiation induced apoptosis of BM cells elicits a strong immune response characterized by enormous fluxes of cytokines through the circulation and in tissues. In addition, CNS exposure to irradiation causes vascular changes that compromise the integrity of the blood-brain barrier. Such experimental confounds associated with irradiation, and in particular, high amounts of circulating cytokines, can lead to the non-physiological transmigration of BM cells into the CNS which can give rise to microglia-like cells. Figures adopted and modified from (Ginhoux and Garel, 2018; Ransohoff, 2007).

Therefore, to further assess whether BM-derived microglia precursors are recruited to the healthy CNS while circumventing the problems associated with irradiation, a subsequent study used parabiosis experiments (Ajami et al., 2007). Parabiosis, a surgical technique that fuses the vasculature of two living

organisms, allowed for the sharing of the blood circulation between wild type and GFP transgenic mice without affecting their blood-brain nor the blood-retinal barrier (Ajami et al., 2007; Kamran et al., 2013). Five months post-surgery, no GFP^+ microglia could be detected in sections obtained from the brain, brainstem or the spinal cord, indicating that under steady-state conditions, CNS microglia were a closed system with the capacity to self-renew and that their maintenance was independent of BM-derived circulating progenitors (Ajami et al., 2007). Furthermore, the authors observed that when facial motoneuron injury was induced in both parabiotic pairs and irradiated/transplanted mice, exogenous GFP^+, Iba-1^+, BM-derived microglia cells could only be detected in the irradiated/transplanted groups, strongly corroborating earlier findings that the replacement of microglia by circulating precursors can be induced by experimental manipulations associated with irradiation (Ajami et al., 2007). In a subsequent landmark study, Ginhoux *et al.* established that microglia residing in the adult CNS in the steady state are derived from primitive myeloid progenitors that migrate from the yolk sac into the brain by embryonic day 9.5, after which the BBB forms and effectively blocks postnatal hematopoietic progenitors from contributing to microglia maintenance (Ginhoux et al., 2010).

To further examine whether microglia renewal and expansion occurred solely from local resident cells, Elmore *et al.* used an inhibitor of colony stimulating factor 1 receptor (CSF1R), PLX3397, to deplete microglia cells in the brain without compromising the integrity of the BBB (Elmore et al., 2014). Findings from the study demonstrated that the brain harbored latent $nestin^+$ microglial progenitors, which following microglia depletion in the brain, undergo rapid proliferation and differentiation to repopulate the entire brain within 1 week of inhibitor cessation (Elmore et al., 2014). Notably, the observed regeneration of microglia in the depleted brain mirrored some aspects of normal development, as embryonic stem cells similarly require a $nestin^+$ stage on their way to becoming microglia (Elmore et al., 2014; Hughes and Bergles, 2014). These findings raised the question whether retinas depleted of microglia could be repopulated in similar fashion from $nestin^+$ precursors (Elmore et al., 2014). To this end, Huang *et al.*

used a selective CSF1R inhibitor, PLX5622, to deplete microglia in the CNS including retina and assess the origin of the repopulated microglia (Huang et al., 2018). In contrast to the brain, the repopulated retinal microglia were not derived from nestin^{+} progenitors, but rather from dual extra retinal origins; residual microglia in the optic nerve which repopulated the retina along the center-to-periphery axis, and macrophages in the ciliary body/iris which repopulated the retina along the periphery and accounted for around 15% of the repopulated microglia (Huang *et al.*, 2018). Of note is that findings from the study uncovered novel radial migratory routes of retinal microglia and demonstrated the presence of peripheral macrophage-derived microglia which were significantly less ramified than their central counterparts (Huang *et al.*, 2018).

1.2.2 Microglia in the healthy retina

Microglia cells play active roles in maintaining normal retinal tissue homeostasis. During the course of embryonic development, amoeboid cells immunopositive for microglia/macrophage markers invade the retina by crossing the vitreal surface and by migrating from nonneural ciliary regions (Santos et al., 2008). These cells are largely confined to the inner half of the retina in close proximity to dying RGCs which are excessively produced during development (Santos et al., 2008). As professional phagocytes, these strategically located amoeboid microglia engage in extensive phagocytic clean-up of apoptotic cellular corpses of the RGCs, thereby preventing leakage of cellular contents that promote inflammation and tissue necrosis (Ravichandran, 2003). Moreover, during the first postnatal days when RGC neurons make exuberant synaptic connections to the lateral geniculate nucleus (LGN) of the thalamus, microglia cells actively engage in pruning of transient, intact retinogeniculate synapses (Schafer et al., 2012). This process is dependent upon neural activity, where microglia preferentially engulf weak synaptic connections (Schafer et al., 2012). Furthermore, microglia mediated synaptic pruning occurs via a complement C3-CR3-dependent mechanism, where activated C3 (iC3b/C3b) selectively labels the weak RGCs terminals triggering a C3-receptor dependent phagocytosis pathway (Schafer et

al., 2012). Indeed, C3 or CR3 knockout mice exhibit striking defects in synaptic pruning during development (Schafer et al., 2012).

Microglia cells in the developing retina also play an essential role in shaping vascular development (Silverman and Wong, 2018). Consistent with this role, microglia have been demonstrated in rodents and humans to populate the retina before developmental vascularization commences (Checchin et al., 2006; Rymo et al., 2011). During retinal vascularization, microglial cells are commonly associated with endothelial tip-cells at the vascular front and have been shown to play an active role in promoting angiogenic sprout anastomosis formation (Checchin et al., 2006; Rymo et al., 2011). This process is however independent of a direct contact between microglia cells and the vessels, and instead occurs via soluble factors secreted by both microglia and vascular endothelial cells (Rymo et al., 2011). Soluble factors released by the vasculature attracts microglial cells and promotes their release of angiogenic factors (Rymo et al., 2011). Consequently, the absence of microglia has been demonstrated to alter CNS vascularization (Arnold and Betsholtz, 2013). In neonatal rats for example, pharmacologic depletion of microglia using clodronate liposomes results in pronounced decreases in the retinal vascular area and density (Checchin et al., 2006). Intriguingly, replenishment of microglia-depleted retinas with exogenous microglia restored vascularity in the developing tissue, strongly indicating a prominent role for microglia in normal retinal blood vessel formation (Checchin et al., 2006). This notwithwithstanding, retinal myeloid cells have also been demonstrated to suppress angiogenic branching of deep retinal vessels via a Wnt-Flt1 pathway, implying that microglia cells can be either anti-angiogenic or pro-angiogenic depending on context (Stefater III et al., 2011).

The outer retina, from the ONL to the RPE, is an immune privileged zone that remains consistently devoid of microglia cells under normal physiological conditions (Silverman and Wong, 2018). RPE cells play a prominently role in development and maintenance of this immunosuppressive microenvironment (Karlstetter et al., 2015; Zamiri et al., 2007). They secrete inhibitory factors such as transforming growth factor-β (TGF-β), thrombospondin-1 (TSP-1) and

somatostatin (SOM) into the subretinal space that actively blocks the undesirable infiltration of microglia and other mononuclear phagocytes into this region (Miyajima-Uchida et al., 2000; Pfeffer et al., 1994; Zamiri et al., 2006). During adulthood, microglia cells are found distributed as horizontal arrays of cells in the IPL and OPL where they exhibit a quiescent phenotype characterized by very small somata and extensively ramified processes that are highly dynamic and motile in nature (Langmann, 2007). They form a mosaic network of evenly distributed non-overlapping cells that allow the neural retina to be continuously sampled every few hours by the continuous movement of the microglial processes (Damani et al., 2011; Karlstetter et al., 2015). The dynamic movement of the processes also serves other housekeeping functions including homeostatic regulation of neuronal activity and the elimination of accumulated metabolic waste products and cellular debris in the retinal microenvironment (Li et al., 2012; Nimmerjahn et al., 2005). In addition, microglia processes which intimately intercalate with neuronal axons and dendrites in the healthy retina plexiform layers are required for the maintenance of synaptic structure and physiology (Wang et al., 2016). Indeed, long-term absence of microglia in the retina results in the degeneration of synapses with concomitant progressive deficits in retina's functional response to light (Wang et al., 2016).

To effectively patrol the retinal environment and limit unnecessary microglia activation, microglia cells are equipped with a versatile subset of different cell-surface proteins that they use to communicate with neighboring neuronal and glial cells (Karlstetter et al., 2015; Kierdorf and Prinz, 2013). CD200R is an important example of an inhibitory receptor expressed predominantly on retinal microglia that actively maintains microglia in a quiescent state when ligated (Broderick et al., 2002; Copland et al., 2007). Its ligand, CD200 (previously known as OX2), is a membrane glycoprotein that is widely expressed in the retina, including in ganglion cells, photoreceptors, vascular endothelium and RPE (Horie et al., 2013; Karlstetter et al., 2015; Langmann, 2007). Previous studies have demonstrated that CD200 deficient mice exhibit augmented pro-inflammatory responses in experimental animal models of uveoretinitis and wet form of age

related macular degeneration (AMD) (Broderick et al., 2002; Copland et al., 2007; Horie et al., 2013). In contrast, pharmacological activation of CD200R using an agonist monoclonal rat anti-mouse CD200R (DX109) antibody ameliorates pathological outcome in optic nerve injury and experimental autoimmune uveoretinitis animal models, suggesting that CD200-CD200R interaction could be harnessed for therapeutic purposes (Copland et al., 2007; Horie et al., 2013).

Another inhibitory factor secreted by neurons to inhibit the inflammatory capacity of microglia is CX3CL1 (fractalkine), a constitutively expressed cleavable chemokine which binds the G_i-protein coupled receptor CX3CR1 on the surface of microglia (Wolf et al., 2013). Numerous studies have demonstrated the neuroprotective and immunomodulatory role of CX3CL1-CX3CR1 interaction in the CNS (Wolf et al., 2013; Zieger et al., 2014). Transplanting mesenchymal stem cells engineered to secrete CX3CL1 in the subretinal space of rats exposed to high-intensity light to induce retinal degeneration inhibited microglia activation and migration to the ONL with concomitant reduction in neuronal demise (Huang et al., 2013). Conversely, in retinal degeneration (rd10) mutant mice deficient of CX3CR1, significantly greater numbers of reactive microglia were shown to infiltrate the ONL and induce a pro-inflammatory milieu that accelerated photoreceptor apoptosis and atrophy when compared with CX3CR1-sufficient rd10 littermates (Zabel et al., 2016). Of note is that delivery of exogenous CX3CR1 to the rd10 mouse eye significantly decreased the density of reactive microglia infiltrating the ONL and slowed the rate of neuronal loss, further underscoring CX3CL1-CX3CR1 signaling axis as an important regulator of microglial reactivity (Zabel et al., 2016).

Microglia also establish important interactions with Müller cells by exchanging functionally significant signals, and this bidirectional communication can act as a mediator of neuron-microglia crosstalk during both physiological and pathophysiological conditions (Madeira et al., 2015; Wang and Wong, 2014). Certain microglia-derived neurotrophic factors such as BDNF and CNTF are consistently shown to be neuroprotective for photoreceptor cells despite these cells not expressing their receptors (Kirsch et al., 2002; Ugolini et al., 1995; Wen

et al., 2008; Wilson et al., 2007). It was later revealed that microglia derived neurotrophic factors interact with Müller cells and induce or inhibit the release of secondary factors including basic fibroblast growth factor (bFGF), leukemia inhibitory factor (LIF) and glial cell line-derived neurotrophic factor (GDNF) that could act directly on photoreceptors and mediate survival or apoptosis during pathophysiological conditions (Harada et al., 2000, 2002; Shen et al., 2013; Wang et al., 2011; Wenzel et al., 2005). Additionally, microglia-Müller cell cross-talk can occur via the translocator protein (TSPO; 18kDa) signaling axis, where Müller cells release an endogenous TSPO ligand, diazepam binding inhibitor (DBI) protein, which binds microglial TSPO and suppresses microglial activation during retinal pathology (Wang et al. 2014).

1.2.3 Microglia in the diseased retina

When the retina suffers from a noxious insult, an immune response is launched by a local defense system that involves the resident microglia cells and the complement system (Chen and Xu, 2015). Microglia cells respond to noxious stimuli by retracting their filopodia-like processes (Figure 3) and upregulating a variety of cell surface molecules including major histocompatibility complex (MHC) class I and II antigens and receptors for cytokines and chemokines (Jurgens and Johnson, 2012).

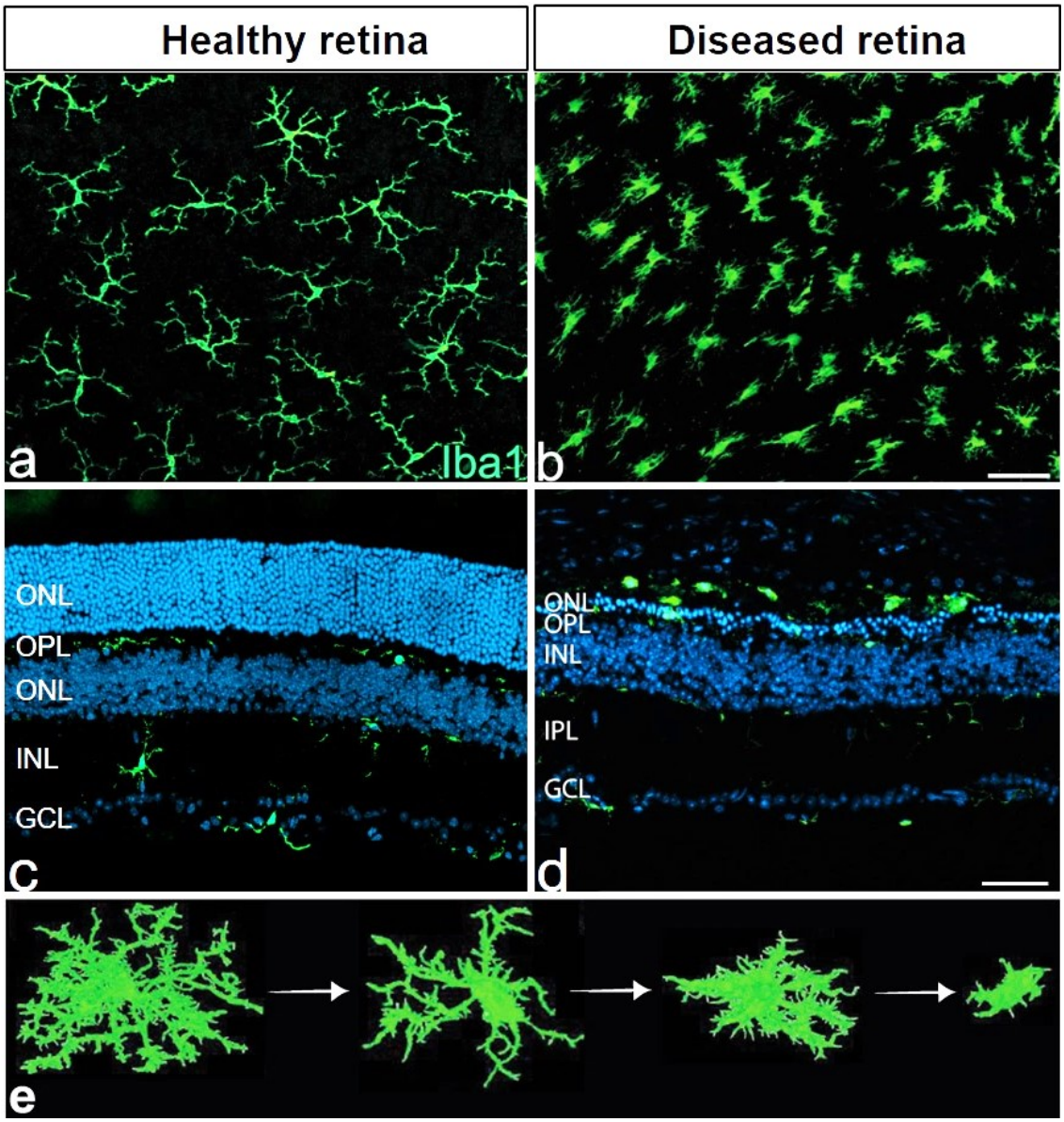

Figure 3: Microglia morphology in health and disease. Flat-mounts (**a & b**) and cross-section (**c & d**) images of Iba1-positive microglial cells in retinas from wild-type **(a & c)** and Fam161a-deficient mouse model of Retinitis Pigmentosa (**b & d**). In the healthy retina **(a & c)**, microglia cells are found in the IPL, OPL and GCL where they form a mosaic network of evenly distributed non-overlapping cells and exhibit a resting but surveillant phenotype characterized by very small somata and extensively ramified processes. In the diseased retina (**b & d**), microglia adopt an amoeboid morphology that is either completely devoid of processes or has very few unbranched processes. They are found in the degenerating ONL and the subretinal space where they not only engage in the phagocytic clearance of cellular corpses and debris, but also actively contribute to the degenerative processes. Panel (**e**) 3D images of Iba-1 stained brain sections generated using Fiji software (NIH, USA) showing the progressive changes in microglial morphology in response to bacterial lipopolysaccharide. Figures **a**, **b** & **d** adopted and

modified from (Dannhausen et al., 2018), figure (**e**) adopted and modified from (Martyanova and Tishkina, 2015).

In addition, microglia alter their transcriptional profiles and undergo a metabolic switch from oxidative phosphorylation (OXPHOS) to glycolysis for the rapid production of energy necessary to fuel inflammatory events (Tannahill et al., 2015). Inflammation-induced metabolic rewiring is also crucial for microglial cellular proliferation since biosynthetic pathways for nucleotides, amino acids and lipid synthesis branch out from glycolysis (Orihuela et al., 2016; Rashid et al., 2018c). Reactive microglia cells subsequently migrate to the site of injury where they produce multiple pro-inflammatory factors including interleukin IL-1β, IL-6, IL-15, interferon gamma (IFN-γ), tumor necrosis factor alpha (TNF-α) and inducible nitric oxide synthase (iNOS) as well as reactive oxygen and nitrogen species (RONS) (Crotti and Ransohoff, 2016; Kierdorf and Prinz, 2013).

Microglia mediated inflammatory processes are aimed at the rapid return of a perturbed tissue back to normal homeostasis. However, if the insults persists, such as in aging and degenerative diseases of the retina, microglia transition from a well-balanced activation state to a hyperreactive state and produce exaggerated levels of pro-inflammatory mediators that contribute to tissue damage and exacerbate disease severity (Chen and Xu, 2015; Karlstetter et al., 2015). In AMD for instance, the widespread accumulation of drusen components provides a prominent chemoattractant stimulus that attracts microglia to the subretinal space (Indaram et al., 2015; Penfold et al., 2001; Rodriguez et al., 2014). Once in the outer retina, reactive microglia or microglia-derived factors induce NLRP3 inflammasome activation in RPE with the concurrent secretion of IL-1β and the degeneration of RPE cells via caspase-1-mediated pyroptosis (Ma et al., 2009; Madeira et al., 2018; Nebel et al., 2017; Tseng et al., 2013). The downstream effects of RPE loss are deleterious, and include choriocapillaris attenuation and secondary photoreceptor demise which ultimately result in loss of visual function (Ambati and Fowler, 2012; Kurihara et al., 2016). Accumulating subretinal microglia and other mononuclear phagocytes can also directly instigate death of photoreceptors in the vicinity by engaging in indiscriminate phagocytosis

of stressed but living photoreceptors (Zhao et al., 2015a). Furthermore, the pro-inflammatory milieu induced by reactive subretinal mononuclear phagocytes can also promote photoreceptor cell death (Scholz et al., 2015c). We have indeed demonstrated in our previous research that conditioned medium obtained from reactive human and murine microglial cells triggers photoreceptor apoptosis (Madeira et al., 2018; Wiedemann et al., 2018).

The presence of reactive microglia in the outer retina is not a phenomenon unique to AMD but is also observed in other retinal degenerative pathologies such as Retinitis pigmentosa (RP) (Gupta et al., 2003). RP is the most prevalent and severe form of inherited retinopathies and is brought about by the primary degeneration of mutation containing rods and the subsequent degeneration of cones (Hartong et al., 2006). Microglia in human RP patients migrate to the photoreceptor layer following cues from apoptotic rods and engage in the phagocytic clearance of cellular corpses and debris (Gupta et al., 2003). Bloated microglia containing rhodopsin-positive cytoplasmic inclusions have indeed been demonstrated in the outer retina of RP patients using immunocytochemistry with microglia and rod cell-specific markers (Gupta et al., 2003). In addition to phagocytic clearance of degenerate cells, bloated infiltrating microglia secrete high levels of pro-inflammatory molecules such as TNF-α, IL-1β, CCL5 (alias RANTES) and CCL2 (alias MCP-1) that kill normal neurons and accentuate the ongoing degenerative process (Zeng et al., 2005). Intriguingly, using the retinal degeneration 10 (*rd10*) mouse model of RP, Guo *et al.* reported that mice deficient in *ccr2* exhibited significantly reduced number of microglia infiltrating the photoreceptor layer compared to *ccr2*$^{+/+}$ *rd10* controls, indicating that the *ccr2/ccl2* signaling pathway plays a key role in mobilizing microglia into the degenerating photoreceptor layer (Guo et al., 2012). Importantly, the reduced microglial infiltration observed in *ccr2*$^{-/-}$ *rd10* mice was associated with increased retinal thickness and function, confirming microglia's involvement in inducing degenerative changes during retinal pathology (Guo et al., 2012).

In diabetic retinopathy (DR), which is the most common ocular complication of diabetes mellitus, hypertrophic and amoeboid microglia are present at different

stages of the disease and are mainly associated with retinal vasculature, cotton-wool spots and microaneurysms in the inner retina (Grigsby et al., 2014; Zeng et al., 2000). In the non-proliferative form of the disease, there is a moderate increase in the number of reactive microglia which are mostly clustered around perivascular region involving arterioles, venules and capillaries as well as around fresh hemorrhages in microaneurysms (Zeng et al., 2008). In the intermediate pre-proliferative disease form, there is a dramatic increase in reactive microglia which cluster around peripheral regions of cotton-wool spots and dilated vessels (Zeng et al., 2008). Lastly, in the proliferative form of the disease characterized by pathological neovascularization, there is a marked increase in the number of reactive microglia in the GCL which heavily surround the new vessels in the nerve fibre layer and the optic nerve head where the proliferative process is most prominent (Zeng et al., 2008). This close topological association between reactive microglia and the perivascular compartments in human DR is postulated to exacerbate vascular permeability via pro-inflammatory mechanisms (Grigsby et al., 2014; Zeng et al., 2008).

Similarly in the human glaucomatous eyes, clusters of large amoeboid microglia are found in the compressed prelaminar and lamina cribrosa regions where they surround blood vessels and form concentric rings (Neufeld, 1999). In addition, reactive microglia occurring either singly or in clusters are found in the parapapillary chorioretinal region (where the RPE and the bruch's membrane terminate) of glaucomatous optic nerve heads (Neufeld, 1999). Of note is that microglia activation in the glaucomatous retina occurs prior to overt RGCs neurodegeneration, suggesting that microglial neuroinflammatory responses play a critical role in the onset and perpetuation of RGC loss (Bosco et al., 2011; Inman and Horner, 2007). (Bosco et al., 2011; Inman and Horner, 2007). The precise mechanisms involved in microglia mediated RGCs neurodegeneration remains poorly understood, but involves, at least in-part, the upregulation of Toll-like receptor (TLR) 4 and the secretion of high amounts of pro-inflammatory mediators TNF-α, IL-6 and nitric oxide (NO) (Echevarria et al., 2017; Neufeld et al., 1997; Sappington and Calkins, 2006; Tezel et al., 2004; Vidal et al., 2006).

Consistently, the depletion of TNF-R1 or IL-6 or the pharmacological inhibition of TLR4 or NO synthesis significantly abrogates the loss of RGCs associated with experimental animal models of glaucoma (Echevarria et al., 2017; Tezel et al., 2004; Vidal et al., 2006).

In summary, ample evidence generated from experimental animal models to human tissue shows unequivocally that microglia play a central role in the pathophysiology of retinal neurodegenerative disorders and thus cannot be simply regarded as “innocent” bystanders of disease. Moreover, microglia responsiveness to noxious stimuli during retinal pathology suggests that these cells have the potential to act as diagnostic biomarkers for predicting disease onset, disease exacerbation, as well as response to treatment (Karlstetter et al., 2015). It is therefore imperative that we clearly understand the mechanisms underlying the establishment, maintenance and regulation of microglia responses during normal and pathological conditions. Such advances will provide an opportunity to better pinpoint candidate molecules and signal-transduction pathways that are dysregulated in overreactive neurotoxic microglia and set the stage for better-informed immunomodulatory strategies.

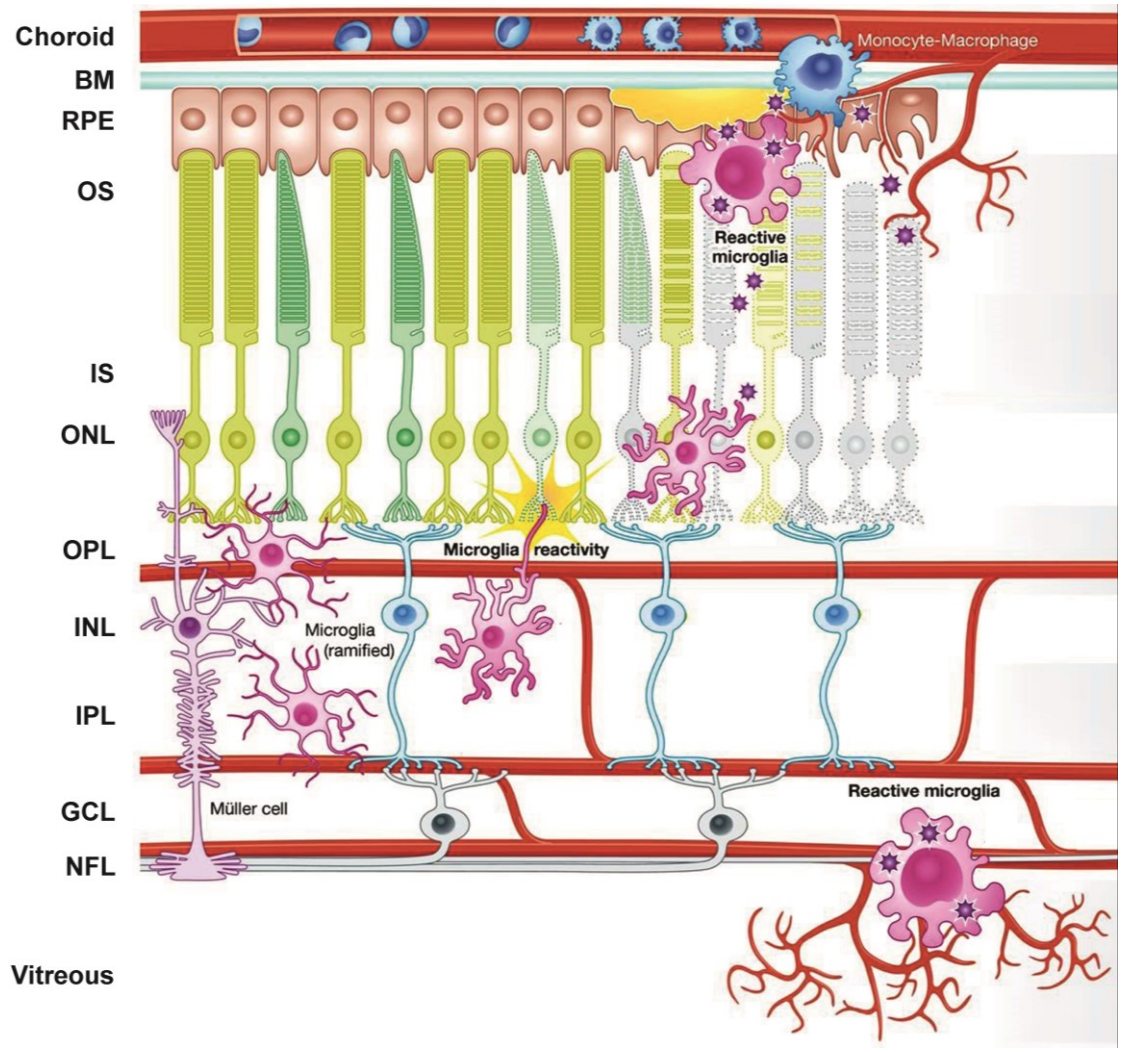

Figure 4: Schematic representation of microglia reactivity in the retina. Under steady state conditions, microglia reside in the plexiform layers where they contribute constitutively to maintaining neuronal synaptic structures, engage in phagocytosis of cell debris and constantly surveil their microenvironment for any disturbance in retinal homeostasis. When retinal neurons or the RPE suffer from noxious insults that lead to alteration in normal cellular function and/or degeneration, microglia become rapidly alerted, transform into amoeboid phagocytes and migrate to the lesion sites in an attempt to restore homeostasis. However, if the insults persist, such as in aging and degenerative diseases of the retina, microglia become pathologically activated and produce exaggerated levels of pro-inflammatory mediators that contribute to tissue damage and exacerbate disease severity. Figure adopted and modified from (Akhtar-Schäfer et al., 2018).

1.2.4 Transcriptional control of microglia phenotypes in health and disease

Much of our understanding of cell-type specific transcriptional regulation has come from detailed analysis of promoter (regulatory) regions which harbor sequence elements that are targets for signal dependent regulation (Holtman et al., 2017). Promoters are primarily occupied by widely expressed transcription factors such as SP1 and GABP which by themselves are incapable of orchestrating cell-type specific gene expression (Holtman et al., 2017). To generate cell-type specific programs of gene expression, distant gene regulatory sequences known as enhancers are required (Holtman et al., 2017; Smale and Natoli, 2014). A classical feature of enhancers is the presence of heterotypic clusters of binding sites for one or more lineage determining transcription factors (LDTF) and for broadly expressed stimulus dependent transcription factors (SDTF) (Figure 5) (Ghisletti et al., 2010; Holtman et al., 2017). In myeloid derived cells, such LDTFs include PU box binding-1 (PU.1), Runt-related transcription factor 1 (RUNX1) and Interferon regulatory factor 8 (IRF8) (Kierdorf et al., 2013). These factors play fundamental roles in microgliogenesis (Ginhoux et al., 2010; Jin et al., 2012; Kierdorf and Prinz, 2013; Satoh et al., 2014). In addition, they have been shown to be constitutively bound to enhancers where they collaborate with other lineage determining factors to induce histone modifications associated with a primed state of activity (Smale and Natoli, 2014).

In macrophages for instance, enhancers controlling endotoxin-stimulated gene expression are almost invariably bound by the lineage dependent Ets transcription factor Pu.1 (Ghisletti et al., 2010). Collaborative DNA binding of Pu.1 with other partner TFs such as C/EBPβ leads to the deposition of monomethyl groups on lysine 4 of histone 3 (H3K4) and the displacement of nucleosomes to expose enhancer DNA sequences (Figure 5) (Ghisletti et al., 2010; Heinz et al., 2010). Notably, the ectopic expression of Pu.1 in NIH-3T3 mouse fibroblast cells results in the depletion of nucleosomes in Pu.1 bound regions as well as several-fold increase in the histone modification H3K4me1 in regions corresponding to

macrophage enhancers (Ghisletti et al., 2010). High levels of the histone mark H3K4me1 is a core chromatin signature of primed enhancers and serves as a beacon for signal-dependent effectors of signaling pathways such as nuclear factor-κB (NFκB), interferon responsive factors (IRFs) and activator protein 1 (AP-1) (Ghisletti et al., 2010; Heinz et al., 2010; Smale and Natoli, 2014). The subsequent binding of SDTFs in the presence of stimulus promotes the recruitment of the ubiquitously expressed histone acetyltransferase (HAT) p300 to the nucleosome depleted enhancer regions with concomitant increase in the acetylation states of various residues of histones H3 and H4 (Heintzman et al., 2007; Smale and Natoli, 2014; Visel et al., 2009). Indeed, p300-mediated histone 3 lysine 27 acetylation (H3K27Ac) has been reported to be a distinct epigenetic mark for active enhancers (Raisner et al., 2018). The observations that SDTFs bind to enhancer landscapes predetermined by LDTFs such as Pu.1 in the presence of stimulus partially explains how broadly expressed TFs can regulate tissue-resident macrophage-specific gene expression (Crotti and Ransohoff, 2016; Holtman et al., 2017)

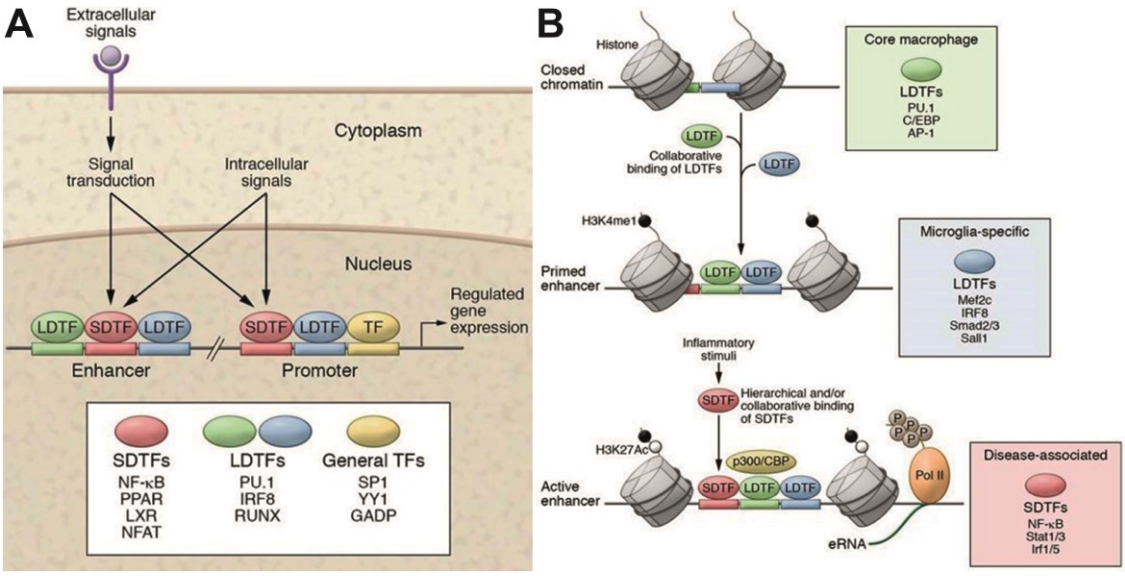

Figure 5: Enhancer-promoter interactions drive cell specific gene expression. (A) Promoters are primarily occupied by broadly expressed transcription factors which by themselves are incapable of orchestrating cell-type specific gene expression. Enhancers occupied by LDTFs and SDTFs interact with promoters to achieve cell type-specific expression and response profiles**. (B)** Initial steps of enhancer selection in closed chromatin regions containing regularly positioned nucleosomes involves the binding of

LDTFs. This results in the depletion/sliding of nucleosomes to expose enhancer DNA sequences. LDTFs also deposit stereotypical histone marks such as H3K4me1 that act as beacons for SDTFs. The net effect of LDTFs binding is the maintenance of inducible genes in a silent, yet primed state which can be rapidly induced in the presence of stimuli**.** Figures **A** and **B** adopted from (Holtman et al., 2017)**.**

Several LDTFs have been shown to play roles in maintaining the unique resting but surveilling phenotype of microglia cells that is characteristic of a healthy CNS (Holtman et al., 2017). RUNX1, which is expressed as early as embryonic day 6.5 in erythromyeloid precursors, has been shown to promote the transition of amoeboid microglia to the ramified deactivated state during brain development (Kierdorf et al., 2013; Zusso et al., 2012). Consistently, mouse primary microglia cells infected with GFP-expressing adenovirus was shown to express significantly high levels of the proinflammatory enzyme iNOS when compared with adenovirus infected primary cultures transduced with Runx1 (Zusso et al., 2012). SALL1, a zinc finger transcriptional repressor whose expression in the CNS is virtually exclusive to adult microglia, is another factor involved in the maintenance of microglia homeostasis (Buttgereit et al., 2016). Ablation of Sall1 results in the conversion of microglia from a ramified phenotype to reactive phenotype characterized by shorter, thicker processes and a larger cell soma (Buttgereit et al., 2016). In addition, Sall1 deletion in microglia induces alterations in neurogenesis that perturb CNS homeostasis (Buttgereit et al., 2016). Another important transcription factor expressed by microglia during their transition from pre-microglia to mature microglia is MAFB (Matcovitch-Natan et al., 2016). Loss of MafB expression in microglia leads to the disruption of developmental genes and the upregulation of interferon and inflammation-related pathways in adult mice (Matcovitch-Natan et al., 2016).

In response to inflammatory stimuli, several SDTFs also play crucial roles in limiting microglia mediated inflammatory responses and inducing neuroprotective behavior. NR4A2 (Nuclear receptor subfamily 4, group A, member 2), also known as Nurr1, is an orphan nuclear receptor that is crucial for the development and homeostasis of dopaminergic neurons (Zetterström et al., 1997). NR4A2 has been shown to protect against loss of dopaminergic neurons by suppressing pro-

inflammatory signaling in microglia and astrocytes (De Miranda et al., 2015; Saijo et al., 2009). The anti-inflammatory mechanism involves the recruitment of NR4A2 to NF-κB-p65 on inflammatory gene promoters and the subsequent recruitment of corepressor for repressor element 1 silencing transcription factor (CoREST) and the nuclear receptor corepressor 2 (NCOR2) (De Miranda et al., 2015; Saijo et al., 2009). The recruitment of CoREST and NCOR2 to the inflammatory gene promoters results in the clearance of NF-κB-p65 and restoration of activated pro-inflammatory gene transcription to a basal state (De Miranda et al., 2015; Saijo et al., 2009).

Ligation of estrogen receptors alpha and beta (ERα & ERβ) by endogenous and synthetic estrogen ligands has also been shown to exert potent immunomodulatory effects in reactive microglia (Arevalo et al., 2015; Bruce-Keller et al., 2000; Saijo et al., 2011). 17β-estradiol (estradiol), produced both in the CNS and in peripheral organs by aromatase-mediated conversion of testosterone, is the most potent estrogen and has been shown in a multitude of studies to attenuate microglia inflammatory responses through both ERα and ERβ activation (Bruce-Keller et al., 2000; Liu et al., 2005; Vegeto et al., 2003; Zhu et al., 2015). Similarly, Androstenediol, an ERβ subtype-specific ligand produced in the brain, has been shown to inhibit the magnitude and duration of microglia inflammatory responses by recruiting C-terminal binding protein (CtBP) corepressor complexes to AP-1 dependent promoters (Saijo et al., 2011). Interestingly, the genetic ablation of ERα leads to a spontaneous reactive phenotype of microglia in the brains of adult ERα-null mice, demonstrating a critical role for this receptor in the maintenance of microglia homeostasis (Vegeto et al., 2003).

NF-E2-related factor-2 (NRF2) is an essential transcription factor for protection against oxidative/xenobiotic stress and inflammation (Kobayashi et al., 2016). NRF2 suppresses inflammation by the upregulation of a battery of antioxidant cytoprotective proteins including hemeoxygenase-1 (HO-1), NAD(P)H quinone oxidoreductase-1 (NQO1), thioredoxins (TRXs) and enzymes of glutathione metabolism (Kobayashi et al., 2016; Lastres-Becker et al., 2014; Li et al., 2004;

Yang et al., 2015). Notably, (Kobayashi et al., 2016) demonstrated that NRF2 can also directly repress inflammation by inhibiting the recruitment of RNA Pol-II to proinflammatory genes such as IL-6 and IL-1β. Besides inhibiting inflammation and boosting the cellular antioxidant capacity, NRF2 activators also been demonstrated to enhance microglia phagocytic capacity via upregulation of the scavenger receptor CD36, suggesting that this pathway might be important in shaping tissue-restorative responses to neurodegenerative conditions (Zhao et al., 2015b). Indeed, in Alzheimer's animal models and patients, stressed neurons signal microglia via fractalkine to activate the NRF2 pathway and attenuate microgliosis (Lastres-Becker et al., 2014).

A large number of SDTFs are similarly involved in mediating pro-inflammatory gene expression in microglia, indicating the complexity of the inflammatory response (Stetson and Medzhitov, 2006). Because of this large number, we focus herein on a few of the best characterized inducers of inflammatory signaling in microglia which include NF-κB, AP-1 and signal transducers and activators of transcription (STAT) family members (Holtman et al., 2017; Medzhitov and Horng, 2009). NF-κB, a family of rapidly inducible transcription factors, was discovered more than 31 years ago and named after the gene it affected and the cell type it was discovered in: nuclear factor binding near the kappa light-chain gene in B cells (Sen and Baltimore, 1986; Zhang et al., 2017). NF-κB family consists of five different members, p65 (RelA), RelB, c-Rel, p50/p105 (NF-κB1) and p52/p100 (NF-κB2) which assemble into several homodimers and heterodimers and regulate different sets of target genes (Liu et al., 2017b). Without stimulation, NF-κB proteins are normally sequestered in the cytoplasm by a dedicated set of inhibitory proteins comprising the inhibitor of κB (IκB) family proteins, IκBα, IκBβ, IκBε, BCL-3, IκBz, IκBNS and the C-terminal portions of the precursor proteins p105 (IκBγ) and p100 (IκBδ) (Hayden and Ghosh, 2008; Zhang et al., 2017). Upon stimulation, IκB subunits undergo phosphorylation by a multi-subunit IκB kinase (IKK) complex composed of two kinase subunits IKKα and IKKβ and a regulatory subunit NF-κB essential modulator (NEMO), resulting in the rapid translocation of NF-κB members into the nucleus to induce

transcription of target genes (Liu et al., 2017b; Zhang et al., 2017). While activation of some NF-κB members such as c-Rel can induce the transcription of genes that confer neuroprotection, the activation of the p50/RelA induces the transcription of apoptotic and inflammatory genes that mediate neurodegenerative processes (Lanzillotta et al., 2015). In microglia, diverse stimuli such as LPS, TNF-α, α-synuclein, amyloid-β, ROS and saturated fatty acids have been shown to activate NF-κB signaling. An unbalanced activation of NF-κB in microglia drives the progression and deterioration of multiple neurodegenerative diseases including Alzheimer's, Parkinson's and Amyotrophic lateral sclerosis (ALS) (Frakes et al., 2014). This has been elegantly demonstrated in a previous study using SOD1-G93A mice model of ALS, where the selective inhibition of microglial NF-κB led to the rescue of motor neurons survival and the extension of lifespan by delaying disease progression by 47% (Frakes et al., 2014). Of note is that suppression of NF-κB signaling in astrocytes was insufficient to attenuate neuronal cell death nor alter survival in the ALS mice, clearly demonstrating that neurodegenerative processes are predominantly driven by NF-κB signaling in pathological activated microglia and infiltrating mononuclear phagocytes (Frakes et al., 2014).

AP-1, a heterodimeric transcriptional regulator comprising various combinations of FOS, JUN, MAF, ATF, and CREB family proteins has been described to function both as an SDTF and a LDTF (Fontana et al., 2015; Holtman et al., 2017; Nomaru et al., 2014; Phanstiel et al., 2017). AP-1 cooperatively binds to DNA sequences together with PU.1 and C/EBP to establish functionally active enhancers that are capable of driving both cell-specific gene expression and signal-dependent responses in macrophages (Heinz et al., 2010; Madrigal and Alasoo, 2018). In addition, AP-1 has been shown to participate in the formation of DNA loops that brings enhancer regions located hundreds of thousands of base pairs away in contact with their target genes (Phanstiel et al., 2017). Indeed, during differentiation of human monocytes to macrophages, both newly formed and pre-existing chromatin loops that acquire enhancer activity were shown to be strongly enriched for AP-1 (Phanstiel et al., 2017). Such gained and activated

loops enriched for AP-1 form hubs that connect multiple distal enhancers to a single gene promoter to drive increased expression of macrophage-specific genes (Figure 6) (Phanstiel et al., 2017).

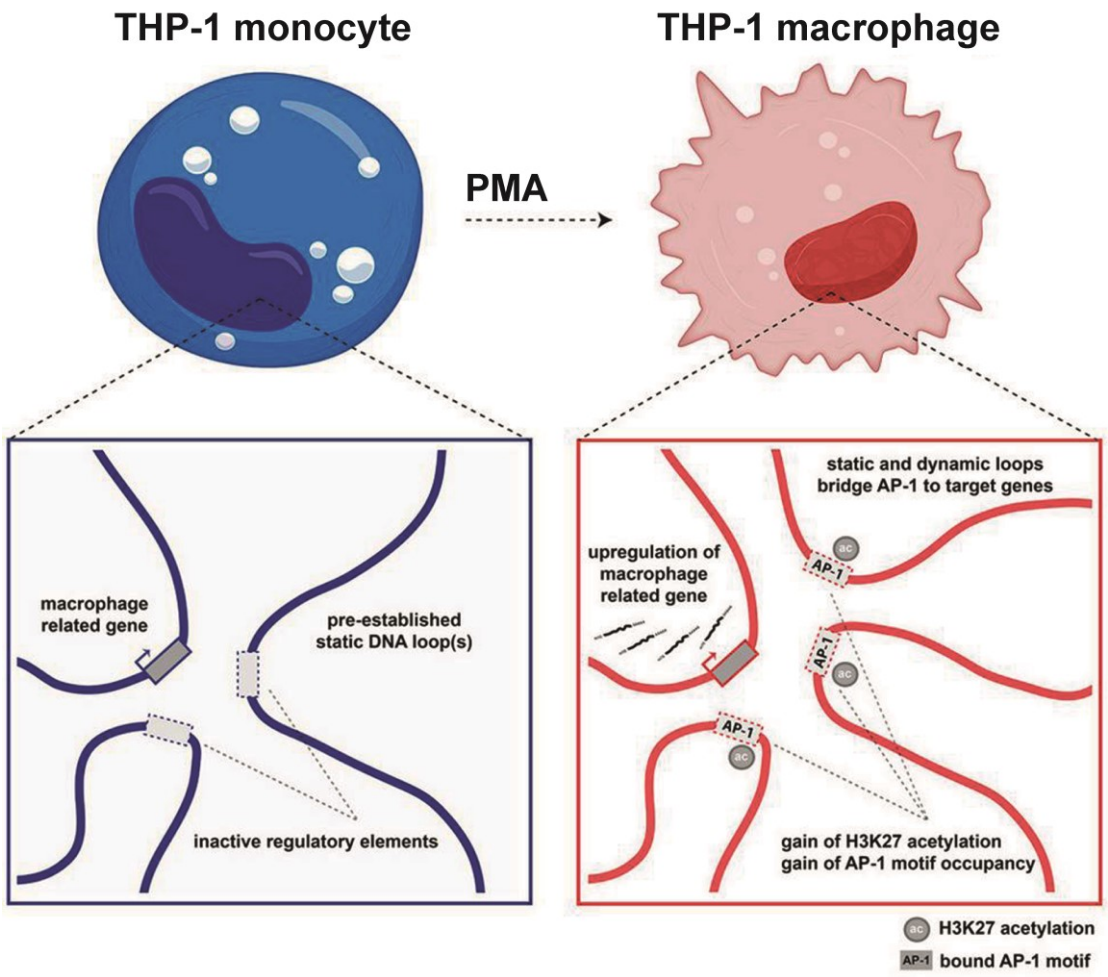

Figure 6: Multi-loop activation hubs that form at key macrophage genes during differentiation are AP-1 enriched. PMA induced differentiation of human monocytes to macrophages leads to the formation of multi-loop activation hubs through both pre-existing and newly acquired DNA loops. These activation hubs form at key macrophage regulatory genes and are enriched for AP-1. They connect multiple distal enhancers to a single gene promoter to induce increased transcription. Figure adopted from (Phanstiel et al., 2017).

In addition to enhancer selection and chromatin looping, AP-1 subunits have been shown to be pivotal in mediating microglia inflammatory responses (Nomaru et al., 2014). Microglia in Fosb-null mice challenged with kainite show significant

reductions in CD68 immunoreactivity and express significantly reduced levels of IL-6, TNF-α as well as anaphylatoxin C5a receptors C5ar1 and C5ar2 when compared to their wild-type counterparts (Nomaru et al., 2014). Similarly, blocking c-Jun N-terminal kinase (JNK) signaling pathway and activation of AP-1 using the flavonoid luteolin markedly reduces LPS-induced production of the pro-inflammatory cytokine IL-6 in microglia (Jang et al., 2008).

Signal transducer and activator of transcription (STAT) protein family are also crucial mediators of microglia inflammatory responses (Chen et al., 2018; Przanowski et al., 2014; Qin et al., 2012). They are activated by a single tyrosine phosphorylation event by Janus kinases (JAKs; JAK1, JAK2, JAK3 and TYK2) which associate with type I and II cytokine receptors (O'Shea and Plenge, 2012; Yan et al., 2018). Phosphorylated STATs form stable homodimers or heterodimers with other STAT proteins before translocating into the nucleus to activate transcription of target genes (O'Shea and Plenge, 2012). Prolonged signalling by pro-inflammatory cytokines via the JAK-STAT pathway is inhibited in a classical negative feedback loop by suppressor of cytokine signaling (SOCS) proteins whose expression is also STAT regulated (Yoshimura et al., 2007). In microglia, the constitutive activation of Stat1 and Stat3 leads to the expression of the histone 3 lysine-27 (H3K27) demethylase JMJD3, which, together with Stat1 and Stat3, drives the expression of numerous pro-inflammatory cytokines and chemokines (Przanowski et al., 2014). Similarly, in experimental autoimmune encephalomyelitis (EAE) mice, myeloid specific ablation of SOCS3 leads to a heightened activation of the STAT3 and induces a more severe form of EAE characterized by enhanced expression of pro-inflammatory mediators and extensive demyelination in the cerebellum compared to the wildtype controls (Qin et al., 2012). In corroboration, experimental autoimmune uveoretinitis (EAU) mice lacking SOCS3 in myeloid cells display an exaggerated retinal inflammatory response characterized by excessive IL-1β, TNF-α and IFN-γ production (Chen et al., 2018). In contrast, inhibition of JAK/STAT1 signaling via the overexpression of SOCS1 in EAU mice lessens disease severity by inhibiting inflammatory chemokine expression and suppressing the recruitment and infiltration of

inflammatory cells into the retina (Yu et al., 2011). Taken together, this evidence suggests that uncontrolled STAT1/STAT3 activity promotes microglia activation and CNS inflammation.

Many factors involved in the transcriptional control of microglia phenotypes in health and disease have been identified; however, there are many more that remain unknown. Alterations in microglia functionality are involved in the pathogenesis of many neurodegenerative diseases (Crotti and Ransohoff, 2016), and therefore a major aim for future research will be to identify specific factors responsible for inhibiting the expression of genes that maintain microglia physiology or overexpressing disease specific genes such as the mitochondrial translocator protein (18 kDa; TSPO) (Karlstetter et al., 2014b; Wang et al., 2014).

1.3 Translocator protein (18 kDa) (TSPO)

The translocator protein (18kDa) (TSPO) was discovered in 1977 as a high affinity benzodiazepine binding site in peripheral tissues that was distinct from the central benzodiazepine receptor, hence the previous denomination peripheral benzodiazepine receptor (PBR) (Braestrup et al., 1977). It is a 5α-helical transmembrane protein that is highly conserved throughout evolution (Figure 7) (Rupprecht et al., 2010). The human TSPO amino acid sequence shares approximately 33.5%, 42.6% and 81.1% identity with the sequence from *Rhodobacter sphaeroides*, *Drosophila melanogaster* and *Mus musculus* respectively (Selvaraj and Stocco, 2015). TSPO homologs, which are not only found in the animal kingdom but also in plants such as *Arabidopsis thaliana* (Balsemão-Pires et al., 2011), show a high degree of functional conservation (Notter et al., 2018; Yeliseev et al., 1997). For instance, when rat Tspo is expressed in TspO^{-} strain of the proteobacterium *Rhodobacter sphaeroides,* it is able to fully rescue the phenotypic changes induced by TspO deletion (Yeliseev et al., 1997).

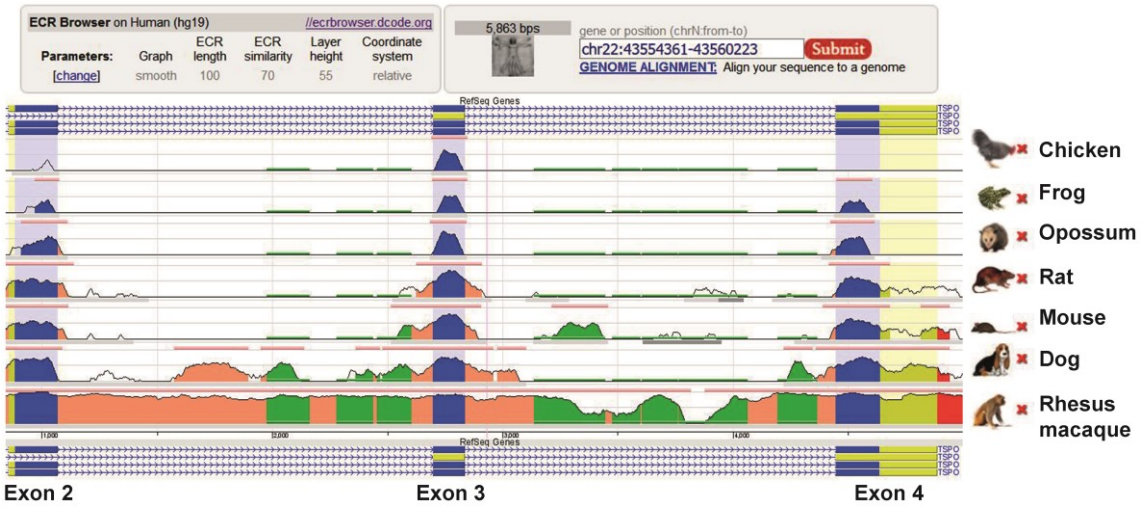

Figure 7: TSPO gene is highly conserved throughout evolution. Analysis of exons 2-4 of the TSPO gene using the Evolutionary Conserved Regions Browser (Ovcharenko et al., 2004) (http://ecrbrowser.dcode.org/) demonstrates sequence conservation between chicken, frog, opossum, rat, mouse, dog and rhesus monkey. Base genome is from human. Exons are presented in blue, untranslated regions (UTRs) in yellow, introns in salmon, simple repeats and transposable elements in green and intergenic sequences in red. Annotated genes are depicted as horizontal blue lines above and below the graph, with strand/transcriptional orientation indicated by arrows.

The TSPO gene consists of four exons, with exon 1 and half of exon 4 remaining untranslated (Lin et al., 1993). The encoded protein is localized primarily to the outer mitochondrial membrane, where it interacts with both outer and inner mitochondrial membrane proteins such as the voltage-dependent anion channel (VDAC) and the adenine nucleotide transporter (ANT) to form a mitochondrial multiprotein complex (McEnery et al., 1992; Veenman et al., 2008). TSPO 2, a less characterized paralogous protein to TSPO, is expressed in developing erythrocytes and is localized to the endoplasmic reticulum and nuclear membranes (Selvaraj and Stocco, 2015). TSPO displays a high constitutive expression in steroidogenic tissues such as adrenal glands, gonads, white and brown adipose tissue, lungs and the placenta, but is very weakly expressed in the healthy brain (Karlstetter *et al.*, 2014; Selvaraj and Stocco, 2015). However, during diverse neuropathological conditions in the brain, there is a dramatic increase in TSPO expression that colocalizes predominantly with activated microglia (Beckers et al., 2018; Daugherty et al., 2013). This robust increase in

microglial TSPO expression from near absence has led to the development of numerous TSPO positron-emission tomography (PET) ligands for the non-invasive imaging of neuroinflammation (Banati et al., 2014; Liu et al., 2014). Similarly during retinal pathology, there is a strong induction in microglial TSPO expression which accurately marks the duration and extent of neuroinflammatory responses in the retina (Karlstetter et al., 2014a; Wang et al., 2014).

The most studied physiological function of TSPO involves the transport of cholesterol from the outer to the inner mitochondrial membrane as a rate limiting step in steroid formation (Midzak et al., 2015). Evidence that linked TSPO function to steroidogenesis came from earlier studies which showed that TSPO binding chemicals like PK11195 could enhance steroid hormone production in Y-1 adrenal tumor cells and that steroidogenesis was significantly hampered in Tspo-negative leydig cells compared to normal cells (Mukhin et al., 1989; Papadopoulos et al., 1997; Selvaraj and Stocco, 2015). Further evidence in support of the steroidogenic role showed that TSPO could strongly bind cholesterol molecules via a cholesterol recognition amino acid consensus (CRAC) motif located at the C-terminus of the protein (Li and Papadopoulos, 1998; Selvaraj and Stocco, 2015). However, recent works from independent research groups have strongly refuted TSPO's involvement in steroidogenesis (Banati et al., 2014; Morohaku et al., 2014; Tu et al., 2014). Findings from these studies showed that steroid hormone production remained unaltered following cell specific or global TSPO knockout in mice and fruit flies (Banati et al., 2014; Morohaku et al., 2014; Tu et al., 2014). In addition, using CRISPR/Cas9 genome editing system to generate $Tspo^{-/-}$ leydig cells, Tu *et al.* demonstrated that the pharmacological effect of PK11195 on steroidogenesis is not mediated through TSPO but rather represent off-target effects (Notter et al., 2018; Tu et al., 2015). However, while these results raise valid concerns, further studies are necessary before TSPO's involvement in steroidogenesis can be invalidated. This is especially so, since recent studies using the most sensitive high-performance liquid chromatography/mass spectrometry technique (HPLC/MS) to evaluate steroid levels support the importance of TSPO as a steroidogenesis regulator particularly under hormonal stimulation and during aging (Barron et al., 2018;

Owen et al., 2017). Of note, Tspo mutant rats showed increased neutral lipid accumulation in the adrenal glands and testis, reduced circulating testosterone and undetectable levels of the neurosteroid allopregnanolone (Owen et al., 2017).

Previous studies using pharmacological ligands or genetic loss of function have also implicated TSPO in cellular bioenergetics (Banati et al., 2014; Liu et al., 2017a). A high-throughput small molecule screen in zebrafish demonstrated that the TSPO ligands PK11195 and Ro5-4864 affect glucose homeostasis and mitochondrial energy production (Gut et al., 2013). Consistently, over-expression of Tspo in Jurkat cells with barely detectable endogenous expression resulted in the upregulation of genes involved in mitochondrial respiration with concomitant increase in mitochondrial ATP production (Liu et al., 2017a). Additionally, it is worth noting that in the retina, TSPO is constitutively expressed in RPE cells which require an active metabolism to maintain outer retina homeostasis, but its expression is robustly induced in microglia only during times of high energy demands to support inflammatory responses (Figure 8) (Orihuela et al., 2016; Scholz et al., 2015b). Moreover, microglia derived from $Tspo^{-/-}$ mice show an altered oxygen consumption rate and significantly reduced ATP production compared to wildtype controls (Banati et al., 2014). However, before TSPO can be conclusively termed as a regulator of mitochondrial energy metabolism, further experiments are needed to determine its precise contribution to this biological process.

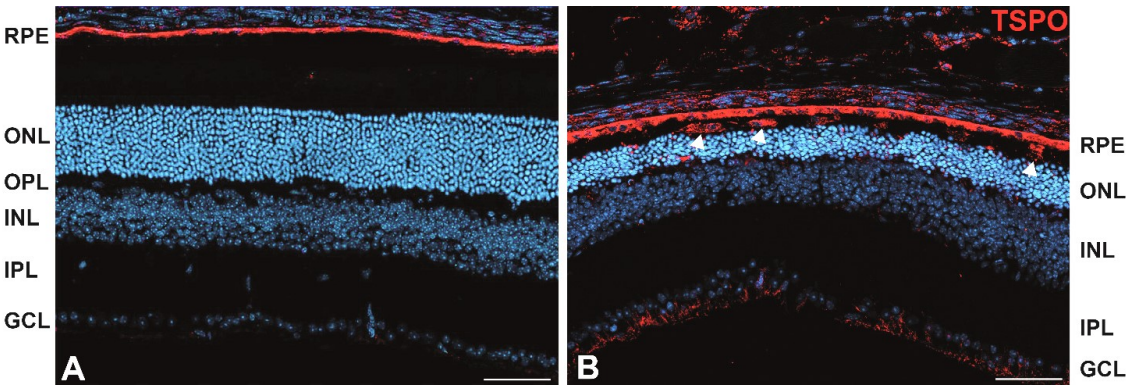

Figure 8: Constitutive and inducible Tspo expression in RPE and microglia cells. Photomicrographs of retina cross-sections from a healthy (**A**) and a light exposed mouse (**B**) stained with anti-TSPO antibody. (**A**) Constitutive expression of Tspo in the retina

pigment epithelium layer (RPE) of the healthy retina. Tspo staining almost non-existent in the plexiform layers where microglia reside. (**B**) Strong upregulation of Tspo expression in reactive amoeboid microglia (white arrow heads) present in the subretinal space of the degenerating retina. Figure (**A**) provided by Katrin Klee, Department of Ophthalmology, University of Zurich, Switzerland. Figure (**B**) provided by Dr. Rebecca Scholz, alumni of the Retinal immunology laboratory, University Hospital of Cologne, Germany.

Other cellular processes where TSPO has been implicated include regulation of the mitochondrial membrane permeability transition pore (MPTP) (Elkamhawy et al., 2017), production of reactive oxygen species (ROS) (Gatliff et al., 2014), cellular proliferation (Rechichi et al., 2008), apoptosis (Veenman and Gavish, 2012), mitochondrial calcium homeostasis (Gatliff et al., 2017), tetrapyrrole biosynthesis (Batoko et al., 2015b, 2015a) and immune modulatory effects (Daugherty et al., 2013; Karlstetter et al., 2014a; Scholz et al., 2015b; Wang et al., 2014).

1.4 Immunomodulatory and neuroprotective effects of TSPO ligands

TSPO is a sensitive biomarker of neuroinflammation and is upregulated in a variety of CNS diseases including multiple sclerosis (MS) (Daugherty et al., 2013), Alzheimer's (Edison et al., 2008), Parkinson's (Ouchi et al., 2005), Huntington's (Messmer and Reynolds, 1998), amyotrophic lateral sclerosis (Turner et al., 2004) and ischemic stroke (Cosenza-Nashat et al., 2009). Although TSPO ligands have been used mostly for non-invasive diagnostic imaging of the affected brain in disease, some studies have also demonstrated their ability to mitigate neuroinflammatory responses and offer neuroprotection (Daugherty et al., 2013). In an experimental autoimmune encephalomyelitis (EAE) mouse model for MS, treatment with the TSPO ligand etifoxine attenuated EAE severity through the reduction of pro-inflammatory cytokine expression (IL-1β, IL-17 and IFN-γ) and peripheral immune cell infiltration in the spinal cord (Daugherty et al., 2013). Moreover, treatment with etifoxine was associated with increased oligodendroglial regeneration following inflammatory demyelination in EAE (Daugherty et al., 2013). In a collagenase mouse model of intracerebral

hemorrhage (ICH), treatment with etifoxine was associated with reduced leukocyte infiltration into the brain, improved BBB integrity and the inhibition of cellular apoptosis and microglia-mediated pro-inflammatory responses (Li et al., 2017). Notably, depletion of microglia using a colony-stimulating factor 1 receptor inhibitor abolished the protective effects of etifoxine, demonstrating that the therapeutic effects of etifoxine require microglia (Li et al., 2017).

Similarly during retinal pathology, we and others have demonstrated that endogenous and synthetic TSPO ligands effectively counter-regulate microgliosis and exert potent neuroprotective effects (Karlstetter et al., 2014b; Wang et al., 2014). Using an endotoxin model of retinal inflammation, Wang *et al.* demonstrated that as reactive retinal microglia upregulate Tspo expression, astrocytes and Müller cells simultaneously upregulate the production and secretion of a 9kDa endogenous TSPO protein ligand, namely diazepine binding inhibitor protein (DBI) (Wang et al., 2014). Secreted DBI is taken up by the retinal microglia, and the interaction between DBI and TSPO serves to limit the magnitude of microglial inflammatory responses and facilitate a return to baseline quiescence (Figure 9) (Wang et al., 2014). Exploiting this endogenous immunomodulatory mechanism, we investigated the ability of a synthetic and highly specific TSPO binding chemical, XBD173 (AC-5216, emapunil), to dampen microglial reactivity in the light-induced retinal degeneration mouse model (Scholz et al., 2015b). Findings from this study revealed that XBD173 strongly inhibited the accumulation of reactive microglia in the outer retina with concomitant preservation of the photoreceptor layer (Scholz et al., 2015b). Moreover, treatment with XBD173 significantly suppressed the expression of pro-inflammatory genes and the morphological transition of microglia towards an amoeboid phenotype in the light-damaged retina (Scholz et al., 2015b). Taken together, these findings highlight the immunomodulatory and neuroprotective properties of TSPO ligands and underscore their potential as pharmacological therapies in the treatment of neurodegenerative disorders.

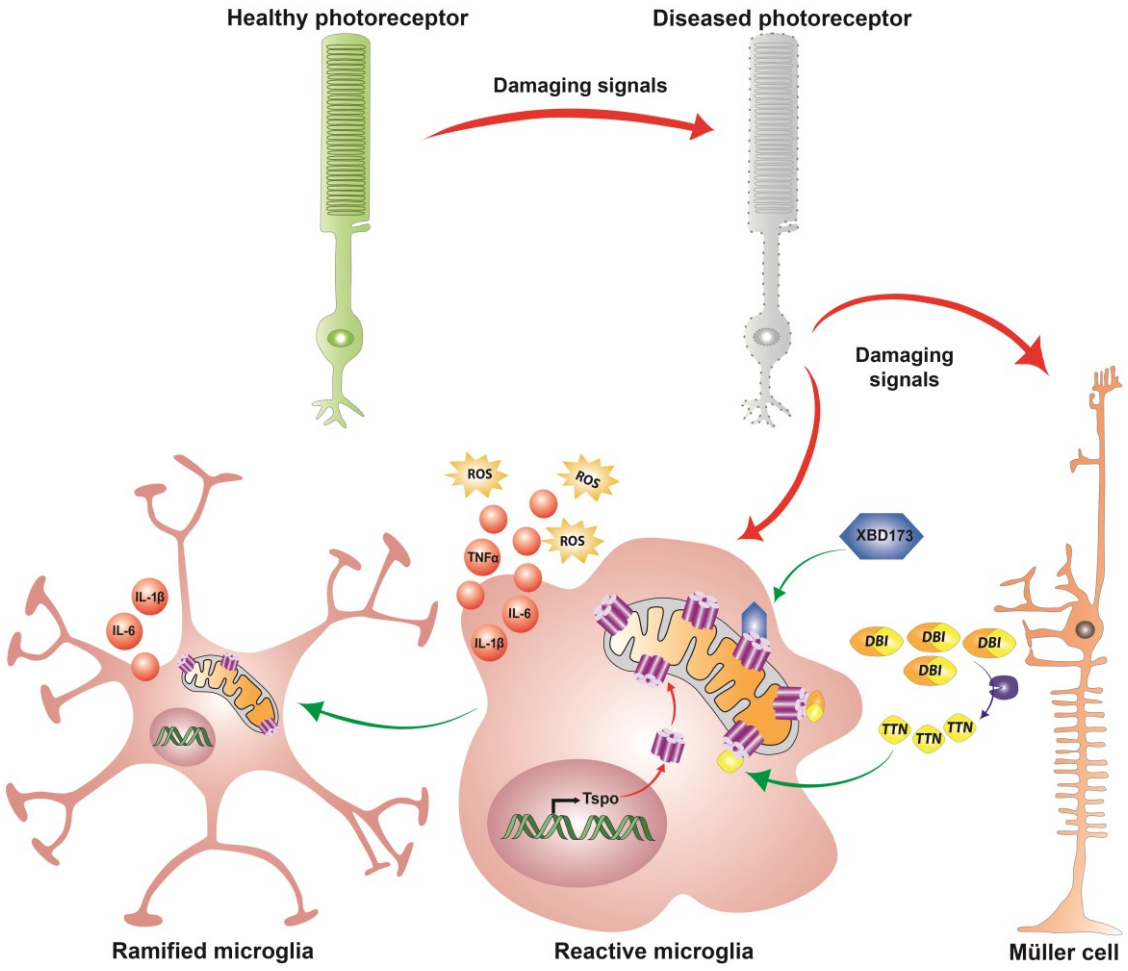

Figure 9: Immunomodulatory effects of endogenous and synthetic TSPO ligands. Specific cues emanating from dying photoreceptors strongly induce TSPO expression in microglia cells. Simultaneously, dying photoreceptors signal Müller cells to upregulate the expression and secretion of the endogenous TSPO ligand Diazepine binding inhibitor (DBI) protein. Secreted DBI and its biologically active cleavage product triakontatetraneuropeptide (TTN) are subsequently taken up by microglia cells. The binding of DBI, TTN or the synthetic ligand XBD173 limits the magnitude and duration of microglia inflammatory responses and promotes their return to baseline quiescence. Figure adopted and modified from (Rashid et al., 2018c).

1.5 Hypothesis and Specific Aims of the Thesis

Neuroinflammation is a key hallmark of neurodegenerative diseases and other CNS pathologies. Microglia, the guard cells of the CNS, play a critical role in orchestrating such neuroinflammatory reactions in response to noxious stimuli. While acute neuroinflammatory responses are beneficial and promote tissue

repair and remodeling, chronic neuroinflammation results in tissue degeneration and exacerbation of disease severity. Therefore, pharmacological approaches that synchronously inhibit dysregulated microglial inflammatory responses while enhancing their beneficial neuroprotective functions presents as promising therapeutic tools for the management and prevention of neurodegenerative diseases. Mitochondrial Translocator Protein (18kDa; TSPO) is lowly expressed in quiescent microglia in the healthy CNS but robustly upregulated in response to injury and neuroinflammation. Importantly, we and others have previously shown that TSPO serves as an attractive therapeutic target for alleviation of immoderate microglia-mediated neuroinflammatory responses during degenerative disorders of the CNS including the retina. However, understanding the molecular mechanisms involved in the aberrant expression of TSPO in microglia during disease is paramount prior to the utilization of this protein as a drug target for interventions aimed at limiting excessive CNS inflammation. Therefore, the main objective of this study was to investigate how TSPO transcriptional regulation is achieved in microglial cells. Given the distinctly different expression in microglia, we hypothesized that the transcriptional regulation of TSPO was achieved, at least in part, via microglia specific factors. To test this hypothesis, functional characterization of the Tspo promoter was carried out in a mouse BV-2 microglial cell line and the minimal sequence necessary to support basal and lipopolysaccharide (LPS) induced promoter activity determined. In addition, the transcriptional regulation of Tspo in BV-2 microglia was compared and contrasted with that of myeloid derived RAW 264.7 macrophage cell line and the retinal pigment epithelial cell line ARPE-19.

2.0 Materials and Methods

2.1 Materials

2.1.1 Mammalian and bacteria cells

Table 1: List of all cell lines and bacteria strain used in the study

Cell lines	Origin
BV-2 murine microglia cell-line	Murine primary microglial cultures isolated from 1-week- old C57BL/6 mice and infected with a v-raf/v-myc recombinant retrovirus (Blasi et al., 1990)
ARPE-19 human retinal pigment epithelial cell-line	A spontaneously arising retinal pigment epithelial (RPE) cell line derived in 1986 from the normal eyes of a 19-year-old male donor (Dunn et al., 1996)
RAW-264.7 macrophage cell-line	Cell-line isolated mice tumors induced with Abelson leukemia virus (A-MuLV). (Raschke et al., 1978)
Bacteria Strain	**Origin**
DH5α	*Escherichia Coli* (E. Coli)

2.1.2 Culture media

Table 2: Reagents and recipes for cell culture and LB media/plates

Reagents	Manufacturer, Cat. No.
Dulbecco's Modified Eagle Medium (DMEM)	Sigma-Aldrich, #D6429
DMEM/F-12	Gibco, # 11554546
Roswell Park Memorial Institute (RPMI) 1640 medium	Gibco, # 21875034
Dulbecco's Phosphate-Buffered Saline (DPBS)	Gibco, #14190
β-mercaptoethanol	Sigma-Aldrich, #M-7154
Fetal Calf Serum (FCS)	Gibco, #10270-106

L-Glutamine (200mM)	Gibco, #25030081
Trypsin/EDTA	Sigma-Aldrich, #T3924
Agar-Agar	Merck, #101614
Ampicillin sodium salt	Roth, #K029.2
Chloramphenicol	Calbiochem, #220551
Sodium chloride (NaCl)	Merck, #106400
Pepton from casein	Roth, #8986
Yeast extract	AppliChem, #A1552

Cell culture media	**Ingredients**
BV-2 cell-line	RPMI 1640 medium
	5 % FCS
	1 % L-Glutamine
	195 nM β-mercaptoethanol
	1 % Penicillin/Streptomycin
RAW 264.7 cell-line	DMEM medium
	10 % FCS
	1 % Penicillin/Streptomycin
ARPE-19 cell-line	DMEM/ F-12 medium
	10 % FCS
	1 % Penicillin/Streptomycin

Lysogeny broth (LB) media	**Recipe**
LB-media	10 g/l Yeast extract
	20 g/l NaCl
	20 g/l Peptone
LB ampicillin media (LB-amp)	100 µg/ml ampicillin in LB-media
LB-amp agar plates	14 g/l agar-agar in LB-amp
LB chloramphenicol media	20 µg/ml chloramphenicol in LB-media
LB chloramphenicol agar plates	14 g/l agar-agar in LB chloramphenicol

2.1.3 Enzymes

Table 3: List of all enzymes and their corresponding buffers used in the study

Enzyme	**Manufacturer, Article number**

PfuUltra II fusion HS DNA polymerase	Agilent Technologies, 600670
10x PfuUltra II Reaction Buffer	Supplied with the enzyme
RevertAid H Minus Reverse Transcriptase	ThermoFisher Scientific, Kit #K1622
5x Reaction Buffer	ThermoFisher Scientific, Kit #K1622
Taq Polymerase (PCR)	Genaxxon, M3001
10x Reaction Buffer	Genaxxon, M3454
FastDigest KpnI	ThermoFisher Scientific, FD0524
FastDigest HindIII	ThermoFisher Scientific, FD0504
10x Fast Digest Buffer	Supplied with the enzymes
10x Fast Digest Green Buffer	Supplied with the enzymes
T4 DNA Ligase	New England Biolabs, M0202S
10x T4 DNA ligase reaction buffer	Supplied with the enzyme
Proteinase K	Merck Chemicals GmbH, 20-298

2.1.4 Antibodies

Table 4: List of all antibodies used in the study

Antibody	Manufacturer, Article number
Anti-SP1 antibody ChIP Grade	Abcam, ab13370
Anti-c-Jun antibody ChIP Grade	Abcam, ab31419
Anti-PBR antibody [EPR5384]	Abcam, ab109497
Sp3 Antibody (D-20) X	Santa Cruz Biotechnology, sc-644 X
Sp4 Antibody (V-20) X	Santa Cruz Biotechnology, sc-645 X
PU.1 Antibody (T-21) X	Santa Cruz Biotechnology, sc-352 X
c-Fos Antibody (4) X	Santa Cruz Biotechnology, sc-52 X
Stat3 Antibody (H-190) X	Santa Cruz Biotechnology, sc-7179 X
GAPDH Antibody (I-19)	Santa Cruz Biotechnology, sc-48166
Actin Antibody (I-19)	Santa Cruz Biotechnology, sc-1616
IgG-HRP (donkey anti-goat)	Santa Cruz Biotechnology, sc-2020
IgG-HRP (goat anti-rabbit)	Agilent Dako, P0448

2.1.5 Buffers and solutions

Table 5: Recipes for buffers and solutions used in this study

Buffer/Solution	Ingredients	Manufacturer, Cat. No.
1x PBS, pH 7.4	137 mM NaCl 2.7 mM Potassium chloride (KCl) 10 mM Disodium phosphate (Na_2HPO_4) 1.8 mM Monopotassium phosphate (KH_2PO_4)	Amresco, #E404 1 tablet/100 ml dH_2O
6x Loading dye	60 % v/v Glycerine 20 mM EDTA 0.25 % w/v Bromophenol blue	Roth, #3783.1 listed above Sigma-Aldrich, #B-6131
1x TBE	1 M Tris, pH 7.5 1 M Boric Acid 20 mM EDTA	Roth, #4855.3 Sigma-Aldrich, #B6768 Merck, #108421
1x TBS-T	150 mM NaCl 200 mM Tris 0.1 % v/v Tween-20	Merck, #106400 listed above Merck, #822184
Complete fixation solution	90 µl of ChIP-IT® fixation buffer 375 µl of 37% formaldehyde 785 µl of nuclease free water	Active Motif, #53038 Sigma-Aldrich, #252549
Antibody solution	5 % w/v Non-fat Milk powder in TBS-T 0.1% Tween-20 (TBS-T) in TBS-T	Roth, #T145.3 listed above
RIPA buffer	50 mM Tris-HCl pH 7.4 150 mM NaCl 1 % v/v NP-40 0.5 % w/v Sodium deoxycholate 0.1 % w/v Sodium dodecyl sulfate (SDS) 2 mM Phenylmethanesulfonylfluoride fluoride (PMSF) cOmplete™ mini protease inhibitor	listed above listed above Calbiochem, #492016 Sigma-Aldrich, #D6750 Serva, #20765.03 AppliChem, #A0999 Roche, #11836153001

Running buffer	192 mM Glycine	AppliChem, #1067
	250 mM Tris	listed above
	0.1 % w/v SDS	listed above
Transfer buffer	192 mM Glycine	listed above
	250 mM Tris	listed above
	20 % v/v Methanol	Chemsolute, #1437.2511
Stripping buffer	192 mM Glycine, pH 2.2	listed above
	0.0001 % w/v SDS	listed above
	0.01 % v/v Tween-20	listed above

2.1.6 Agarose and SDS-PAGE gels

Table 6: Recipes for agarose and SDS-PAGE gels

Gels	Ingredients	Manufacturer, Cat. No.
Agarose gel (1 & 2%)	1-2 % w/v Agarose	Biozyme, #840004
	0.5 µg/ml Ethidium bromide in TBE	Sigma-Aldrich, #46067
Running gel (15%)	15% Acrylamide v/v	Roth, #A124.1
	0.4 M Tris pH 8.8	listed above
	0.1 % w/v SDS	listed above
	0.1 % w/v Ammonium persulfate (APS)	Sigma-Aldrich, #A3678
	0.01 % v/v TEMED	Roth, #2367.1
Stacking gel	5 % v/v Acrylamide	listed above
	0.125 M Tris pH 6.8	
	0.1 % w/v SDS	
	0.1 % w/v APS	
	10µl 0.005 % v/v TEMED	

2.1.7 Kits

Table 7: Commercially available kits used in this study

Kit	Manufacturer, Cat. No.
LightCycler® 480 Probes Master	Roche Applied Science, #04707494001
NucleoSpin® Plasmid	Macherey-Nagel, #740588

NucleoBond® Xtra Midi	Macherey-Nagel, #740410.100
NucleoBond® Xtra Midi EF	Macherey-Nagel, #740420.50
NucleoSpin® RNA	Macherey-Nagel, #740955
NucleoSpin® Gel and PCR Clean-up	Macherey-Nagel, #740609
ONE-Glo™ Luciferase Assay System	Promega, #E6110
Pierce™ BCA Protein Assay Kit	ThermoFisher Scientific, #23225
Pierce™ ECL Western Blotting Substrate	ThermoFisher Scientific, #32109
SignalFire™ Elite ECL Reagent	Cell Signaling Technology, #12757
Q5® site-directed mutagenesis kit	New England Biolabs, #E0554S
Magna ChIP™ G -ChIP Kit	Merck, #17-611

2.1.8 Chemicals and reagents

Table 8: List of chemicals and reagents used in this study

Chemicals and reagents	Manufacturer, Cat. No.
2-Nitrophenyl b-D-galactopyranoside	Carbosynth, #EN06363
5X siRNA Buffer	Dharmacon, #B-002000-UB-100
Dimethylsufoxid (DMSO)	Serva, #20385.01
dNTP-Set	Genaxxon, #M3015
Ethanol	Applichem, #A3678
Ethanol 70%	Applichem, #A2192
Hydrochloric acid (HCL) 37%	Roth, #X942
Isopropanol	Merck, #100995
Laemmli sample buffer	Bio-Rad, #161-0747
Lipofectamine™ 3000 Transfection Reagent	ThermoFisher Scientific, L3000015
LPS from *E. coli* :B4	Sigma-Aldrich, #L4391
Magnesium chloride (2M solution in H_2O)	Sigma-Aldrich, #68475
MassRuler DNA Ladder	ThermoFisher Scientific, #SM0403
PageRuler™ Prestained Protein Ladder	ThermoFisher Scientific, #26616
RNase away	Molecular Biopro., #70003
Sodium carbonate	Roth, #P028.1
TransIt-LT1 Transfection reagent	Mirus, #MIR 2305
Trichostatin A	Sigma-Aldrich, #T8552
Trypan blue	Biochrom AG, #L6323

2.1.9 Devices

Table 9: List of devices used in the study

Device	Manufacturer
7900 HT Fast Real-Time PCR System	AB Applied Biosystems
Adventurer Pro balance	Ohaus®
Bacterial incubator	VWR International
BlueMarine™ 200 Electrophoresis unit	SERVA Electrophoresis GmbH
Centrifuge 5415 R	Eppendorf
Centrifuge Mini Star	VWR International
DynaMag™-2 magnet	ThermoFisher Scientific
Explorer R Ex 124 balance	Ohaus®
Galaxy 170S CO_2 incubator	Eppendorf / New Brunswick Scientific
Heraeus Labofuge 400 R	Thermo Scientific
Infinite®F200 Pro plate reader	Tecan
Intas Gel iX20 Imager	Intas
LightCycler® 480 Instrument II	Roche Applied Science
Matrix™ Multichannel Pipettes	ThermoFisher Scientific
Mini-Protean® Tetra System	Bio-Rad
MiniTrans-Blot® Cell Module	Bio-Rad
MSC-Advantage hood	Thermo Scientific
MultiImageII	Alpha Innotech
NanoDrop 2000 Spectrophotometer	Thermo Scientific
Neubauer counting chamber	OptikLabor
Orbital incubator S1500	Stuart®
PCR workstation	VWR International
peQSTAR 2x cycler	peQlab
See-saw rocker SSL4	Stuart®
Thermomixer compact	Eppendorf
TW20 watherbath	Julabo
Vibracell 75115 Sonicator	Fisher Bioblock Scientific
Vortex-genie®	Scientific IndustriesTM
VWR Electrophoresis Power Source 250V	VWR International

2.1.10 Software

Table 10: List of software used in the study

Software	Manufacturer
A plasmid Editor (ApE)	M. Wayne Davis, University of Utah
AlphaView FluorChem FC2	Cell Biosciences
CSl Adobe Creative Suite	Adobe Systems
GraphPad Prism version 6.07	GraphPad Software, Inc.
ImageJ 1.51j8	National Institutes of Health
Intas Gel Documentation 3.39 software	IntasScience Imaging
LightCycler® 480 software 1.5.1	Roche Applied Science
SDS 2.3 Applied Biosystems	SDS 2.3 Applied Biosystems
MatInspector software	Genomatix Software, Inc.
Mendeley version 1.19.2	Elsevier
Microsoft office 365 pro plus	Microsoft Corporation
Nanodrop 2000/2000c software	ThermoFisher Scientific

2.2 Methods

2.2.1 Cell culture

Cell lines used in this study included murine BV-2 microglia and Raw-264.7 macrophages and human ARPE-19 cells. Culture medium used to grow and maintain the cells is detailed in Table 1. For routine maintenance, cultures were grown in T75 flasks and maintained at 37°C in a humidified atmosphere of 5% CO_2. At 80-90% confluence, BV-2 and Raw-264.7 cells were rinsed gently with 1x PBS and detached from the flasks by gentle scraping in 5 mls of warmed fresh medium. ARPE-19 cells were grown to confluency and detached by incubation with 5 mL trypsin at 37°C, 5% CO_2 for 5 mins. Trypsin reaction was stopped by adding complete growth medium and the cell suspension transferred to a 50 ml falcon tube. Centrifugation was then done at 800 x g for 10 mins to separate the cells from the trypsin containing medium. All cells were split by a 1:5 dilution factor and appropriate volume resuspended in 10 mls of warmed medium. Cells were kept in culture until passage 20.

2.2.2 Plasmid construction

Mouse BAC clone RP23-352L10 (RPCI) (Source BioScience, Nottingham, United Kingdom; GenBank accession number 712558) was used as template in a PCR reaction to amplify a 2.812 kb Tspo promoter sequence using modified primers containing KpnI and Hind-III restriction sites in the forward and reverse primers respectively. The PCR reactions were set-up as described in table 11 and run using the temperature profile outlined in table 12

Table 11: PCR recipe to amplify Tspo promoter from mouse BAC clone

Reaction component	Amount
Template DNA	100 ng
Forward primer	1 µl (200 nM)
Reverse primer	1 µl (200 nM)
deoxynucleotide (dNTP) solution mix	1 µl (800 µM of total dNTP)
PfuUltra II fusion HS DNA polymerase	0.5 µl
PfuUltra II 10x PCR buffer	5 µl (final 1x $MgCl_2$ concentration of 2 mM)
Nuclease free dH_2O	Up to 50 µl

Table 12: PCR temperature profile

Step	Temperature	Time
Initial Denaturation	95°C	5 mins
35 cycles	95 °C	40 seconds
	50°C	44 seconds
	72 °C	80 seconds
Final Extension	72 °C	10 mins
Hold	8 °C	

The PCR reactions were carried out in triplicate, and 10 µl of each PCR reaction was mixed with 2 µl of 6x loading dye and analyzed on a 1% agarose gel. The remaining 40 µl of the PCR product from the 3 reactions was pooled together and cleaned using the NucleoSpin Gel and PCR clean-up kit. The purified PCR product

was then cut using high fidelity fast digest restriction enzymes as detailed in Table 13 below.

Table 13: Restriction digest protocol

Reaction component	Amount
Purified PCR product	30 µl (~ 1.5 µg)
10x Fast digest buffer	5 µl
KpnI	5 µl
Hind-III	5 µl
Nuclease free dH_2O	Up to 50 µl

Fifteen micrograms of the promoterless pGL4.10 firefly luciferase vector was also subjected to a double restriction digest using the same protocol outlined in Table 12. The restriction digest products were then separated on a 1 % agarose gel before being excised out with clean scalpel and purified. The digested Tspo promoter fragment was then ligated into the promoterless pGL4.10 firefly luciferase reporter vector to generate plasmid pGL4.10-2733/+79. The recipe used to set up the ligation reaction is summarized in Table 14 below.

Table 14: Ligation protocol

Reaction component	Amount
Reporter vector (pGL4.10) DNA	2 µl (~ 200 ng)
Insert (Tspo promoter sequence) DNA	14.5 µl (~ 320 ng)
T4 DNA ligase	1.5 µl
10x T4 DNA ligase reaction buffer	2 µl

The ligated plasmid was transformed into *E. coli* bacterial strain DH5-α. Single colonies of the transformed bacteria were selected and transferred to 5 mls of LB broth containing 100 µg/ml ampicillin and grown overnight at 37 °C with vigorous shaking (170 rpm). Plasmid DNA was extracted from the bacterial culture using the NucleoSpin® Plasmid kit and tested for the presence of the insert by a double-digest with restriction enzymes used earlier in the cloning steps (Table 15). Correct promoter sequences and orientation was verified by sanger sequencing using primers listed in Table 17. Plasmids pGL4.10-1915/+79, -1455/+79, -845/+79, -791/+79, -733/+79, -680/+79, -593/+79, -520/+79, -168/+79, -143/+79, -125/+79

and pGL4.10-39/+79, carrying progressive unidirectional 5′ → 3′ deletions on the promoter were then generated by PCR using plasmid pGL4.10-2733/+79 as template and primers listed in Table 16.

Table 15: Test digest protocol

Reaction component	Amount
Plasmid DNA	11 µl
10x Fast digest buffer	5 µl
KpnI	0.5 µl
Hind-III	0.5 µl
Nuclease free dH_2O	Up to 20 µl

Table 16: Primers used to generate reporter plasmids

Plasmid	Primer sequences 5' → 3' including restriction site
pGL4.10-2733/+79	FP_ ccc**GGTACC**gctgaggaaagaagaaaacaaca
pGL4.10-2733/+79	RP_ ccc**AAGCTT**ctggcctcagtttccctttt
pGL4.10-1915/+79	FP_ ccc**GGTACC**agaccagggtgatgtcgaac
pGL4.10-1455/+79	FP_ ccc**GGTACC**tggcaagagctctaggagga
pGL4.10-845/+79	FP_ cccGGTACCattggcaaggctgcagag
pGL4.10-791/+79	FP_ ccc**GGTACC**ctgctgtgctgctggttaag
pGL4.10-733/+79	FP_ ccc**GGTACC**cgcatgctcacctttacctt
pGL4.10-680/+79	FP_ ccc**GGTACC**cctgtgttaaaaccctgggtatag
pGL4.10-593/+79	FP_ ccc**GGTACC**cccagccagcctactctaat
pGL4.10-520/+79	FP_ ccc**GGTACC**gcgcctagggccttactaac
pGL4.10-168/+79	FP_ ccc**GGTACC**gcatctctcccctctgtgtc
pGL4.10-143/+79	FP_ ccc**GGTACC**cccacgatgaggagagaaaa
pGL4.10-125/+79	FP_ ccc**GGTACC**aaaagaggggtgcctggtt
pGL4.10-39/+79	FP_ cccGGTACCgcatctctcccctctgtgtc

The same reverse primer was used to construct all plasmids. GGTACC, *KpnI* restriction site, AAGCTT, *Hind-III* restriction site.

Table 17: List of sequencing primers used in this study

Name	Sequence	Region
mTspo_Seq_F1	agattttggaagctgaggaaa	-2744 to -2723

mTspo_Seq_F2	ggaggggaggactaaagaa	-2403 to -2383
mTspo_Seq_F3	gaccagggtgatgtcgaact	-1914 to -1894
mTspo_Seq_F4	ccactgagagggaagatgct	-1412 to -1392
mTspo_Seq_F5	ggcgcagagagactgaaaag	-906 to -886
mTspo_Seq_F6	gcgtgcacagaaagtactcc	-425 to -405
mTspo_Seq_R1	agagcttgccagatgtggtt	-2598 to -2578
mTspo_Seq_R2	ctgagccatttctccagctc	-2083 to -2063
mTspo_Seq_R3	ttcttgctacagcctgtggat	-1599 to -1578
mTspo_Seq_R4	gtgaaaccaagtgggaccag	-1074 to -1054
mTspo_Seq_R5	ccctcaacctcttcctgtga	-569 to -549
mTspo_Seq_R6	gacactgcgcacagaggtt	-28 to -9

2.2.3 Site directed mutagenesis

MatInspector software (http://www.genomatix.de) was used to perform sequence analysis of all potential substitution mutants to ensure that the mutated sequence did not create a known consensus DNA binding motif. Thereafter, *in-vitro* site directed mutagenesis was performed by PCR using the Q5® site-directed mutagenesis kit, a mutagenic primer and plasmid pGL4.10-845/+79 as template. Custom non-overlapping mutagenic primers were designed using the NEBaseChanger tool (https://nebasechanger.neb.com/). Non-overlapping primers are preferred over complementary primers for mutagenesis since they minimize primer-primer interactions and therefore favor the use of plasmid DNA as the template (Liu and Naismith, 2008). Two to five bp mismatches in the core-binding motif of the transcription factor binding sites (TFBSs) were incorporated in the center of the forward primer. A PCR containing 12.5 µl of the Q5 hot start high-fidelity 2x master mix, 1.25 µl (0.5 µM) of the forward and reverse primer, 1 µl (25 ng) of template DNA and 9 µl of nuclease free water in a total reaction volume of 25 µl was performed using the temperature profile outlined in the Table 18 below

Table 18: Site directed mutagenesis PCR temperature profile

Step	Temperature	Time
Initial Denaturation	98 °C	30 seconds

25 cycles	98 °C	10 seconds
	60-70 °C	30 seconds
	72 °C	2 mins, 30 seconds
Final Extension	72 °C	2 mins
Hold	8 °C	

Annealing temperature: TFBSs Sp1.4, Ets.2 and Nkx 3.1/Sp1/3/4, 60 °C, TFBSs Ap-1, Ets.1, AR/PR, 66 °C, TFBSs Sp 1.1, Sp 1.2/3, 70 °C.

The PCR products were then treated with a KLD (Kinase, Ligase and DpnI) enzyme mix in a reaction that included the following components; 1 µl of the PCR product, 5 µl of the 2x KLD reaction buffer, 1 µl of the 10x KLD enzyme mix and 3 µl of nuclease free water. The ingredients were mixed well by pipetting up and down and incubated at room temperature (RT) for 5 mins. Five microliters of the KLD mix was then used to transform NEB 5-alpha competent *E. coli* cells (provided for in the kit) by heat shock. Plasmid DNA was isolated from single colonies using the NucleoSpin® Plasmid kit and sequenced to verify the mutations. *E. coli* hosts harboring the mutated variants were grown in LB medium containing 100 µg/ml ampicillin at 37 °C with vigorous shaking (170 rpm) overnight before plasmid DNA was extracted with using NucleoBond® Xtra Midi EF (endotoxin-free) kits (Macherey & Nagel, Dueren, Germany).

2.2.4 Transient transfections, luciferase and β-Gal assays

All transfections were performed in antibiotic free medium. Cells were seeded in 12-well plates and left overnight for attachment and recovery. One hour prior to transfection, pre-warmed fresh medium was added to the cells. Transfection complexes were then prepared by mixing 0.5 µg of plasmid DNA (diluted in 5 µl of ddH_20), 3 µl of TransIT-LT1 transfection reagent (Mirus, Madison, WI, USA) and 100 µl of serum free medium. A second transfection mix containing 0.4 µg of the pSV beta-galactosidase control vector (Promega) was also prepared. The mixtures were vortexed and incubated at RT for 30 mins before being added dropwise to the cells. Where indicated, the compounds LPS and Trichostatin A (TSA) were added to cells in fresh medium 24 h post transfection and incubated for a further 6 h. LPS was added to the cells at 250 ng/ml final concentration. BV-2 and ARPE-19 cells were treated with 50 and 200 nM of TSA respectively. After

time lapse, cells were washed once with 1x phosphate-buffered saline (PBS) and lysed in 250 µl of 1x Glo lysis buffer (Promega, Madison, WI, USA). Cell lysates were then transferred to a 1.5 ml microfuge tube and centrifuged for 3 mins at 13000rpm. Luciferase activity was then determined by combining 40 µl of the lysates with 40 µl of the luciferase assay reagent (Promega) in a 96-well white flat-bottom plate (Corning) and measuring light emission. For measurement of β-galactosidase activity, 50 µl of β-galactosidase assay reagent was mixed with 50 µl of the cell lysates and incubated at RT for 30 mins. One hundred and fifty microliters of stop solution (1M Na_2CO_3) was then added to the mixture and absorbance measured at 405 nm. Tecan Infinite F200 pro reader (Tecan, Austria) was used to measure both luminescence and light absorbance.

2.2.5 Chromatin immunoprecipitation (ChIP)

Chromatin immunoprecipitation (ChIP) was performed with the Magna ChIP™ G Kit according to the manufacturer's instructions with slight modifications. BV-2 cells were propagated in T-75 flasks until they reached ~80-90% confluence. The cells were then cross-linked at RT for 10 mins in 9 mls of serum free medium and 1 ml of complete fixation solution (Table 5). Final concentration for formaldehyde in the culture medium was 1%. Quenching of unreacted formaldehyde was done with 1 ml of 10x glycine (provided in the kit) for 5 mins at RT. Thereafter, plates were washed thrice with ice cold 1X PBS supplemented with protease inhibitors (1 mM PMSF, 1 µg/ml aprotinin and 1 µg/ml pepstatin A) before being scraped and pelleted by centrifugation at 2000 x g for 5 min at 4 °C. Cell pellets from three flasks were resuspended in 0.5 mls of cell lysis buffer (provided in the kit) and incubated on ice for 15 mins with vortexing every 5 mins. The cell suspension was then centrifuged at 1000 x g for 5 mins at 4 °C and the supernatant discarded. The resulting cell pellet was resuspended in 0.5 mls nuclear lysis buffer (provided in the kit) containing protease inhibitors and kept on ice. Chromatin was sheared to an average size of 200–800 bp with a Vibracell 75115 Sonicator (Bioblock Scientific) using twelve 10 s pulses at 20% amplitude. Sheared chromatin was then transferred to fresh 1.5 mls microfuge tubes in 50 µl aliquots before 450 µl of dilution buffer (provided in the kit) containing protease inhibitors was added to each aliquot. Twenty microliters of protein G magnetic beads (provided in the kit)

was added to the diluted chromatin and immunoprecipitation performed with 2.5 µg of anti-Pu.1, 4µg of Sp3, Sp4, cFos, Stat3 (Santa Cruz Biotechnology), Sp1 and cJun (Abcam, Cambridge, UK) overnight at 4 °C with rotation. Protein G magnetic beads with the captured antibody/antigen immune complexes were separated from the immunoprecipitation fractions using a magnetic separation rack and subjected to a series of washing steps with provided buffers. Protein complexes were eluted from the magnetic beads with 100 µl of ChIP elution buffer (provided in the kit) containing proteinase K and reverse cross-linking performed by incubating in a thermoblock at 62 °C for 2 h with shaking. The immunoprecipitated DNA was purified and analyzed by PCR and qRT-PCR using primers specific for mouse Tspo proximal and distal promoter regions (Table 19). ChIP positive and negative controls included DNA precipitated with anti-RNA polymerase-II and normal mouse IgG (provided in the kit) respectively. QRT-PCR analysis of DNA immunoprecipitated with anti-RNA polymerase-II was performed using a positive control primer set that amplifies a 93 bp fragment in intron 5 of the mouse Gapdh gene (Active Motif, Carlsbad, CA, USA). For ChIP after LPS stimulation, BV-2 cells were grown in T-75 flasks until reaching ~ 80-90% confluency before being stimulated with 1 µg/ml LPS or 1 x PBS as vehicle for 1 h. Cross-linking was performed thereafter, and ChIP carried out using the same procedure described above.

Table 19: Primer sequences (5' → 3') used in ChIP experiments

	Forward Primer	Reverse Primer	Product size
Distal promoter -832 to -694 bp	cagaggtgtgctgagagatgt	ctcagatcctggtgtctgca	138 bp
Distal promoter -613 to -477 bp	cagattggtggggctccttg	actaaccgctttctgcctct	136 bp
Proximal promoter -314 to -196 bp	agaattcagccaggcacagt	cagaggtggcacatgtttgt	118 bp

2.2.6 RNA-Isolation and reverse transcription

At the end of the culture experiments, old medium was removed, and the cells washed once with 1x PBS. Cell lysis was done with 350 µl of RA1 buffer supplemented with 3.5 µl of β-mercaptoethanol before total RNA was extracted using the NucleoSpin® RNA Mini Kit according to the manufacturer's (Macherey & Nagel, Dueren, Germany) instructions. After purification, RNA was eluted from the silica-based columns with 40 µl of nuclease free water and the concentrations determined spectrophotometrically using a NanoDrop 2000 (Thermo Fisher Scientific). First strand cDNA synthesis was then performed with 1 µg of RNA in a 20 µl final volume using the RevertAid™ H Minus First strand cDNA Synthesis Kit (Thermo Fisher Scientific). The resulting cDNA was diluted with nuclease free water to a final volume of 50µl (final conc. 20ng/µl) and used as a template for real-time PCR.

2.2.7 Quantitative RT-PCR

Real-time qPCR was performed in 10 µl final reaction volume by combining the components listed in Table 20. The reaction mixtures were then run using the temperature profile outlined in Table 21.

Table 20: qRT-PCR recipe

Reaction component	Amount
cDNA	50 ng (2.5 µl)
Forward primer	1 µl (1 µM)
Reverse primer	1 µl (1 µM)
Fast Start Universal Probe Master (Rox)	5 µl (800 µM of total dNTP)
dual-labelled UPL probe	0.125 µl
Nuclease free dH_2O	0.375 µl

Table 21: qRT-PCR cycling conditions

Step	Temperature	Time
Initial Denaturation	95°C	10 mins

40 cycles	95 °C 60°C	15 seconds 60 seconds
Hold	8 °C	

ATP synthase subunit-β (ATP5B) was used as internal control. Sequences of primers used and their corresponding UPL probe numbers are outlined in Table 22. ChIP-qPCR analysis was performed in a reaction containing 1.5 µl of the immunoprecipitated DNA, 0.5 µl (500 nM) of the forward and reverse primer, 12.5 µl of the GoTaq® qPCR Master Mix (Promega, Madison, WI, USA), 0.2 µl of the carboxy-X-rhodamine (CXR) reference dye and 9.8 µl of nuclease free water. PCR cycling conditions were as follows: 2 min 95 °C hold, followed by 40 cycles of 15 s 95 °C melt and 1 min 60 °C anneal/extension. Melting curve analysis (95 °C for 15 s, and then 60 °C for 15 s until 95 °C) followed each qPCR run to verify that a single product has been amplified. All qPCR reactions were carried out in an Applied Biosystems 7900 HT Fast Real-Time PCR system (Applied Biosystems, Carlsbad, CA, USA).

Table 22: Primer sets used for qRT-PCR

Gene	Forward primer (5' → 3')	Reverse primer (5' → 3')	UPL Probe #
Sp1	atgcccctattgcaaagaca	tggatgtgacaaatgtgctgt	103
Sp3	ttgcacctgtcccaactgta	tgttgcttctttttcccaaga	77
Sp4	cagggagttccagtaacaatca	caggagctatagtagcttgttgga	58
Pu.1	ggagaagctgatggcttgg	caggcgaatctttttcttgc	94
cJun	ccagaagatggtgtggtgttt	ctgaccctctcccttgc	11
cFos	gggacagcctttcctactacc	agatctgcgcaaaagtcctg	67
Stat3	gttcctggcaccttggatt	caacgtggcatgtgactctt	71
ATP5B	ggcacaatgcaggaaagg	tcagcaggcacatagatagcc	77

2.2.8 siRNA-mediated gene silencing

All siRNAs used in the current study were ON-TARGETplus SMART pool siRNAs which combine four different siRNAs sequences per gene (Table 23) to reduce off-target effects (GE Healthcare Dharmacon, Lafayette, CO, USA). The following ON-TARGETplus SMARTpool siRNAs were used: Sp1 (L-040633-02-0005), Sp3 (L-040397-01-0005), Sp4 (L-043282-01-0005), Pu.1(Spi1) (L-041420-00-0005), cJun (L-043776-00-0005), cFos (L-041157-00-0005), Stat3 (L-040794-01-0005) and the non-targeting negative control pool (D-001810-10-05). One vial of 5 nM siRNA (in dry pellet form) was reconstituted using 250 µl of 1x siRNA buffer (diluted from a 5x stock solution with RNAse free water) to prepare 20 µM stock solutions which were stored in -20 °C until use. Transfection was carried out as described in a previous report (Rosner et al., 2010). BV-2 cells were plated at a density of 2 x 10^5 cells per well in 12-well plates and left overnight for attachment and recovery. The next day and 30 mins before transfection, cells were washed once with 0.5 mls of warmed Dulbecco's PBS (DPBS) and the medium changed to Opti-MEM I reduced serum media (900 µl per well). The siRNA/lipid complexes were then prepared by combining 5 µl of siRNA duplex (final concentration 100 nM), 3 µl of lipofectamine 3000 transfection reagent (Invitrogen) and 100 µl of Opti-MEM I medium and incubating for 20 mins at RT. The siRNA/lipid solutions were then added dropwise to each well and the cells incubated for 48 h for mRNA analysis. For ARPE-19 experiments, cells were seeded and grown until confluent before being transfected with 1 µg of the Sp1, Sp3 and Sp4 siRNA (Santa Cruz, Biotechnology) using lipofectamine 3000. For simultaneous knockdown of two genes, the amount of siRNA used per target gene was reduced by half to 50 nM and 0.5 µg for BV-2 and ARPE-19 cells respectively, thereby keeping the overall amount of siRNA per transfection constant. Twenty four hours post siRNA transfection, BV-2 and ARPE-19 cells were transfected with plasmid pGL4.10-845/+79 and incubated for an additional 24 h prior to measuring luciferase activity.

Table 23: ON-TARGETplus SMARTpool siRNA sequences

Gene	Target sequence (5′–3′)	Antisense (5′–3′)	Cat. No.
Sp1	ACGCAGGACUCGUCGGGAA	UUCCCGACGAGUCCUGCGU	J-040633-21
	GACAGUGAUUCCUGGAUUA	UAAUCCAGGAAUCACUGUC	J-040633-22

	GAUCAUACCAGGUGCAAAC	GUUUGCACCUGGUAUGAUC	J-040633-23
	GCUUAUGCUAAAUCGGUUA	UAACCGAUUUAGCAUAAGC	J-040633-24
Sp3	CCUAACACAUUUACGAGUA	UACUCGUAAAUGUGUUAGG	J-040397-09
	AAUCAAUAGUGUCGAUCUA	UAGAUCGACACUAUUGAUU	J-040397-10
	AAACUCAAGUAGUCGCUAA	UUAGCGACUACUUGAGUUU	J-040397-11
	CCGAUGGACAUUUGAUAAA	UUUAUCAAAUGUCCAUCGG	J-040397-12
Sp4	GUACAAAACCCAAGCGGUA	UACCGCUUGGGUUUUGUAC	J-043282-9
	GGAAGAAUUCUGAAACGUU	AACGUUUCAGAAUUCUUCC	J-043282-10
	AGGGAUUGCUAAUGCGACA	UGUCGCAUUAGCAAUCCCU	J-043282-11
	CUAACUGACAAUAGGGAUA	UAUCCCUAUUGUCAGUUAG	J-043282-12
Pu.1	GGAUGUGCUUCCCUUAUCA	UGAUAAGGGAAGCACAUCC	J-041420-05
	CCAUAGCGAUCACUACUGG	CCAGUAGUGAUCGCUAUGG	J-041420-06
	GUCCAAUGCAUGACUACUA	UAGUAGUCAUGCAUUGGAC	J-041420-07
	GCAAGACAGGCGAGGUGAA	UUCACCUCGCCUGUCUUGC	J-041420-08
cJun	CCAAGAACGUGACCGACGA	UCGUCGGUCACGUUCUUGG	J-043776-05
	GCAGAGAGGAAGCGCAUGA	UCAUGCGCUUCCUCUCUGC	J-043776-06
	GAAACGACCUUCUACGACG	CGUCGUAGAAGGUCGUUUC	J-043776-07
	GAACAGGUGGCACAGCUUA	UAAGCUGUGCCACCUGUUC	J-043776-08
cFos	GCGCAGAGCAUCGGCAGAA	UUCUGCCGAUGCUCUGCGC	L-041157-05
	GGAGGAGGGAGCUGACAGA	UCUGUCAGCUCCCUCCUCC	L-041157-06
	GGAUUUGACUGGAGGUCUG	CAGACCUCCAGUCAAAUCC	L-041157-07
	GCGCAGAUCUGUCCGUCUC	GAGACGGACAGAUCUGCGC	L-041157-08
Stat3	CUCAGAGGGUCUCGGAAAU	AUUUCCGAGACCCUCUGAG	J-040794-09
	CCGCCAACAAAUUAAGAAA	UUUCUUAAUUUGUUGGCGG	J-040794-10
	GAGUUGAAUUAUCAGCUUA	UAAGCUGAUAAUUCAACUC	J-040794-11
	CAGUUUACCACGAAAGUCA	UGACUUUCGUGGUAAACUG	J-040794-12

2.2.9 Western Blots

BV-2 and ARPE-19 cells were seeded in 6-well plates at a density of 4 x 10^5 cells per well. For BV-2 cells, transfection with siRNA was performed 24 h later as earlier described. After 24 h, culture media was replaced, and the cells stimulated with 1 µg/ml LPS for an additional 72 h. For ARPE-19, cells plated in the 6-well plates were allowed to grow until confluency before being transfected with 1.5 µg

of Sp1, Sp3 and Sp4 siRNA (Santa Cruz, Biotechnology) for 72 h as earlier described. After incubation with siRNA, cells were washed once with ice-cold DPBS and lysed in 150 µl of 1x cold RIPA buffer (Table 5) supplemented with protease inhibitor cocktail (Roche). Protein concentration was estimated with the Pierce™ Bicinchoninic Acid (BCA) Protein Assay Kit as per the manufacturer's instructions. Briefly, albumin protein standard (provided for in the kit at a concentration of 2 mg/ml) was serially diluted to 1.5, 1.0, 0.75, 0.5, 0.25, 0.125 and 0.025 mg/mL and the protein samples were diluted 1:20 with 1x RIPA buffer. 25 µl of each standard or unknown sample was pipetted in a 96-well plate and combined with 200 µl of working reagent (50 parts of BCA Reagent A mixed with 1 part of BCA Reagent B). The mixture was incubated at 37°C for 30 mins and after cooling to room temperature, absorbance was measured at 570 nm with a Tecan Infinite F200 pro reader (Tecan, Austria). Equal amounts of protein (~20 µg) and 8 µl of PageRuler pre-stained protein ladder (Thermo Scientific) were separated on 15% tris-glycine polyacrylamide gels at 100 V for 120 mins and then transferred onto 0.45 µm nitrocellulose membranes (Bio-Rad, Munich, Germany). The membranes were then placed in blocking solution (same as antibody solution listed in Table 5) for 1 h to prevent non-specific binding and afterwards probed with primary antibodies (Table 4) directed against TSPO (dilution 1:1000) and Actin (dilution 1:1000). Primary antibody incubations were done overnight on a rotating platform at 4 °C. The next day, the blots were washed thrice in TBS-T for 15 mins before incubation with secondary goat anti-rabbit IgG-HRP (dilution 1:4000) or rabbit anti-goat IgG-HRP (dilution 1:2500) antibodies for 1 h at RT. Membranes were developed with SignalFire™ Elite ECL reagent and protein bands visualized and imaged with the MultiImage II system (Alpha Innotech, Santa Clara, CA, USA). Band intensities were quantified using Image J software (NIH).

2.2.10 Statistical analysis

Statistical analysis was carried out with Prism Graph pad version 6.0 (GraphPad Software Inc., San Diego, CA) and a p value of < 0.05 was considered to be statistically significant. Relative changes in gene expression were calculated with the $2^{-\Delta\Delta Ct}$ method to generate relative quantification (RQ) values which were subsequently analyzed by Prism Graph pad. For ChIP experiments, data obtained

by qRT-PCR for each specific antibody was normalized by subtracting the adjusted input (Ct_{input} − Log2 (Input dilution factor)) values to obtain ΔCt values. ΔΔCt values were then calculated by subtracting the ΔCt value of negative control (IgG) from the ΔCt values of the target ChIP samples. Fold enrichment was subsequently calculated as 2 to the power of negative ΔΔCt values ($2^{-\Delta\Delta Ct}$). Student's t-test was used for two groups comparison, one-way ANOVA with Tukey's post-hoc test for multiple group comparison and two-way ANOVA with Dunnett's post-hoc test for multiple group comparisons involving two factors. The data are expressed as mean ± standard deviation (SD) unless indicated otherwise.

3.0 Results

3.1 Basal activity of the Tspo promoter in BV-2 microglia

A 2.812Kb Tspo promoter region, including 79 bp downstream of the previously mapped transcription initiation site (Giatzakis and Papadopoulos, 2004), was amplified by PCR using Mouse BAC clone RP23-352L10 (RPCI) as template. The amplified PCR fragments were directionally cloned into the promoter-less pGL4.10-Basic firefly luciferase reporter vector using KpnI and Hind-III restriction sites to generate plasmid pGL4.10–2733/+79. Sequencing was carried to confirm that the cloned constructs had the correct reading frame and were in correct orientation. Thereafter to dissect *cis*-regulatory elements that are critical for Tspo promoter activity in microglia, unidirectional 5' deletions of the promoter sequence were introduced using PCR to generate plasmids pGL4.10-1915bp, 1455bp, 845bp, 520bp, 168bp, and pGL4.10-39bp. The activity of the reporter plasmids was then investigated in the BV-2 mouse microglia cell line. To control for transfection efficiency, cells were co-transfected with pSV-β-Galactosidase control vector. As shown in figure 10A, transfection of plasmid pGL4.10–2733/+79 resulted in consistently high promoter activity in BV-2 cells on the order of 150–200 times the background measured using the promoterless plasmid. No significant differences ($p > 0.05$) in promoter activity could be detected between cells transfected with the reporter vector containing either the first 845 bp of the Tspo promoter or the full-length promoter (pGL4.10–2733/+79). These results implied that the minimal promoter required to reconstitute near maximal activity in BV-2 cells was contained in the first 845 bp upstream of the transcription start site (TSS). Additional deletions from -845 to -520 bp and from -168 to -39 bp led to a significant decrease in promoter activity, suggesting the presence of positive regulatory elements in these regions. To further localize the positive regulatory sequences in these regions, 6 additional constructs (pGL4.10-797, -733, - 680, -593, -145, and pGL4.10-125) were generated; 4 between -845 and -520bp (pGL4.10-797, 733, -680 and pGL4.10-593) and 2 between -168 and -39 (pGL4.10-145 and pGL4.10-125). Deletion of the area between -845 to -593 resulted in a significant loss of promoter activity. Notably, subsequent deletion to nucleotide −520 resulted in a striking decrease in promoter activity, suggesting

that most of the positive regulatory elements are likely localized between this region (Figure 10B). Moreover, deletion of sequences between -125 and -39 decreased promoter activity to near baseline levels, implying that additional factors necessary for eliciting basal transcriptional activity are contained in this region.

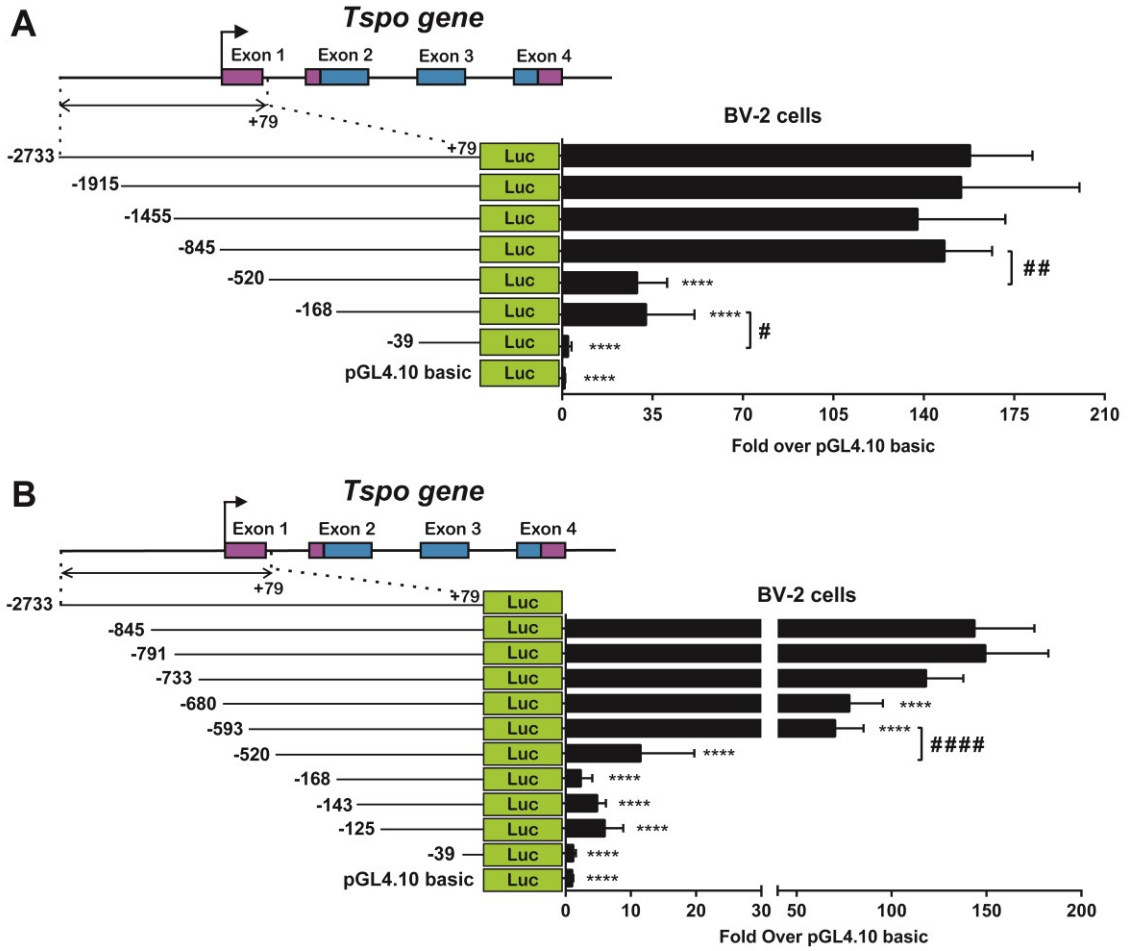

Figure 10: Functional characterization of the mouse Tspo promoter. BV-2 cells were transfected with equimolar amounts of the various 5'-deletion constructs and 24 h later they were lysed, and their luciferase activity measured. Luciferase activity is shown as fold over background obtained with pGL4.10-basic. (**A**) -845 bp upstream constitutes the minimal promoter region required to drive near maximal promoter activity in BV-2 cells. Deletion of sequences between -845 and -520 bp and between -168 and -39 bp results in a significant loss in promoter activity. $^{\#\#}p < 0.01$, $^{\#}p < 0.05$, $^{****}p < 0.0001$ vs. full (-2733/+79) promoter. (**B**) Additional reporter plasmids were constructed to localize positive regulatory elements between the -845-520 and -168-39 regions. Deletion of the -593−520 area led to a dramatic decrease in promoter activity, implying that most of the positive regulatory elements were likely localized between this region. Deletion of the -125−39 sequences abolished promoter activity. Error bars represent SD from three independent biological replicates each measured in duplicate. $^{\#\#\#\#}p < 0.0001$, $^{****}p < 0.0001$ vs. -845/+79 promoter.

3.2 LPS stimulation increases Tspo promoter activity

In our previous research, we have demonstrated that lipopolysaccharide (LPS) strongly induces Tspo mRNA and protein levels in BV-2 microglia cells (Karlstetter et al., 2014b). Therefore, the current study set out to investigate whether the LPS-induced increase in Tspo expression is transcriptionally mediated. To this end, BV-2 cells were transfected with the luciferase reporter plasmids for 24 h after which old medium was changed, and the cells stimulated with 250 ng/ml LPS for an additional 6 h. Our findings demonstrated that cells transfected with the reporter plasmid containing the full-length promoter (pGL4.10–2733/+79) exhibited up to 3-fold increase in luciferase activity upon LPS exposure when compared to the unstimulated controls. Similarly, the luciferase activity of cells transfected with reporter plasmids containing promoter sequences between -845 to -593 was significantly increased following LPS stimulation. Of note, the effect of LPS on Tspo promoter activity in the BV-2 cells was abolished when sequences between -593– 520 bp were deleted (Figure 11), suggesting that these sequences harbour *cis*-acting regulatory elements that drive Tspo expression in response to pro-inflammatory stimuli.

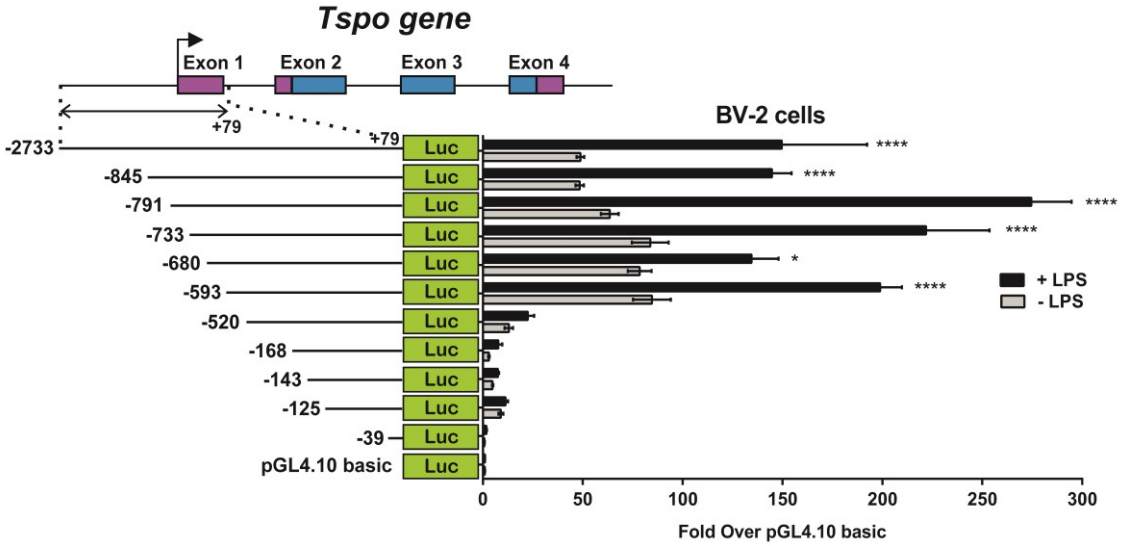

Figure 11: LPS significantly induces Tspo promoter activity. BV-2 cells were transfected with equimolar amounts of the various 5'-deletion constructs for 24 hrs, then stimulated with LPS 100ng/ml for an additional 6 hrs. Values are derived from three biological replicates measured each measured in duplicate. ****$p < 0.001$, *$p < 0.05$

3.3 Ap-1, Ets and Sp binding sites are strong positive elements regulating the expression of Tspo in BV-2 microglia

Next, to localize strong positive elements in the identified regulatory regions, *in-silico* analysis was performed using MatInspector software (http://www.genomatix.de). Bioinformatic analysis of the promoter revealed the presence of numerous putative TFBS; far too many to all have biological relevance. Therefore, comparison to previous Tspo promoter characterization studies in non-immune cells as well as screening for transcription factors implicated in the immune response was done to identify TFBS likely to be functional. Two consensus motifs for Ets (v-ets erythroblastosis virus E26 oncogene homolog) binding sites, a half consensus motif for androgen/progesterone receptors, one Ap-1 motif, one motif for Nkx3.1 which has previously been shown to serve as a non-canonical binding site for Sp1/3, and four Sp1/3/4 consensus motifs (GC boxes) located in a CpG island 125 bp upstream of the TSS (Figure 12) were identified.

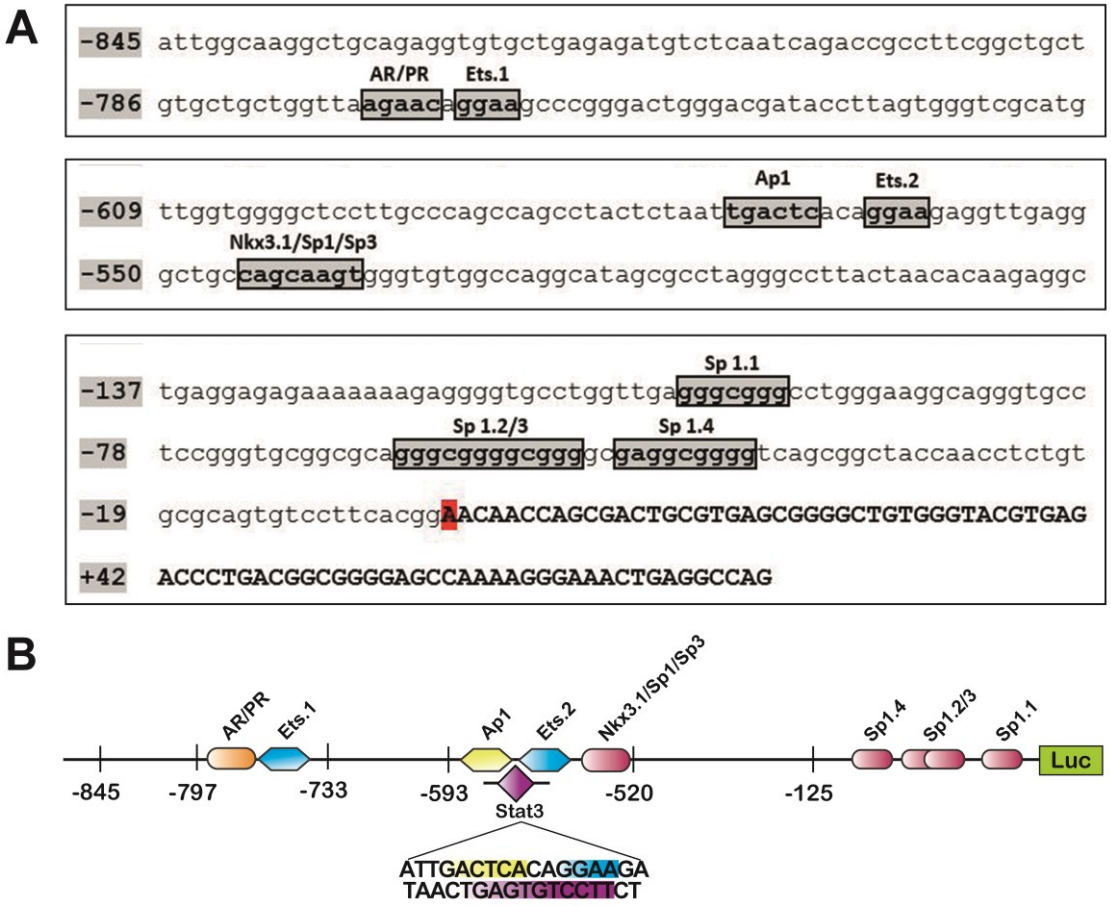

Figure 12: Regulatory DNA sequences within the Tspo promoter. (A) Part of exon 1 sequences are included and shown in capital letters and in bold. TSPO transcriptional

start site (TSS-1) is highlighted in red and the core central motifs of the putative transcription factor binding sites are highlighted with grey boxes. (**B**). Schematic representation of the minimal TSPO promoter and putative transcription factor binding sites essential for transcriptional activity in BV-2 cells.

To determine the role of these of *cis*-acting elements in the regulation of Tspo promoter activity in BV-2 microglia, we used the plasmid pGL4.10-845/+79 to construct a series of substitution mutants. For each mutant plasmid, 2-5 bp in the core biding motif of the TFBS were exchanged for mutated sequences as described earlier in the methods section (Figure 13).

Figure 13: Sanger sequencing validation of the introduced mutations

As shown in figure 14A, compared to the wild-type construct, mutation of the overlapping 2nd and 3rd Sp1/3/4 binding sites, termed as Sp1.2/3 in a previous report (Giatzakis and Papadopoulos, 2004) markedly reduced Tspo promoter

activity by around 96% (Fig. 9). Mutation of the other two GC boxes in the proximal promoter, Sp1.4 and Sp1.1, and of Ap-1, Ets.2 (2nd Ets site further downstream) and Nkx3.1/Sp1/3 site also resulted in significant loss in promoter activity compared to the wild type control. However, since site-directed mutagenesis of the Ap-1 or Ets.2 sites in the Tspo promoter alters a Stat3 binding site that occurs on the complementary strand spanning Ap-1 and Ets.2 sites in the -593-520 region (Batarseh et al., 2011), it is plausible that part of the decrease in promoter activity following Ap-1 or Ets.2 mutation might emanate from disruption of the Stat3 binding site. Furthermore, due to the close proximity of the Ap-1 and Ets.2 site (3 bp apart), we also generated a plasmid carrying mutations in both sites to investigate possible interactions. However, no synergistic effects on promoter activity were observed when both Ap-1 and Ets.2 sites were mutated (Figure 14B). Mutation of the AR/PR site in this cell line resulted in a significant increase in promoter activity. These results suggest that the GC boxes, Ap-1, Ets.2 and Nkx3.1 sites are essential for basal transcriptional activity of the -845/+79 minimal promoter in BV-2 microglia cells.

To examine whether the same transcription factor binding sites were crucial for Tspo transcriptional activity in other myeloid derived immune cells, substitution mutants were transfected into the mouse macrophage cell line, RAW 264.7. Our findings closely mirrored those obtained from BV-2 cells. Mutation of Sp1.1, Sp1.2/3, Nkx3.1/Sp1/3, Ets.2, Ap-1 but not Sp1.4 led to significant decreases ($p < 0.001$) in promoter activity when compared to the wild type control (Figure 14C). Similarly, mutation of the AR/PR site led to a slight but non-significant increase in promoter activity. These results demonstrate that Ap-1, Ets.2, Nkx3.1/Sp1/3 and Sp1/3/4 binding sites on the promoter are were important for a myeloid lineage-dependent transcriptional control of Tspo.

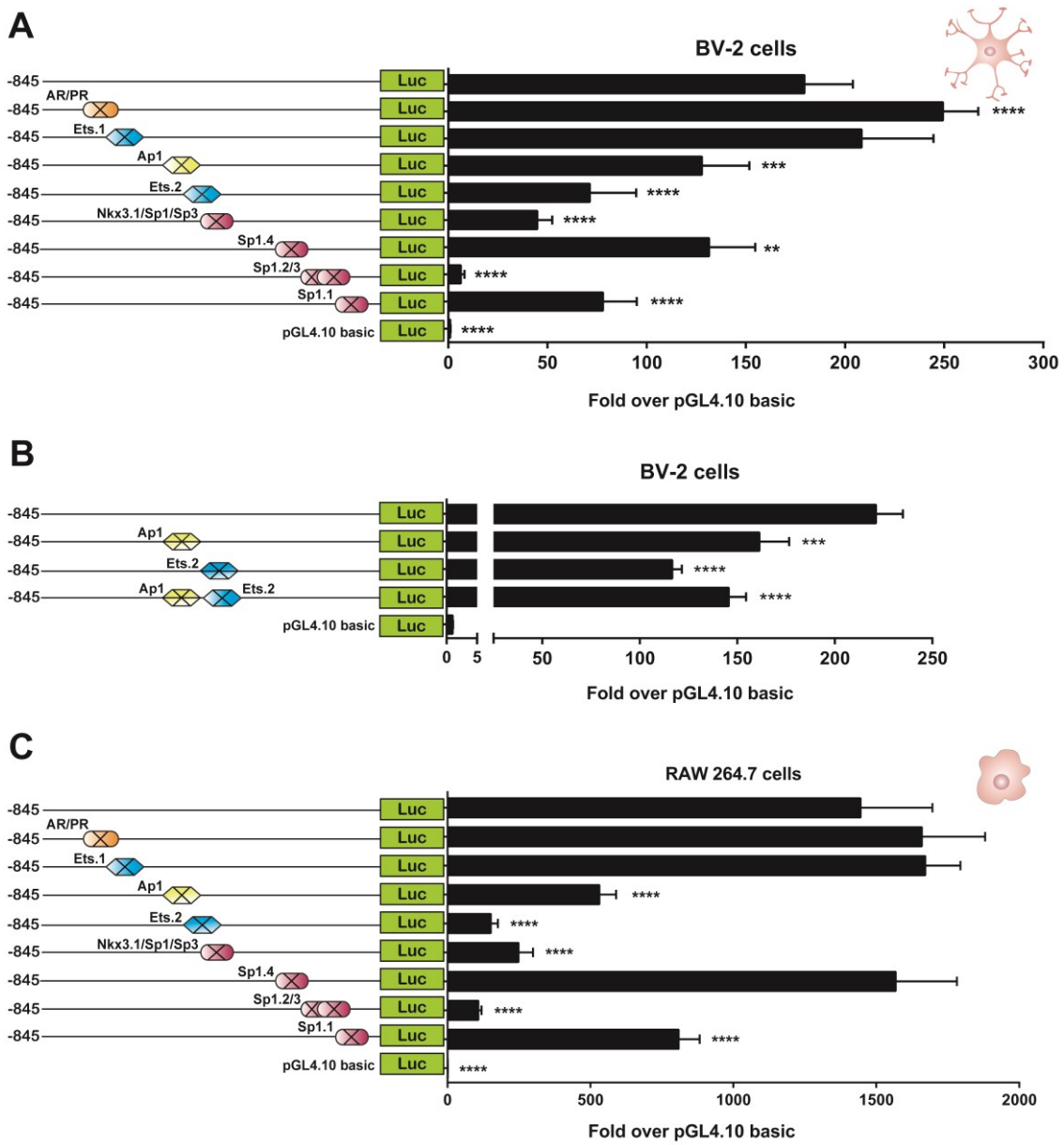

Figure 14: Ap-1, Ets.2, Nkx3.1/Sp1/3 and the conserved GC boxes in the proximal promoter are crucial for TSPO promoter activity. (**A**) A series of luciferase reporter plasmids carrying mutations in the core motifs of the potential regulatory elements within the positively identified regulatory regions were constructed using the −845/+79 plasmid as template. The wildtype and mutant reporter plasmids were then transiently transfected into BV-2 cells. After 24 h, the cells were harvested, and luciferase activity measured (**B**) Due to the proximity of the Ap-1 and Ets.2 site (3 bp apart) on the Tspo promoter, a plasmid carrying mutations in both sites was constructed. BV-2 cells were transfected with equimolar amounts of the indicated reporter constructs for 24hrs, and their luciferase activity measured. No synergistic effects on promoter activity were observed when both Ap-1 and Ets.2 sites were mutated. (**C**) RAW 264.7 macrophage cells were transfected with wildtype and the generated mutant reporter plasmids for 24 h after which the cells were harvested, and luciferase activity measured. Luciferase activity is shown as fold over background obtained with pGL4.10-basic. Error bars represent the SD from two independent biological replicates each measured in duplicate. ****p < 0.0001, ***p < 0.001 vs wild type promoter -845/+79.

3.4 Pu.1, cJun, cFos, Stat3, Sp1, Sp3 and Sp4 binds the endogenous Tspo promoter in BV-2 microglia

Based on the distinctly different Tspo expression in microglia cells in the CNS including the retina, we sought to investigate using chromatin immunoprecipitation (ChIP) whether microglia specific factors are bound to the endogenous Tspo promoter in BV-2 cells. Since Pu.1 is largely responsible for a microglia specific gene expression signature (Crotti and Ransohoff, 2016) and that mutation of an Ets consensus binding site on the Tspo promoter results in a significant loss in promoter activity, we sought to determine whether Pu.1 binds the Ets sites on the endogenous promoter in intact BV-2 cells. To this end, formaldehyde cross-linked chromatin from BV-2 microglia was immunoprecipitated with a specific antibody against Pu.1 and the immunoprecipitated DNA subjected to PCR analysis following reverse-cross linking and purification steps. Findings from both ChIP-PCR and ChIP-qPCR experiments revealed that the Ets.2 site, located in the -593-520 region, but not Ets.1 found further upstream in the Tspo promoter, is bound by Pu.1 (Figure 15). These results corroborated our initial site directed mutagenesis findings that mutation of the Ets.2 site, but not the Ets.1 site significantly reduced Tspo promoter activity in both BV-2 microglia and RAW 264.7 macrophages.

We next tested using ChIP whether Sp1, Sp3, Sp4, cJun, cFos, and Stat3 binds to their respective TFBS on the endogenous Tspo promoter in BV-2 microglia cells. Our data demonstrates that both the proximal promoter harboring sites Sp1.4, Sp1.2/3 and Sp1.1, and the Nkx3.1 site which also serves as a non-canonical site for Sp family of GC box binding proteins (Giatzakis and Papadopoulos, 2004) are highly enriched for Sp1, Sp3 and Sp4 proteins (Figure 16). Similarly, the Ap-1 and Stat3 sites were enriched for cJun, cFos, and Stat3 proteins (Figure 16).

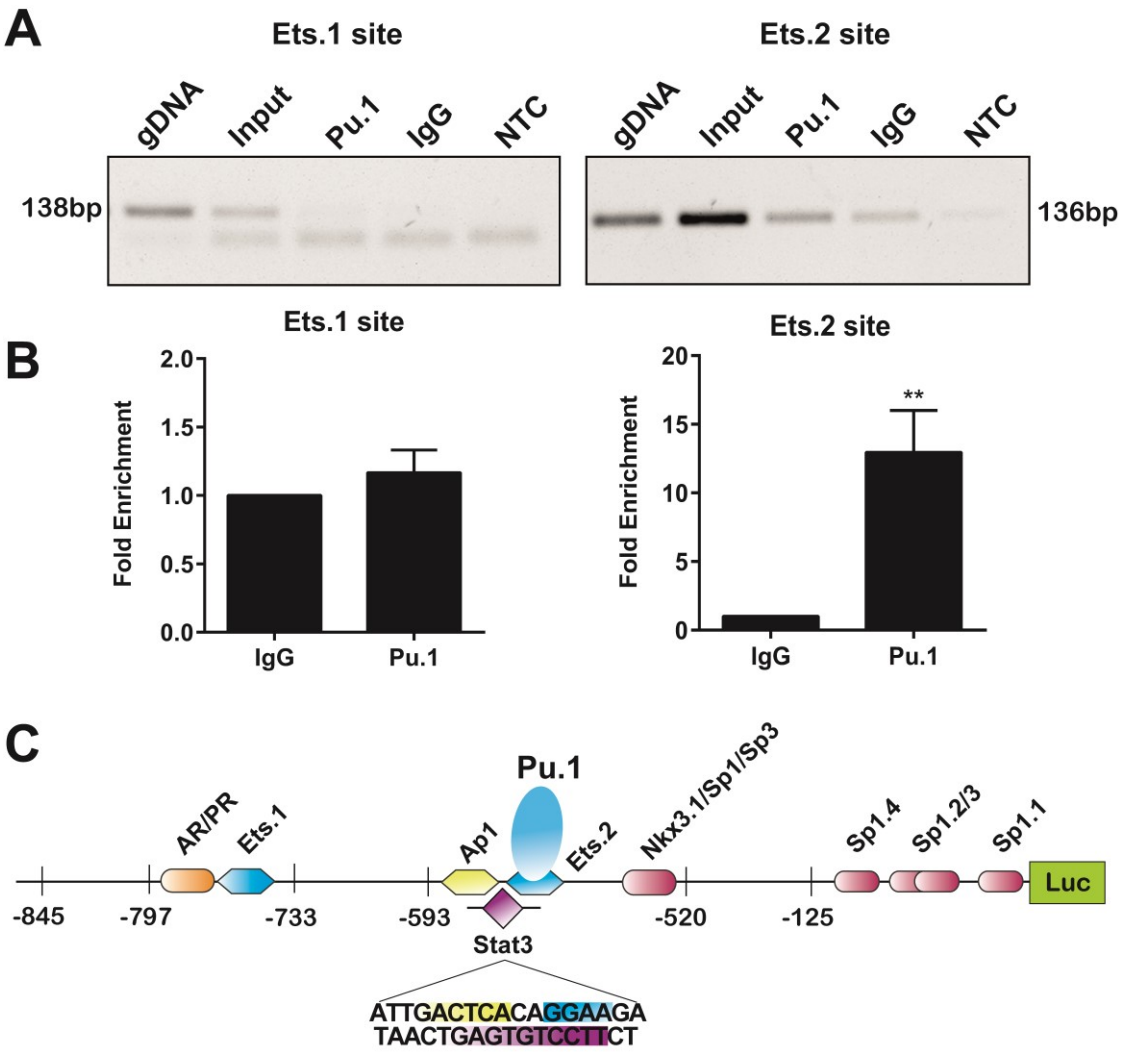

Figure 15: Pu.1 binds to the endogenous Tspo promoter in BV-2 microglia. (**A**) Crosslinked, sheared chromatin was prepared from BV-2 cells and immunoprecipitated with antibodies specific for Pu.1. Precipitated DNA was amplified by PCR with primers spanning the first (-832-694) and second Ets sites (-613 to -477) on the Tspo promoter (Table 4). Products were visualized on a 1% agarose-gel. Input represents PCR products obtained from the chromatin samples before immunoprecipitation and served, together with genomic DNA (gDNA), as a positive control. Normal rabbit IgG served as a negative control. ChIP DNA was substituted for water in the non-template control (NTC) reactions. The images shown are representative of 3 independent experiments (**B**) ChIP DNA was amplified by qRT-PCR using the same primers outlined in Table 4. Data is presented as mean ± SD of at least three biological replicates and expressed as fold-enrichment calculated as described earlier in Methods. (**C**) Schematic diagram illustrating Pu.1 occupancy in the second, but not first, Ets site on the Tspo promoter.

3.5 LPS induces Pu.1, cJun, cFos, Sp1, Sp3 and Sp4 recruitment to the Tspo promoter in BV-2 microglia

Given that LPS strongly induced Tspo promoter activity in BV-2 cells with concomitant increase in Tspo mRNA and protein levels (Karlstetter et al., 2014a),

we sought to investigate whether this induction involves the additional recruitment of transcription factors to the Tspo promoter. For this, BV-2 cells in T-75 flasks were stimulated with 1 µg/ml LPS for 1 h after which the cells were cross-linked with 1% formaldehyde and subjected to ChIP analysis as described in the methods section. ChIP-qPCR analysis of immunoprecipitated DNA demonstrated that Pu.1, cJun, cFos, Sp1, Sp3 and Sp4 occupancy at the Tspo promoter was significantly ($p < 0.05$) enhanced following LPS stimulation (Figure 16). In contrast, Stat3 binding to the Tspo promoter was not LPS inducible, implying that the enhanced binding of Ap-1 and Pu.1 to the Tspo promoter may influence Stat3 binding to this partially overlapping site (Figure 16).

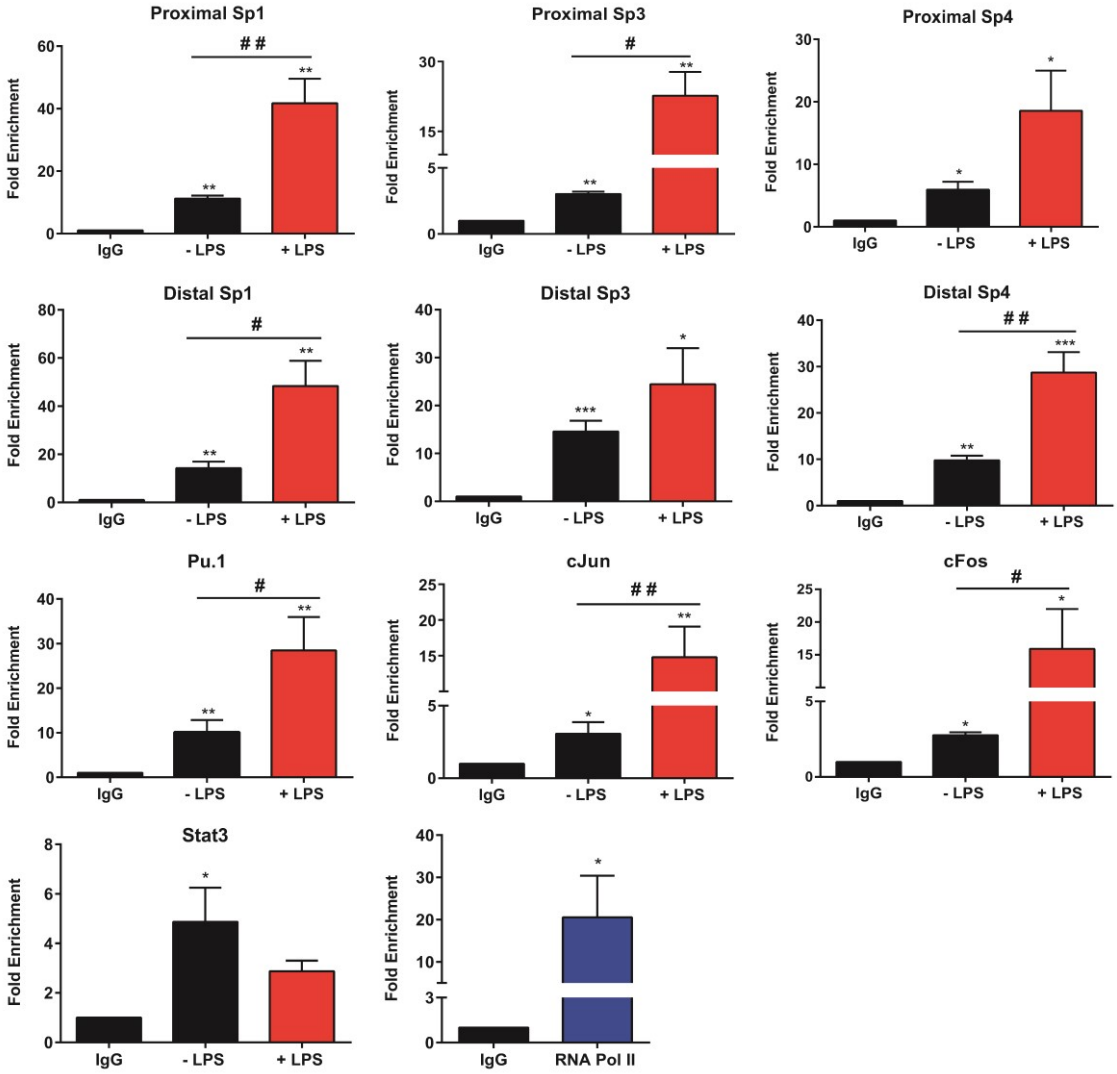

Figure 16: LPS stimulates recruitment of transcription factors Pu.1, Ap-1 (cJun/ cFos) Sp1, Sp3 and Sp4 to the endogenous Tspo promoter in BV-2 microglia. BV-2 cells were stimulated with 1 µg/ml LPS or 1x PBS for 1 h before crosslinking and chromatin shearing. Sheared chromatin was immunoprecipitated with antibodies specific

for Pu.1, cJun, cFos, Stat3, Sp1, Sp3, Sp4 and RNA polymerase-II. Precipitated DNA was amplified by qRT-PCR with primers spanning -613-477 (distal) and -314-196 (proximal) regions on the Tspo promoter (Table 4). DNA precipitated with anti-RNA polymerase-II was analyzed by qRT-PCR using a positive control primer set that amplifies a 93 bp fragment in intron 5 of the mouse Gapdh gene. Data is presented as mean ± SD of at least three biological replicates and expressed as fold-enrichment calculated as described earlier in Methods. Normal mouse IgG served as a negative control. $^{\#}p < 0.05$, $^{\#\#}p < 0.01$. $^{*}p < 0.05$, $^{**}p < 0.01$, $^{***}p < 0.001$.

3.6 Pu.1, Sp1, Sp3, Sp4, cJun, cFos and Stat3 siRNA significantly reduce Tspo promoter activity in BV-2 microglia

To determine the role of Pu.1, cJun, cFos, Stat3, Sp1, Sp3, and Sp4 in regulating Tspo promoter activity, RNAi mediated gene silencing was performed. The knockdown efficiency was verified at the mRNA level by qPCR (Figure 17A). As shown on figure 17C, down-regulation of Pu.1, cJun, cFos, Sp1, Sp3, Sp4 and Stat3 by siRNA transfection strongly diminished ($p < 0.0001$) Tspo promoter activity in BV-2 cells. No synergistic effects were observed when some of the siRNA pools were combined. These results further suggested that these transcription factors may participate in the regulation of Tspo expression in BV-2 microglia cells.

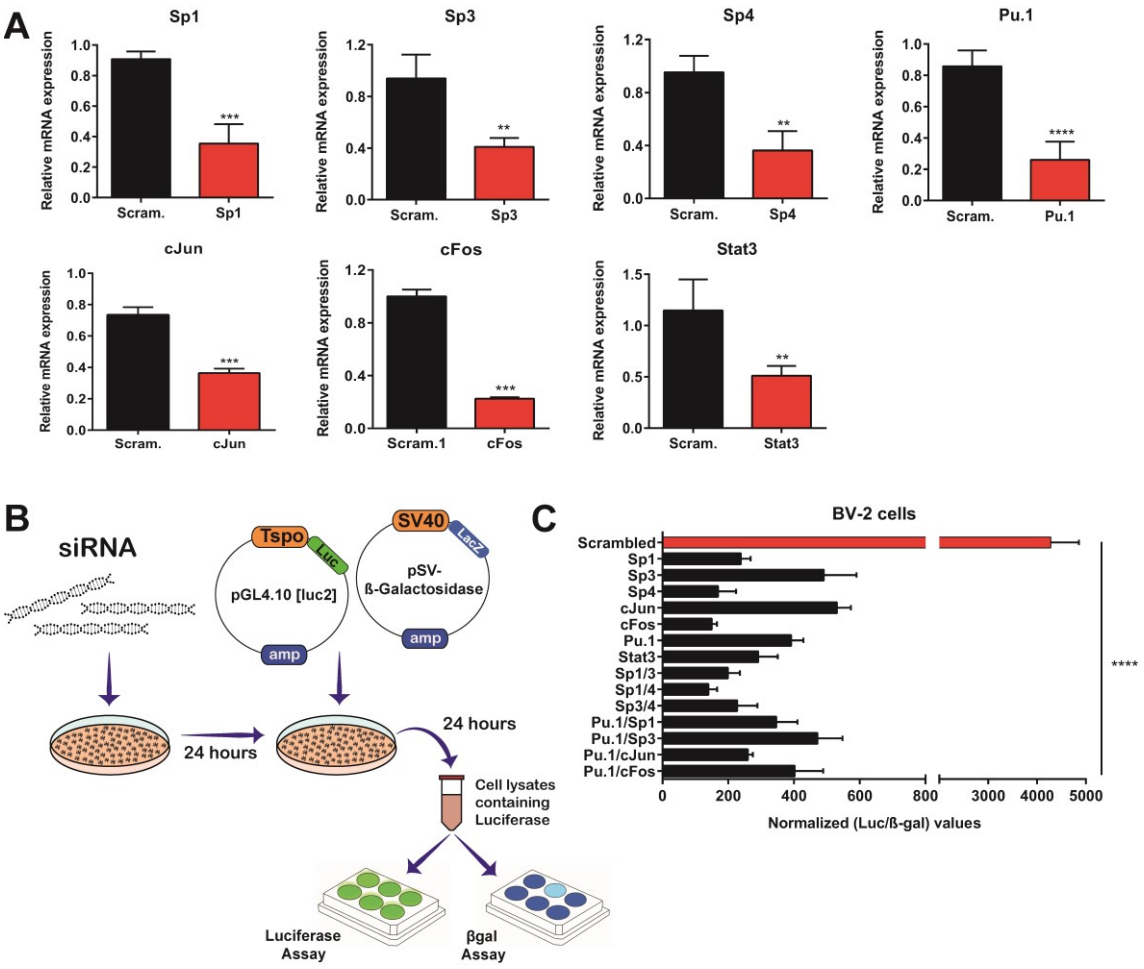

Figure 17: Pu.1, cJun, cFos, Stat3, Sp1, Sp3 and Sp4 regulate Tspo promoter activity in BV-2 microglia cells. (**A**) BV-2 cells were transfected with 100nM of the indicated siRNAs for 48 h, and levels of Pu.1, cJun, cFos, Stat3, Sp1, Sp3 and Sp4 mRNA were quantified using real time PCR. Data are derived from three independent experiments performed in duplicate and presented as mean ± SD. (**B**) Schematic representation of experimental setup (**C**) BV-2 cells were transfected with 100nM of siRNA in 12-well plates and 24 h later, transfected with the pGL4.10-845/+79 reporter construct and the pSV β-gal control vector for an additional 24 h prior to measurement of luciferase activity. Data are derived from two independent experiments performed in triplicate and presented as mean ± SEM. *p <0.05, **p <0.01, ***p <0.001, ****p <0.001

3.7 Ap-1 mediates LPS-induced increase in Tspo protein expression in BV-2 microglia

Because we observed that down-regulation of Pu.1, cJun, cFos, Stat3, Sp1, Sp3, and Sp4 significantly reduced Tspo promoter activity in BV-2 cells, we next set out to determine whether siRNA-mediated inhibition of these transcription factors could influence Tspo expression in BV-2 microglia. In this experiment, cells seeded in 6-well plates were transfected with 100nM siRNA for 72 h before harvesting in RIPA lysis buffer and analyzing Tspo expression via western blots.

Our findings revealed that under basal conditions, RNAi mediated gene silencing of these transcription factors did not alter Tspo protein expression in BV-2 cells. In contrast, a combined depletion of cJun and cFos blocked LPS induced increase in Tspo protein expression in BV-2 microglia (Figure 18), strongly suggesting that the dimeric transcription factor Ap-1 plays an instrumental role in the upregulation of Tspo in microglia during pathophysiological conditions.

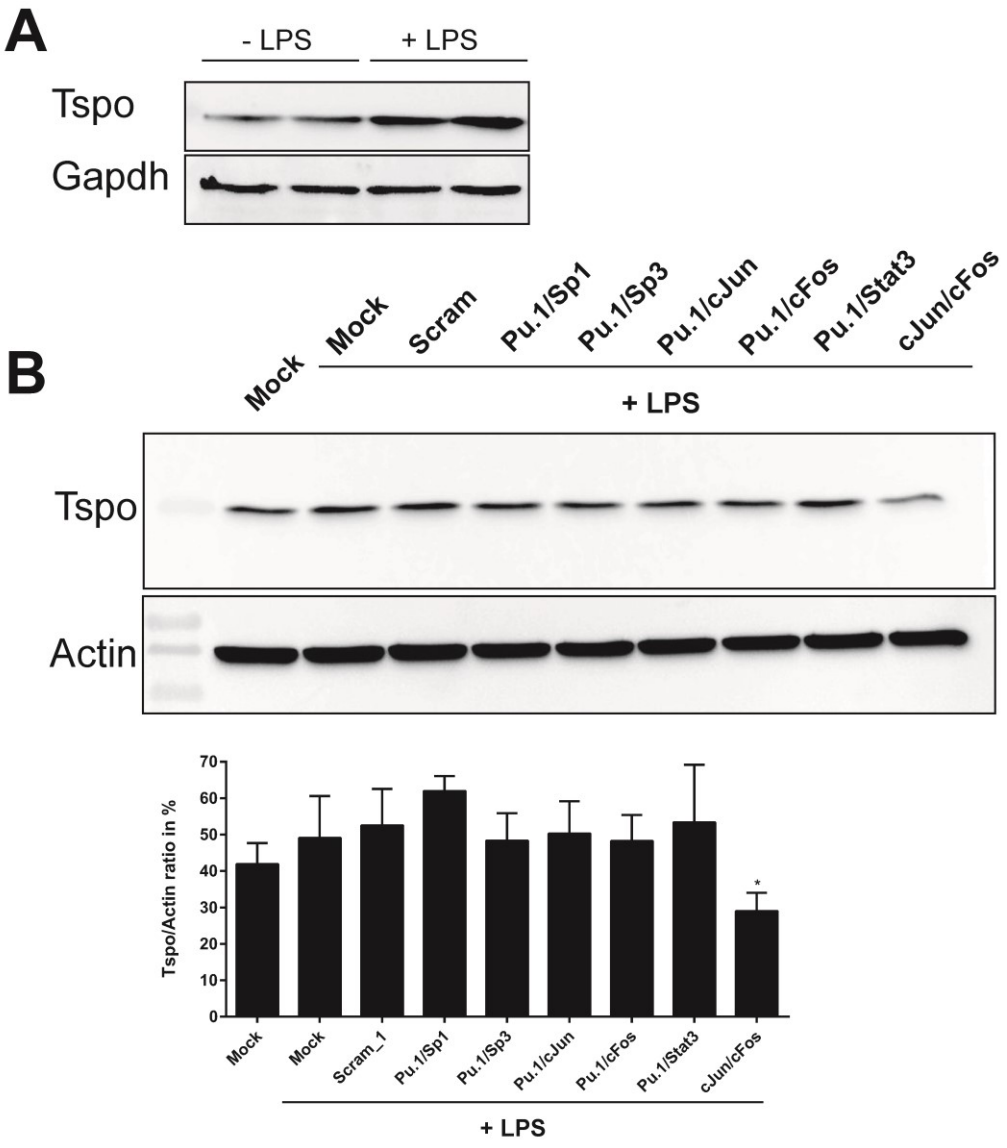

Figure 18: LPS-induced expression of Tspo in BV-2 cells is mediated by Ap-1. (**A**) Stimulation of BV-2 microglia with LPS leads to the induction of Tspo protein levels. Cells were stimulated with 1µg/ml LPS for 72 h after which they were lysed and Tspo protein levels analyzed by western blot analysis (**B**) Combined knockdown of cJun/cFos inhibits LPS induced increase in Tspo protein expression in BV-2 microglia. Cells were transfected with 100nM of siRNA pools for 24 h before change of medium and stimulation with 1µg/ml LPS for an additional 72 h. (**C**) The densitometry of each band was measured using Image J software (NIH), and values obtained from Tspo bands were normalized to

Actin. Data are derived from three independent immunoblots and presented as mean ± SD. *p <0.05.

3.8 Differential utilization of the Tspo promoter between BV-2 microglia and ARPE-19 cells

We have previously shown that unlike microglia cells which express very low levels of Tspo during homeostasis, retinal pigment epithelial (RPE) cells express constitutively high levels of Tspo in the retinal tissue (Scholz et al., 2015a). Therefore in the current study, we explored whether the differential regulation of Tspo expression in microglia and RPE cells in the retina was a direct consequence of differential promoter usage between the two cell types. To this end, ARPE-19 cells were transfected with our series of reporter plasmids carrying Tspo promoters with progressive 5'-truncations and their luciferase activity compared with that in BV-2 microglia. As shown in figure 9, the proximal promoter retained very high activity in ARPE-19 cells, with as little as 125 bp of 5'-flanking sequence required for near maximal promoter activity (Figure 19A). These findings were in stark contrast to our earlier findings in BV-2 microglia cells where 845 bp upstream of the TSS were needed for near maximal promoter activity (Figure 10A). Indeed, comparison of relative promoter activity (expressed as a percentage of the -845/+79 promoter activity) of constructs -168/+79, -143/+79, -125/+79 and -39/+79 clearly revealed that the proximal promoter was preferentially very active in ARPE-19 cells when compared to BV-2 (Figure 19B). These results indicated that the first 125 bp upstream of the TSS contained all the core promoter elements necessary to direct TSPO transcription in ARPE-19 cells.

In-silico analysis had earlier identified a series of four GC boxes in this region, two of which were overlapping (Sp1.2/3 site). Of note is that these GC-boxes are highly conserved between humans and mouse (Batarseh et al., 2012a). Therefore, we sought to determine whether these GC boxes in the proximal promoter were specifically required for TSPO promoter activity in ARPE-19. For this, cells were transfected with reporter plasmids carrying 2-3 bp substitution mutations in the core binding motif of the various GC boxes. Our results demonstrate that mutations targeting either of the GC boxes significantly reduced Tspo promoter activity in ARPE-19 cells, with the greatest loss in activity

observed in mutations targeting the overlapping GC boxes (Figure 20A). Consistent with these findings, siRNA-mediated silencing of GC box binding proteins Sp1, Sp3 and Sp4 significantly lowered Tspo promoter activity in ARPE-19 cells, with Sp1 knockdown evoking the greatest loss in promoter activity when compared to Sp3 or Sp4 (Figure 20B).

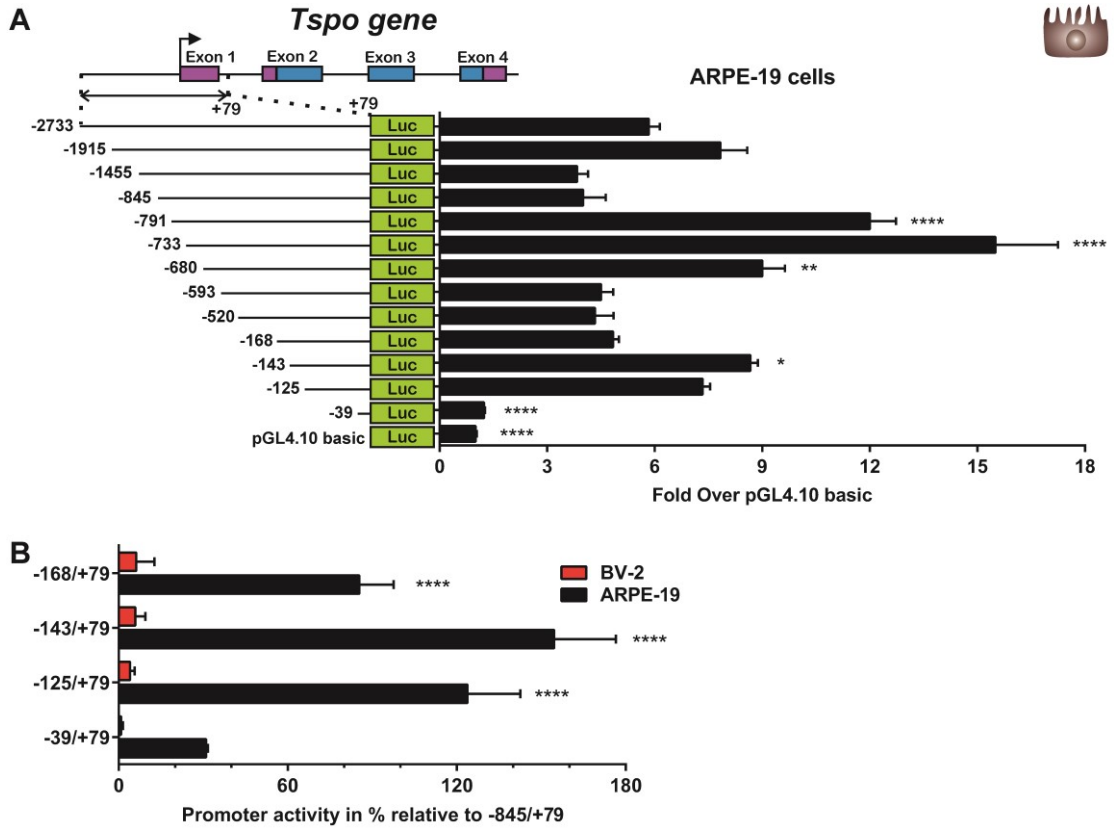

Figure 19: Functional characterization of the Tspo promoter in ARPE-19 cells. (**A**) Cells were transfected with equimolar amounts of the various 5'-deletion constructs and 24 h later they were lysed, and their luciferase activity measured. Luciferase activity is shown as fold over background obtained with pGL4.10-basic. As few as 125 bp of flanking sequence is needed to achieve near maximal promoter activity in ARPE-19 cells. $^{**}p < 0.01$, $^{****}p < 0.0001$ vs. -2733/+79 promoter. (**B**) Comparison of proximal promoter activity between ARPE-19 and BV-2 cells. Promoter activity obtained from the indicated reporter constructs was calculated as a percentage relative to the -845/+79 construct. Error bars represent SD from three independent biological replicates each measured in duplicate. $^{****}p < 0.0001$, $^{***}p < 0.001$ vs. -845/+79 promoter.

To ascertain the role of Sp1, Sp3 and Sp4 in the regulation of TSPO expression in ARPE-19 cells, siRNA mediated knockdown effects were analyzed at protein level. ARPE-19 cells seeded in 6-well plates were transfected with 1.5 µg of Sp1, Sp3 and Sp4 siRNA (either singly or in combination) and incubated for 72 h before harvesting protein and analyzing TSPO expression via western blots. Our

results revealed that individual knockdowns of Sp3 or Sp4 effectively reduced ($p = 0.0062$) TSPO protein levels when compared to the non-targeting scrambled control (Figure 20C). Sp1 knockdown also induced low to moderate decreases in TSPO protein levels, although these differences were not statistically significant. Notably, the simultaneous knockdown of either Sp1/Sp3, Sp1/Sp4 or Sp3/Sp4 resulted in a prominent reduction in TSPO protein levels, implying overlapping and/or compensatory mechanisms for Sp family of GC box-binding factors in the regulation of TSPO in ARPE-19 cells. Taken together, these results indicate that the minimal promoter region for driving TSPO expression in RPE cells is located within a 125 bp region upstream of the TSS and that the GC boxes contained in this region have to be intact for full transcriptional activity.

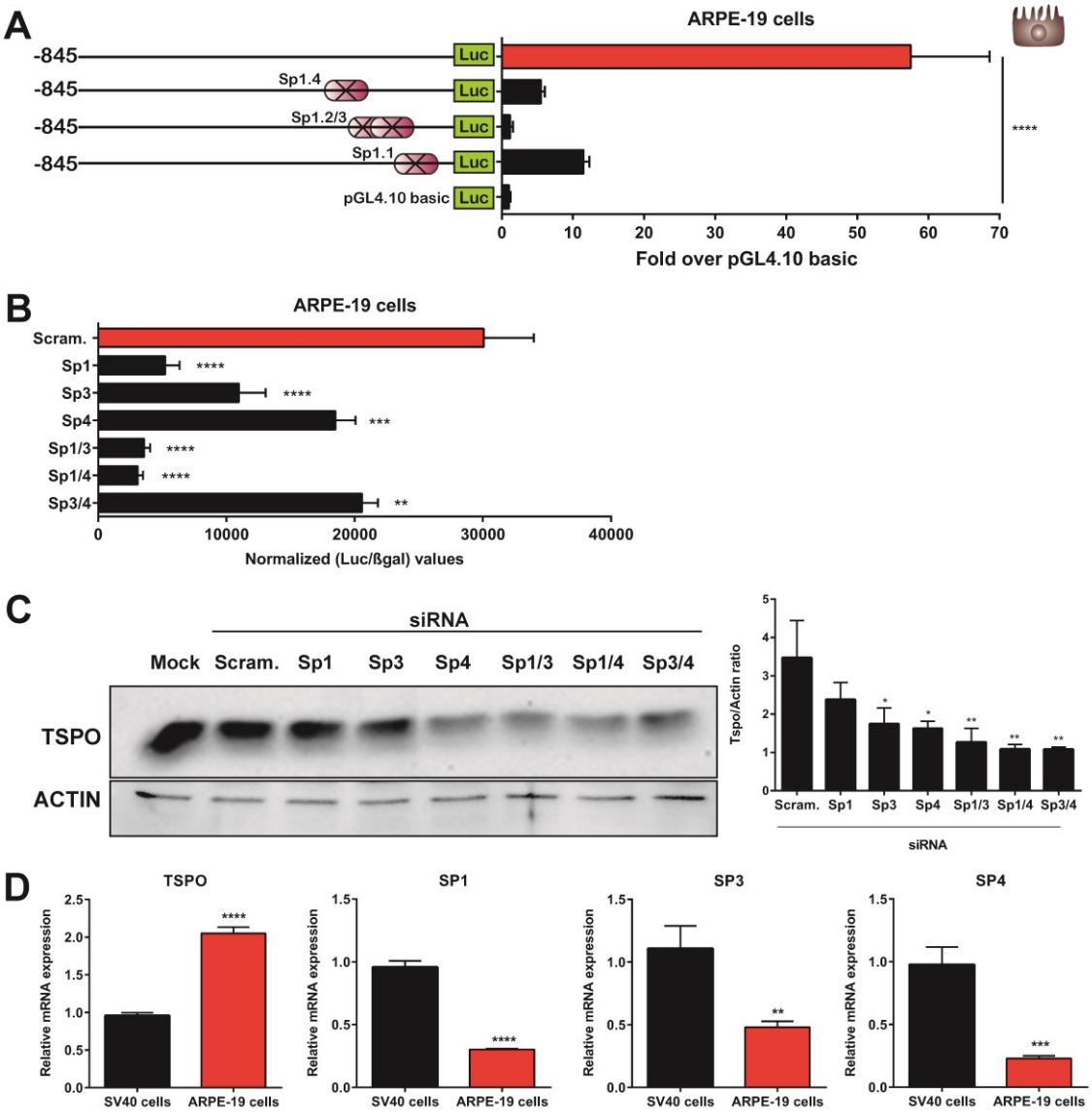

Figure 20: GC box binding proteins Sp1, Sp3 and Sp4 regulate TSPO transcriptional activity in ARPE-19 cells. (**A**) Luciferase reporter plasmids carrying mutations in the core motifs of the GC boxes located in the Tspo proximal promoter (-125 bp upstream) were constructed using the −845/+79 plasmid as template. The wildtype and mutant reporter plasmids were then transiently transfected into ARPE-19 cells and 24 h later, the cells were harvested and luciferase activity measured. Data are derived from three independent experiments performed in triplicate. ****$p < 0.001$ vs. vs wild type promoter -845/+79 **(B)** ARPE-19 cells were transfected with 1 µg of siRNA in 12-well plates and 24 h later, medium was changed, and the cells transfected with the pGL4.10-845/+79 reporter construct and the pSV β-gal control vector for an additional 24 h. Cells were lysed 24 h later and luciferase activity measured. Data are derived from three independent experiments performed in triplicate. **$p < 0.01$, ***$p < 0.001$, ****$p < 0.001$ vs. non-targeting scrambled siRNA **(C)** ARPE-19 cells were transfected with 1.5 µg of siRNA in 6-well plates for 72 h after which they were lysed and Tspo protein levels analyzed by western blot analysis. The densitometry of each band from three independent immunoblots was measured using Image J software (NIH), and values obtained from TSPO bands were normalized to Actin. Data are presented as mean ± SD. *$p < 0.05$, **$p < 0.01$ vs. non-targeting scrambled siRNA (**D**) Levels of TSPO, SP1, SP3 and SP4 mRNA in SV-40 microglia and ARPE-19 cells were quantified using real time qPCR. Data are derived from two independent experiments performed in duplicate and presented as mean ± SD. **$p < 0.01$, ***$p < 0.001$, ****$p < 0.001$.

Lastly, we investigated whether the higher strength of the proximal promoter and the enhanced expression of TSPO in RPE cells when compared to microglia could be attributed to differential levels of GC box binding Sp factors between the two cell lines. For this experiment, human SV-40 immortalized microglia cell line was used to avoid species related differences. Real time qPCR analysis revealed that contrary to our expectations, SV-40 microglia cells expressed significantly higher levels of Sp1, Sp3 or Sp4 when compared to ARPE-19 cells, indicating that the differential activity of the Tspo proximal promoter between RPE and microglia cells could not be explained by differential levels of Sp factors.

3.9 Trichostatin A (TSA) can induce Tspo promoter activity in ARPE-19 cells but not in BV-2 microglia

Previous studies have demonstrated that Trichostatin A (TSA), a histone deacetylase (HDAC) inhibitor, could induce the recruitment of Sp1 and Sp3 to promoter regions (Huang et al., 2005; Kuan et al., 2016; Schnur et al., 2007; Won et al., 2002). Therefore, to further verify the contribution of GC box binding Sp proteins in the regulation of Tspo promoter activity, BV-2 and ARPE-19 cells were transfected with the reporter plasmids for 24 h and later stimulated with 50nM

and 200nM of TSA for 6 h and 24 h respectively. Our results demonstrate that TSA can significantly boost Tspo promoter activity in ARPE-19 cells, but not in BV-2 microglia (Figure 21). Infact, TSA induced a significant loss of promoter activity in the -845/+79 deletion construct in BV-2 cells. These results were consistent with our earlier findings and suggested that BV-2 cells, unlike ARPE-19, require additional *cis*-acting regulatory elements and factors upstream for inducible Tspo promoter activity.

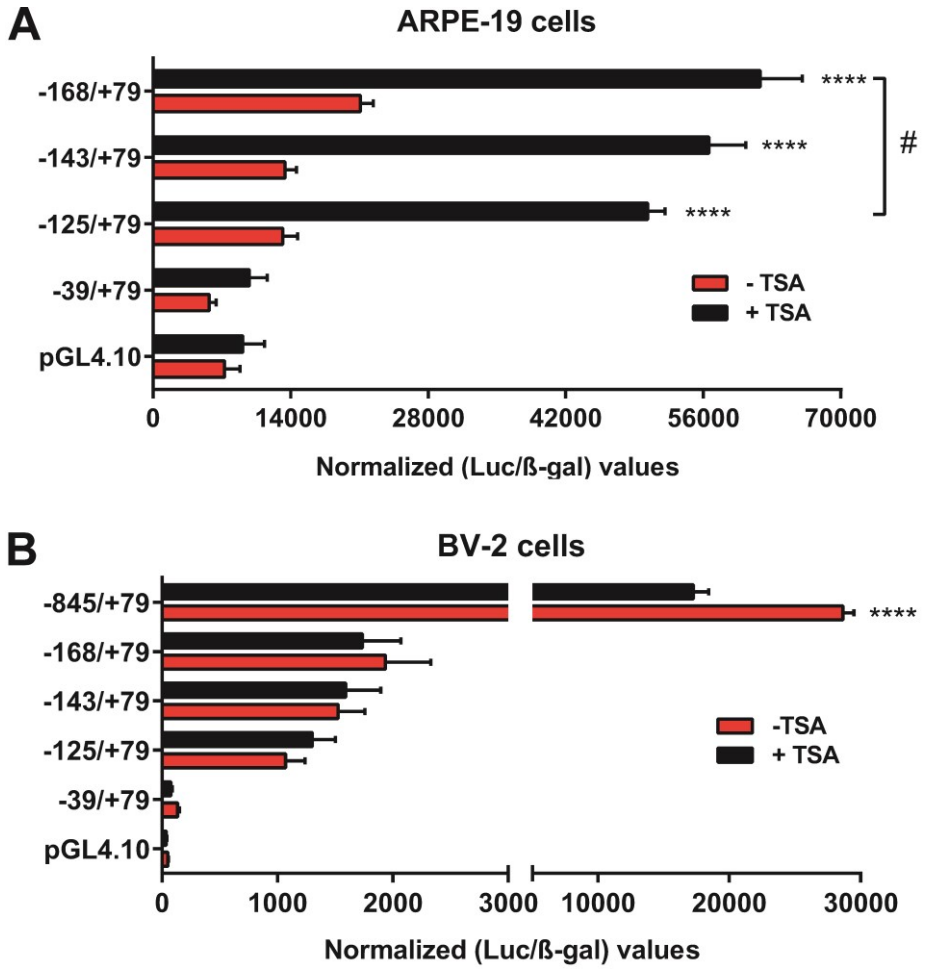

Figure 21: TSA induces TSPO promoter activity in ARPE-19 but not in BV-2 cells. ARPE-19 and BV-2 cells were transfected with equimolar amounts of the indicated deletion constructs and 24 h later, medium was changed, and the cells treated with 200nM and 50nM of the histone deacetylase inhibitor Trichostatin A for 24 h and 6 h respectively. Cells were later lysed and their luciferase activity measured. Data are derived from three independent experiments performed in triplicate and presented as mean ± SEM. $^{\#}p$ <0.05, $^{****}p$ <0.001.

4.0 Discussion

Since its initial discovery in 1977 as a secondary binding site for benzodiazepine anxiolytic drugs (Braestrup et al., 1977), multiple studies, including our own, have demonstrated that the Translocator protein (18kDa; TSPO) is a reliable biomarker of inflammation in the CNS including the retina (Daugherty et al., 2013; Karlstetter et al., 2014b; Scholz et al., 2015b; Wang et al., 2014). TSPO expression is strongly induced in numerous neuropathological conditions including Alzheimer's, Parkinson's, Multiple sclerosis, HIV encephalitis as well as neurodegenerative diseases of the retina (Cosenza-Nashat et al., 2009; Daugherty et al., 2013; Karlstetter et al., 2015; Yasuno et al., 2008). Immunohistochemistry studies show that increased TSPO expression during CNS pathology is concentrated in reactive microglia/infiltrating macrophages, while increased expression of diazepine binding inhibitor protein (DBI), an endogenous TSPO ligand, is concentrated in macroglia cells (Müller cells and astrocytes (Christian and Huguenard, 2013; Karlstetter et al., 2014b; Wang et al., 2014). Importantly, we and others have shown that the interaction between TSPO and its endogenous or synthetic ligands limits the magnitude of microglia mediated inflammatory responses with concomitant neuroprotection (Scholz et al., 2015b; Wang et al., 2014). However, despite its importance as a biomarker and as an attractive therapeutic target for immunomodulation of microglia, studies focused on understanding the underlying molecular mechanisms of TSPO gene regulation in immune cells remain largely non-existent. Research carried out so far aimed at understanding TSPO's transcriptional regulation has been conducted using steroidogenic and non-steroidogenic cell lines (Batarseh et al., 2011, 2012a; Giatzakis and Papadopoulos, 2004). As such, findings from these studies have mostly attributed TSPO regulation to ubiquitous transcription factors such as Sp1, Sp3 and GABP which by themselves cannot confer microglia specific expression (Christoforos et al., 2008; Giatzakis and Papadopoulos, 2004). To address this, we have performed an extensive functional analysis of the Tspo promoter in BV-2 cells in an attempt to identify important *cis*-regulatory elements and trans-acting factors required for both basal and inducible Tspo expression in microglia cells.

In the current study, the full length Tspo promoter was cloned into the pGL4.10-Basic reporter vector upstream of the luciferase gene. Then, to identify the minimal promoter, a series of 5'-unidirectional truncation mutants were generated by PCR and transfected into BV-2 murine microglia cells. These cells were previously generated by infecting primary microglial cell cultures with a raf/myc oncogene carrying retrovirus, and represents the most extensively used cell line in microglial research (Blasi et al., 1990; Henn, 2009). Transfection of BV-2 cells with the reporter vector containing the full-length promoter resulted in consistently high luciferase activity, in the order of 150–200 times the background measured using the promoterless plasmid. Deletion of promoter sequences between -2733 (full promoter) and −845 resulted in no significant difference in promoter activity, implying that approximately 845 bases upstream of the transcription start site were enough to activate near maximal Tspo transcription in microglia. Thus, for the remainder of the study, we analyzed the regulatory mechanisms acting on the −845/+79 construct. Deletion of only 73 bp from the −593/+79 construct resulted in a striking decrease in basal promoter activity to levels close to background, implying that strong positive *cis*-regulatory elements are likely localized in this region. Interestingly, deletion of the same region (-593 to -520) led to a significant loss in LPS induced promoter activity, suggesting that this region also harbours *cis*-acting regulatory elements that drive induced Tspo expression in response to LPS stimulation. Computer based analysis (MatInspector) of these promoter sequences revealed the existence of one Ap-1, Ets and Nkx3.1 site previously shown to bind Sp1/Sp3 factors in murine MA-10 Leydig cells and NIH-3T3 fibroblasts (Giatzakis and Papadopoulos, 2004). Notably, Tspo promoter activity decreased significantly upon targeted point mutations of these TFBSs, indicating that these consensus binding motifs must be intact for full basal promoter activity in BV-2 microglia cells. Similar results were obtained when RAW 264.7 murine macrophage cells were transfected with wild-type or Ap-1, Ets.2 or Nkx3.1/Sp1/3/4 mutant reporter constructs, implying that the same TFBS's are required for Tspo promoter activity in other myeloid derived cells. Simultaneous mutagenesis of Ap-1 and Ets.2 core motifs, which lie 3 bp apart, had no additive effect, implying that only one of the two sites may be utilized at any time, at least during basal conditions.

Microglia cells display distinct expression of TSPO when compared to other CNS cell types (Guilarte et al., 2016; Karlstetter et al., 2014b; Rupprecht et al., 2010). In the normal CNS milieu, quiescent microglia express very low levels of TSPO as opposed to reactive microglia in the diseased CNS which express strikingly elevated levels (Karlstetter et al., 2014b; Scholz et al., 2015b). In the current study, we demonstrate that the induction of Tspo by reactive microglia during pathophysiological conditions is mediated at the transcriptional level. Furthermore, congruent with the distinct Tspo expression pattern in microglia, we demonstrate for the first time that the essential myeloid lineage determining transcription factor PU box binding-1 (Pu.1) binds to a distal regulatory region (-593 to -520) of the Tspo promoter. Pu.1 is a member of the Ets family of transcription factors, and its deficiency in animals leads to a complete lack of B cells, monocytes and tissue macrophages including Kupffer cells and microglia (Crotti and Ransohoff, 2016). Pu.1 binds to purine rich sequences containing a 5'-GGAA/T-3' core and induces a myeloid-specific gene expression signature (Nerlov and Graf, 1998; Weigelt et al., 2007, 2009). It is therefore conceivable that Pu.1 binding to the promoter might partly explain the Tspo specific expression pattern observed in microglia and other myeloid lineage cells during pathophysiological conditions (Rashid et al., 2018a).

Similarly, the current study provides evidence that Ap-1 (cJun/cFos), Stat3, Sp1, Sp3 and Sp4 are bound to their respective *cis*-elements in the distal regulatory region (-593 to -520) of the Tspo promoter. In addition, stimulation of BV-2 cells with LPS led to an additional recruitment of the aforementioned transcription factors, including Pu.1 (excluding Stat3) to the Tspo promoter. Of note, previous studies have demonstrated that these transcription factors are activated in response to inflammatory stimuli resulting in the transcription of specific subsets of proinflammatory genes (Boutillier et al., 2007; Brightbill et al., 2000; Carver et al., 2013; Liu et al., 2015; Lodie et al., 1997). Interestingly, the transcription of such inflammatory response genes is regulated by a proximal promoter and, for most or all genes, one or more distant regulatory regions (Smale, 2010; Smale and Natoli, 2014). These distant promoter sequences are bound by multiple transcription factors in response to diverse inflammatory stimuli, and this process is critical for the selective activation of these genes (Smale, 2010; Smale and

Natoli, 2014). Take the human IFNβ gene for instance, an inflammatory response gene whose regulatory region consists of a short 55 bp DNA sequence (Thanos and Maniatis, 1995). Inflammatory stimuli such as a virus infection induces the recruitment and binding of a multitude of inducible transcription factors including NF-kB, IRF3, IRF7, ATF-2 and c-Jun to activate transcription (Smale, 2010; Thanos and Maniatis, 1995). Therefore, based on the findings of the current study that LPS-induced transcription of Tspo is strongly dependent upon a distal regulatory region and the recruitment of multiple inflammation responsive transcription factors, it is reasonable to speculate, at least in immune cells, that the underlying physiological function of Tspo may involve the subtle and complex mediation of the inflammatory response (Rashid et al., 2018a).

However, despite observations in the current study that LPS stimulation induced the recruitment of Pu.1, Ap-1 and Sp family of GC-box binding transcription factors to the Tspo promoter, their precise role in mediating LPS-induced expression of Tspo remains largely elusive. Nonetheless, we show herein that the dimeric transcription factor Ap-1 (cJun/cFos) is essential for the upregulation of Tspo expression in BV-2 microglia following LPS stimulation. Consistently, previous research has also demonstrated that siRNA-mediated gene silencing of the Ap-1 subunit, cJun, is sufficient to significantly reduce Tspo levels in MA-10 leydig and NIH-3T3 mouse fibroblasts cells (Batarseh et al., 2011). However, in the current study, single knockdown of either cJun or cFos did not inhibit basal nor LPS-induced Tspo expression in microglia. Our results also provide no insights into the mechanisms of Ap-1-mediated induction of Tspo expression in LPS-stimulated BV-2 cells. However, it is noteworthy that Ap-1 has previously been shown to play a fundamental role in the maintenance of chromatin “accessibility”, and by extension, the recruitment of inducible transcription factors to the chromatin (Biddie et al., 2011). Therefore, whether Ap-1 plays a similar role in the regulation of inducible Tspo expression in microglia by binding to its specific *cis*-element within the distal regulatory region and maintaining an open chromatin configuration for the recruitment of Pu.1 and Sp factors remains to be determined. Notwithstanding this uncertainty, findings from the current study showing that deletion or substitution mutation of the Ap-1-site in the distal promoter significantly inhibited basal and LPS induced Tspo promoter activity further

highlights the importance of Ap-1 in the regulation of Tspo in microglia (Rashid et al., 2018b).

The TSPO proximal promoter, spanning approximately 150 bp upstream of the TSS, is situated in a CpG island and is very well conserved among humans, rats and mice (Batarseh and Papadopoulos, 2010). Sequence comparison of mouse and rat proximal promoters reveals up to 90% homology while that of mouse and human reveals approximately 70% homology (Batarseh and Papadopoulos, 2010). Findings from the current study indicated that this proximal promoter retains very low basal activity in BV-2 microglia cells, in contrast to ARPE-19 cells where it was highly active and accounted for most of the promoter activity observed in this cell line. Previous studies have demonstrated that in MA-10 leydig and Y1 adrenocortical cells which display high constitutive Tspo expression similar to ARPE-19 cells, this region constitutes the minimal promoter and contains all sequence components necessary for Tspo transcription initiation (Giatzakis and Papadopoulos, 2004). Bioinformatic analyses of the Tspo proximal promoter revealed the presence of four GC boxes, corroborating a previous report (Giatzakis and Papadopoulos, 2004). To analyze the importance of these GC boxes in regulating Tspo expression in ARPE-19 and BV-2 cells, we used siRNA to selectively down-regulate the expression of GC box binding factors Sp1, Sp3 or Sp4 either singly or in combination. Consistent with our prior findings showing high activity of the proximal promoter in ARPE-19 cells, individual knockdown of Sp3 or Sp4 and double knockdowns of Sp1/Sp3, Sp1/Sp4 or Sp3/Sp4 significantly reduced TSPO protein expression in ARPE-19 cells but not in BV-2 microglia. To verify that the GC box binding Sp factors were important in cell-line specific activation of Tspo transcription, the effect of the histone deacetylase inhibitor, TSA, on Tspo promoter activity in BV-2 and ARPE-19 cells was assessed. TSA has been shown in previous studies to augment promoter activity by enhancing the recruitment of Sp1 and Sp3 to GC boxes (Schnur et al., 2007). Moreover, treatment of MDA-MB-231 cells with TSA has been shown to strongly induce TSPO promoter activity via GC-rich elements within the proximal promoter, with the overexpression of Sp1 and Sp3 potentiating TSA effects (Batarseh et al., 2012b). In the current study, we demonstrate that TSA treatment strongly activates the Tspo promoter in ARPE-

19 cells but not in BV-2 microglia cells. Altogether, these results indicate that the proximal promoter harboring a series of GC boxes as binding sites for Sp factors is sufficient for the effective activation of TSPO transcription in RPE cells, but not in microglia where additional distal elements and factors are required to activate transcription. Furthermore, these findings indicate that distinct regions of the promoter direct constitutive and inducible transcription of Tspo. Indeed, 805 bp upstream of the TSS are required for near maximal promoter activity in NIH-3T3 cells whose Tspo expression can be induced by phorbol-12-myristate 13-acetate (PMA), in contrast to 123 bp required for most promoter activity in MA-10 cells which display high constitutive levels of Tspo that is non-responsive to PMA stimulation (Batarseh et al., 2008; Giatzakis and Papadopoulos, 2004).

Despite the weak activity of the proximal promoter in BV-2 microglia cells, deletion of sequences between -168 to -39 led to a significant loss in promoter activity to levels slightly above background measured using the promoterless plasmid. Likewise, mutagenesis of the GC boxes located in the proximal promoter or siRNA-mediated knockdown of Sp factors resulted in significant decreases in promoter activity in BV-2 and RAW 264.7 cells. Mutations within the overlapping GC boxes caused the greatest decrease in promoter activity (90-95%) in both cell lines. Given that the TSPO promoter, similar to housekeeping genes, lacks TATA and CCAAT boxes, the observation that disruption of proximal GC boxes significantly diminished promoter activity was to be expected (Azizkhan et al., 1993). Previous research has demonstrated that GC boxes and Sp factors are critical for the initiation of transcription in promoters that lack TATA and CCAAT motifs (Azizkhan et al., 1993). Consistently, our findings from ChIP analyses confirmed that the GC boxes in the proximal promoter are bound by Sp1, Sp3, and Sp4, and that additional recruitment of these transcription factors to the promoter occurs as part of a series of events that facilitate the inducible expression of Tspo in microglia in response to inflammatory stimuli such as LPS (Rashid et al., 2018b).

5.0 Conclusion and future perspectives

In summary, findings of the current study show that a 845 bp fragment upstream of the transcription initiation site constitutes the minimal Tspo promoter sufficient to drive full transcriptional activity in BV-2 microglia cells. The present findings further indicate that a complex interplay between proximal and distal promoter elements within the 845 bp fragment exists to regulate Tspo expression in BV-2 microglia (Figure 22). Additionally, results presented herein reveal the presence of a strong positive distal regulatory region, spanning from -593 to -520 relative to the TSS, that is bound by Ap-1(cJun/cFos), Pu.1, Stat3 and Sp factors and whose deletion abolishes basal as well as LPS induced promoter activity. Moreover, the current results indicate that LPS-induced Tspo expression in BV-2 cells is mediated, at least in part, at the transcriptional level via the additional recruitment of Pu.1, Ap-1 (cJun/cFos), Sp1, Sp3 and Sp4 factors to the distal and proximal regulatory sequences. Notably, we show that the dimeric transcription factor Ap-1 (cJun/cFos) is indispensable for LPS-induced Tspo expression in BV-2 microglia cells. Consistent with the presence of important distal elements, we demonstrate that the proximal region extending -125 bp upstream of the TSS which contains four GC-boxes is necessary but insufficient to support basal or LPS-induced Tspo promoter activity in BV-2 cells. In contrast, the sequence elements contained in the proximal promoter are sufficient to drive full promoter activity in ARPE-19 cells. Taken together, these findings provide new insights into the molecular mechanisms responsible for Tspo regulation in BV-2 microglia during basal as well as LPS-induced inflammatory conditions. In addition, findings presented herein suggest that important distal elements may account for the cell-specific differences in Tspo expression patterns between BV-2 microglia and ARPE-19 cells.

However, while the current findings are extensive and serve as a good starting point for the identification of signaling pathways via which TSPO is overexpressed, they only partially explain how Tspo regulation is achieved in microglia and leave a lot of open questions to be addressed in the future. Examples of these questions include; i) How do the identified transcription factors interact with chromatin structure and enhancer landscapes to selectively regulate Tspo expression in microglia? ii) Is the promoter region -593 to -520, shown herein to be bound by lineage and signal dependent transcription factors, a functional enhancer that can activate Tspo transcription

independent of orientation and position relative to the TSS? iii) Are there other distant enhancers that are involved in the transcriptional activation of TSPO in microglia in response to noxious stimuli in the CNS? To what extent are these findings translatable to murine microglia in-vivo or to human microglia?

New genetic tools and techniques can be used to address some of these questions. For instance, the CRISPR/Cas9 system can be used to generate mice with defined point mutations in the genome and subsequently examine the relevance of the in-vitro findings presented herein. New genome-wide approaches such as Hi-C could also be used to unravel the complex enhancer(s)-promoter interactions that are responsible for coordinating changes in TSPO transcription in microglia in response to inflammatory stimuli. High-throughput technologies such as Chromatin immunoprecipitation sequencing (ChIP-seq) can be adopted to identify more distant regulatory elements. Consequently, deciphering the mechanisms involved in TSPO regulation in microglia is likely to yield information about the protein's function which currently remains unknown as well as aid current efforts to selectively target TSPO for immunotherapeutic benefit.

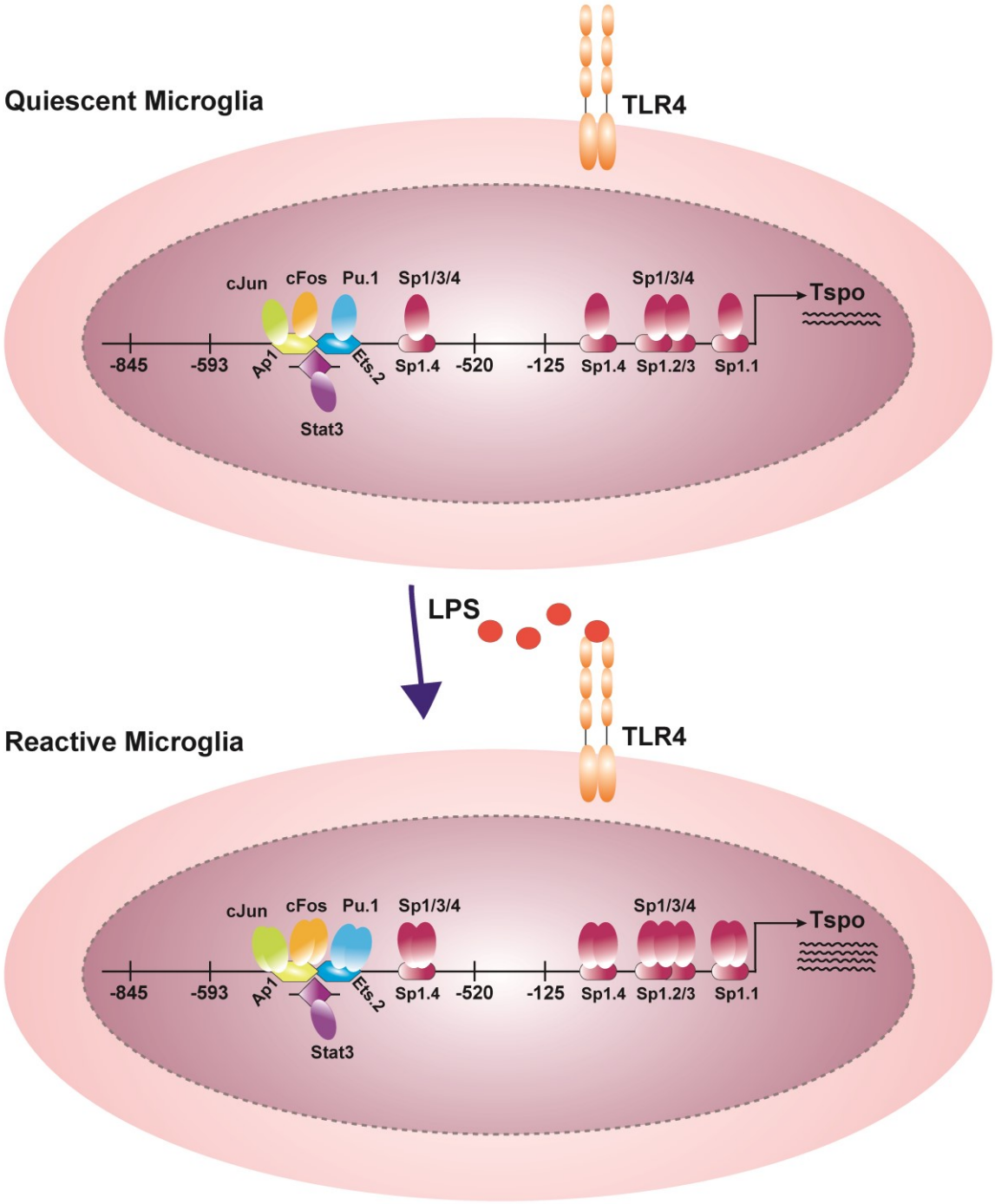

Figure 22: Schematic representation of *cis*-elements and transcription factors regulating Tspo gene transcription in BV-2 microglia during physiological and LPS-induced pathophysiological conditions. Pu.1, Ap-1 (cJun/cFos), Stat3, Sp1, Sp3 and Sp4 factors binding proximal and distal elements on the Tspo promoter work in concert to regulate Tspo transcription. Pathological stimulus such as LPS induces an enhanced recruitment of these factors to the promoter to augment transcription, resulting in strongly upregulated Tspo levels in Microglia (Rashid et al., 2018b).

References

Adams, N. A., Awadein, A., and Toma, H. S. (2007). The Retinal Ciliopathies. *Ophthalmic Genet.* 28, 113–125. doi:10.1080/13816810701537424.

Ajami, B., Bennett, J. L., Krieger, C., Tetzlaff, W., and Rossi, F. M. V (2007). Local self-renewal can sustain CNS microglia maintenance and function throughout adult life. *Nat. Neurosci.* 10, 1538–1543. doi:10.1038/nn2014.

Akhtar-Schäfer, I., Wang, L., Krohne, T. U., Xu, H., and Langmann, T. (2018). Modulation of three key innate immune pathways for the most common retinal degenerative diseases. *EMBO Mol. Med.* 10, e8259. doi:10.15252/emmm.201708259.

Ambati, J., and Fowler, B. J. (2012). Mechanisms of age-related macular degeneration. *Neuron* 75, 26–39. doi:10.1016/j.neuron.2012.06.018.

Amoaku, W. M. K., Frew, L., Mahon, G. J., Gardiner, T. A., and Archer, D. B. (1989). Early ultrastructural changes after low-dose X-irradiation in the retina of the rat. *Eye* 3, 638–646. doi:10.1038/eye.1989.98.

Arevalo, M.-A., Azcoitia, I., and Garcia-Segura, L. M. (2015). The neuroprotective actions of oestradiol and oestrogen receptors. *Nat. Rev. Neurosci.* 16, 17–29. doi:10.1038/nrn3856.

Arnold, T., and Betsholtz, C. (2013). The importance of microglia in the development of the vasculature in the central nervous system. *Vasc. Cell* 5, 4. doi:10.1186/2045-824X-5-4.

Azizkhan, J. C., Jensen, D. E., Pierce, A. J., and Wade, M. (1993). Transcription from TATA-less promoters: dihydrofolate reductase as a model. *Crit. Rev. Eukaryot. Gene Expr.* 3, 229–54.

Balsemão-Pires, E., Jaillais, Y., Olson, B. J., Andrade, L. R., Umen, J. G., Chory, J., et al. (2011). The Arabidopsis translocator protein (AtTSPO) is regulated at multiple levels in response to salt stress and perturbations in tetrapyrrole metabolism. *BMC Plant Biol.* 11, 108. doi:10.1186/1471-2229-11-108.

Banati, R. B., Middleton, R. J., Chan, R., Hatty, C. R., Wai-Ying Kam, W., Quin, C., et al. (2014). Positron emission tomography and functional characterization of a complete PBR/TSPO knockout. *Nat. Commun.* 5, 1–12. doi:10.1038/ncomms6452.

Barron, A. M., Ji, B., Kito, S., Suhara, T., and Higuchi, M. (2018). Steroidogenic

abnormalities in translocator protein knockout mice and significance in the aging male. *Biochem. J.* 475, 75–85. doi:10.1042/BCJ20170645.

Batarseh, A., Barlow, K. D., Martinez-Arguelles, D. B., and Papadopoulos, V. (2012a). Functional characterization of the human translocator protein (18kDa) gene promoter in human breast cancer cell lines. *Biochim. Biophys. Acta* 1819, 38–56. doi:10.1016/j.bbagrm.2011.09.001.

Batarseh, A., Barlow, K. D., Martinez-Arguelles, D. B., and Papadopoulos, V. (2012b). Functional characterization of the human translocator protein (18kDa) gene promoter in human breast cancer cell lines. *Biochim. Biophys. Acta* 1819, 38–56. doi:10.1016/j.bbagrm.2011.09.001.

Batarseh, A., Giatzakis, C., and Papadopoulos, V. (2008). Phorbol-12-myristate 13-Acetate Acting through Protein Kinase C ε Induces translocator protein (18-kDa) TSPO gene expression. *Biochemistry* 47, 12886–12899.

Batarseh, A., Li, J., and Papadopoulos, V. (2011). Protein kinase Cε regulation of translocator protein (18 kDa) Tspo gene expression is mediated through a MAPK pathway targeting STAT3 and c-Jun transcription factors. *Biochemistry* 49, 4766–4778. doi:10.1021/bi100020e.Protein.

Batarseh, A., and Papadopoulos, V. (2010). Regulation of translocator protein 18 kDa (TSPO) expression in health and disease states. *Mol. Cell. Endocrinol.* 327, 1–12. doi:10.1016/j.mce.2010.06.013.

Batoko, H., Jurkiewicz, P., and Veljanovski, V. (2015a). Translocator proteins, porphyrins and abiotic stress: new light? *Trends Plant Sci.* 20, 261–263. doi:10.1016/j.tplants.2015.03.009.

Batoko, H., Veljanovski, V., and Jurkiewicz, P. (2015b). Enigmatic Translocator protein (TSPO) and cellular stress regulation. *Trends Biochem. Sci.* 40, 497–503. doi:10.1016/j.tibs.2015.07.001.

Beckers, L., Ory, D., Geric, I., Declercq, L., Koole, M., Kassiou, M., et al. (2018). Increased expression of Translocator Protein (TSPO) marks pro-inflammatory microglia but does not predict neurodegeneration. *Mol. Imaging Biol.* 20, 94–102. doi:10.1007/s11307-017-1099-1.

Biddie, S. C., John, S., Sabo, P. J., Thurman, R. E., Johnson, T. A., Schiltz, R. L., et al. (2011). Transcription factor AP1 potentiates chromatin accessibility and glucocorticoid receptor binding. *Mol. Cell* 43, 145–155. doi:10.1016/j.molcel.2011.06.016.

Blasi, E., Barluzzi, R., Bocchini, V., Mazzolla, R., and Bistoni, F. (1990). Immortalization of murine microglial cells by a v-raf/v-myc carrying retrovirus. *J. Neuroimmunol.* 27, 229–37.

Boije, H., Shirazi Fard, S., Edqvist, P.-H., and Hallböök, F. (2016). Horizontal Cells, the Odd Ones Out in the Retina, Give Insights into Development and Disease. *Front. Neuroanat.* 10, 77. doi:10.3389/fnana.2016.00077.

Bosco, A., Steele, M. R., and Vetter, M. L. (2011). Early microglia activation in a mouse model of chronic glaucoma. *J. Comp. Neurol.* 519, 599–620. doi:10.1002/cne.22516.

Boutillier, S., Lannes, B., Buée, L., Delacourte, A., Rouaux, C., Mohr, M., et al. (2007). Sp3 and sp4 transcription factor levels are increased in brains of patients with Alzheimer's disease. *Neurodegener. Dis.* 4, 413–23. doi:10.1159/000107701.

Braestrup, C., Albrechtsen, R., and Squires, R. F. (1977). High densities of benzodiazepine receptors in human cortical areas. *Nature* 269, 702–704. doi:10.1038/269702a0.

Brightbill, H. D., Plevy, S. E., Modlin, R. L., and Smale, S. T. (2000). A prominent role for Sp1 during lipopolysaccharide- mediated induction of the IL-10 promoter in macrophages. *J. Immunol.* 164, 1940–1951. doi:10.4049/jimmunol.164.4.1940.

Bringmann, A., Pannicke, T., Biedermann, B., Francke, M., Iandiev, I., Grosche, J., et al. (2009). Role of retinal glial cells in neurotransmitter uptake and metabolism. *Neurochem. Int.* 54, 143–160. doi:10.1016/j.neuint.2008.10.014.

Broderick, C., Hoek, R. M., Forrester, J. V., Liversidge, J., Sedgwick, J. D., and Dick, A. D. (2002). Constitutive retinal CD200 expression regulates resident microglia and activation state of inflammatory cells during experimental autoimmune uveoretinitis. *Am. J. Pathol.* 161, 1669–1677. doi:10.1016/S0002-9440(10)64444-6.

Bruce-Keller, A. J., Keeling, J. L., Keller, J. N., Huang, F. F., Camondola, S., and Mattson, M. P. (2000). Anti-inflammatory effects of estrogen on microglial activation. *Endocrinology* 141, 3646–3656. doi:10.1210/endo.141.10.7693.

Buttgereit, A., Lelios, I., Yu, X., Vrohlings, M., Krakoski, N. R., Gautier, E. L., et al. (2016). Sall1 is a transcriptional regulator defining microglia identity and

function. *Nat. Immunol.* 17, 1397–1406. doi:10.1038/ni.3585.

Carver, B. J., Plosa, E. J., Stinnett, A. M., Blackwell, T. S., and Prince, L. S. (2013). Interactions between NF-κB and SP3 connect inflammatory signaling with reduced FGF-10 expression. *J. Biol. Chem.* 288, 15318–25. doi:10.1074/jbc.M112.447318.

Chaya, T., Matsumoto, A., Sugita, Y., Watanabe, S., Kuwahara, R., Tachibana, M., et al. (2017). Versatile functional roles of horizontal cells in the retinal circuit. *Sci. Rep.* 7, 5540. doi:10.1038/s41598-017-05543-2.

Checchin, D., Sennlaub, F., Levavasseur, E., Leduc, M., and Chemtob, S. (2006). Potential Role of Microglia in Retinal Blood Vessel Formation. *Investig. Opthalmology Vis. Sci.* 47, 3595. doi:10.1167/iovs.05-1522.

Chen, M., and Xu, H. (2015). Parainflammation, chronic inflammation, and age-related macular degeneration. *J. Leukoc. Biol.* 98, 713–725. doi:10.1189/jlb.3RI0615-239R.

Chen, M., Zhao, J., Ali, I. H. A., Marry, S., Augustine, J., Bhuckory, M., et al. (2018). Cytokine Signaling Protein 3 Deficiency in Myeloid Cells Promotes Retinal Degeneration and Angiogenesis through Arginase-1 Up-Regulation in Experimental Autoimmune Uveoretinitis. *Am. J. Pathol.* 188, 1007–1020. doi:10.1016/j.ajpath.2017.12.021.

Christian, C. A., and Huguenard, J. R. (2013). Astrocytes potentiate GABAergic transmission in the thalamic reticular nucleus via endozepine signaling. *Proc. Natl. Acad. Sci. U. S. A.* 110, 20278–83. doi:10.1073/pnas.1318031110.

Christoforos, G., Batarseh, A., Dettin, L., and Papadopoulos, V. (2008). The role of Ets transcription factors in the basal transcription of the translocator protein (18kDa). *Biochemistry* 46, 4763–4774. doi:10.1021/bi062208o.The.

Copland, D. A., Calder, C. J., Raveney, B. J. E., Nicholson, L. B., Phillips, J., Cherwinski, H., et al. (2007). Monoclonal Antibody-Mediated CD200 Receptor Signaling Suppresses Macrophage Activation and Tissue Damage in Experimental Autoimmune Uveoretinitis. *Am. J. Pathol.* 171, 580–588. doi:10.2353/ajpath.2007.070272.

Cosenza-Nashat, M., Zhao, M.-L., Suh, H.-S., Morgan, J., Natividad, R., Morgello, S., et al. (2009). Expression of the translocator protein of 18 kDa by microglia, macrophages and astrocytes based on immunohistochemical localization in abnormal human brain. *Neuropathol. Appl. Neurobiol.* 35,

306–328. doi:10.1111/j.1365-2990.2008.01006.x.

Crotti, A., and Ransohoff, R. M. (2016). Microglial Physiology and Pathophysiology: Insights from Genome-wide Transcriptional Profiling. *Immunity* 44, 505–515. doi:10.1016/J.IMMUNI.2016.02.013.

Damani, M. R., Zhao, L., Fontainhas, A. M., Amaral, J., Fariss, R. N., and Wong, W. T. (2011). Age-related alterations in the dynamic behavior of microglia. *Aging Cell* 10, 263–276. doi:10.1111/j.1474-9726.2010.00660.x.

Dannhausen, K., Rashid, K., and Langmann, T. (2018). "Microglia Analysis in Retinal Degeneration Mouse Models," in *Methods in molecular biology (Clifton, N.J.)*, 159–166. doi:10.1007/978-1-4939-7720-8_10.

Daugherty, D. J., Selvaraj, V., Chechneva, O. V, Liu, X.-B., Pleasure, D. E., and Deng, W. (2013). A TSPO ligand is protective in a mouse model of multiple sclerosis. *EMBO Mol. Med.* 5, 891–903. doi:10.1002/emmm.201202124.

De Miranda, B. R., Popichak, K. A., Hammond, S. L., Jorgensen, B. A., Phillips, A. T., Safe, S., et al. (2015). The Nurr1 Activator 1,1-Bis(3'-Indolyl)-1-(p-Chlorophenyl)Methane Blocks Inflammatory Gene Expression in BV-2 Microglial Cells by Inhibiting Nuclear Factor B. *Mol. Pharmacol.* 87, 1021–1034. doi:10.1124/mol.114.095398.

Dhande, O. S., and Huberman, A. D. (2014). Retinal ganglion cell maps in the brain: implications for visual processing. *Curr. Opin. Neurobiol.* 24, 133–42. doi:10.1016/j.conb.2013.08.006.

Dunn, K. C., Aotaki-Keen, A. E., Putkey, F. R., and Hjelmeland, L. M. (1996). ARPE-19, A Human Retinal Pigment Epithelial Cell Line with Differentiated Properties. *Exp. Eye Res.* 62, 155–170. doi:10.1006/exer.1996.0020.

Echevarria, F. D., Formichella, C. R., and Sappington, R. M. (2017). Interleukin-6 Deficiency Attenuates Retinal Ganglion Cell Axonopathy and Glaucoma-Related Vision Loss. *Front. Neurosci.* 11, 318. doi:10.3389/fnins.2017.00318.

Edison, P., Archer, H. A., Gerhard, A., Hinz, R., Pavese, N., Turkheimer, F. E., et al. (2008). Microglia, amyloid, and cognition in Alzheimer's disease: An [11C](R)PK11195-PET and [11C]PIB-PET study. *Neurobiol. Dis.* 32, 412–419. doi:10.1016/j.nbd.2008.08.001.

Elkamhawy, A., Park, J., Hassan, A. H. E., Pae, A. N., Lee, J., Park, B.-G., et al. (2017). Design, synthesis, biological evaluation and molecular modelling of

2-(2-aryloxyphenyl)-1,4-dihydroisoquinolin-3(2 H)-ones: A novel class of TSPO ligands modulating amyloid-β-induced mPTP opening. *Eur. J. Pharm. Sci.* 104, 366–381. doi:10.1016/j.ejps.2017.04.015.

Elmore, M. R. P., Najafi, A. R., Koike, M. A., Dagher, N. N., Spangenberg, E. E., Rice, R. A., et al. (2014). Colony-Stimulating Factor 1 Receptor Signaling Is Necessary for Microglia Viability, Unmasking a Microglia Progenitor Cell in the Adult Brain. *Neuron* 82, 380–397. doi:10.1016/j.neuron.2014.02.040.

Fontana, M. F., Baccarella, A., Pancholi, N., Pufall, M. A., Herbert, D. R., and Kim, C. C. (2015). JUNB Is a Key Transcriptional Modulator of Macrophage Activation. *J. Immunol.* 194, 177–186. doi:10.4049/jimmunol.1401595.

Forrester, J. V., Dick, A. D., McMenamin, P. G., R., and F., Pearlman, E. (2015). *The eye: Basic Sciences in Practice . Elsevier Health Sciences.*

Frakes, A. E., Ferraiuolo, L., Haidet-Phillips, A. M., Schmelzer, L., Braun, L., Miranda, C. J., et al. (2014). Microglia Induce Motor Neuron Death via the Classical NF-κB Pathway in Amyotrophic Lateral Sclerosis. *Neuron* 81, 1009–1023. doi:10.1016/j.neuron.2014.01.013.

Gatliff, J., East, D. A., Singh, A., Alvarez, M. S., Frison, M., Matic, I., et al. (2017). A role for TSPO in mitochondrial Ca2+ homeostasis and redox stress signaling. *Cell Death Dis.* 8, e2896. doi:10.1038/cddis.2017.186.

Gatliff, J., East, D., Crosby, J., Abeti, R., Harvey, R., Craigen, W., et al. (2014). TSPO interacts with VDAC1 and triggers a ROS-mediated inhibition of mitochondrial quality control. *Autophagy* 10, 2279–2296. doi:10.4161/15548627.2014.991665.

Ghisletti, S., Barozzi, I., Mietton, F., Polletti, S., De Santa, F., Venturini, E., et al. (2010). Identification and Characterization of Enhancers Controlling the Inflammatory Gene Expression Program in Macrophages. *Immunity* 32, 317–328. doi:10.1016/j.immuni.2010.02.008.

Giatzakis, C., and Papadopoulos, V. (2004). Differential utilization of the promoter of peripheral-type benzodiazepine receptor by steroidogenic versus nonsteroidogenic cell lines and the role of Sp1 and Sp3 in the regulation of basal activity. *Endocrinology* 145, 1113–23. doi:10.1210/en.2003-1330.

Ginhoux, F., and Garel, S. (2018). The mysterious origins of microglia. *Nat. Neurosci.* 21, 897–899. doi:10.1038/s41593-018-0176-3.

Ginhoux, F., Greter, M., Leboeuf, M., Nandi, S., See, P., Gokhan, S., et al. (2010).

Fate mapping analysis reveals that adult microglia derive from primitive macrophages. *Science* 330, 841–5. doi:10.1126/science.1194637.

Goldman, D. (2014). Müller glial cell reprogramming and retina regeneration. *Nat. Rev. Neurosci.* 15, 431–42. doi:10.1038/nrn3723.

Greene-Schloesser, D., Robbins, M. E., Peiffer, A. M., Shaw, E. G., Wheeler, K. T., and Chan, M. D. (2012). Radiation-induced brain injury: A review. *Front. Oncol.* 2, 73. doi:10.3389/fonc.2012.00073.

Grigsby, J. G., Cardona, S. M., Pouw, C. E., Muniz, A., Mendiola, A. S., Tsin, A. T. C., et al. (2014). The role of microglia in diabetic retinopathy. *J. Ophthalmol.* 2014, 705783. doi:10.1155/2014/705783.

Guilarte, T. R., Loth, M. K., and Guariglia, S. R. (2016). TSPO Finds NOX2 in Microglia for Redox Homeostasis. *Trends Pharmacol. Sci.* 37, 334–343. doi:10.1016/j.tips.2016.02.008.

Guo, C., Otani, A., Oishi, A., Kojima, H., Makiyama, Y., Nakagawa, S., et al. (2012). Knockout of ccr2 alleviates photoreceptor cell death in a model of retinitis pigmentosa. *Exp. Eye Res.* 104, 39–47. doi:10.1016/j.exer.2012.08.013.

Gupta, N., Brown, K. E., and Milam, A. H. (2003). Activated microglia in human retinitis pigmentosa, late-onset retinal degeneration, and age-related macular degeneration. *Exp. Eye Res.* 76, 463–471. doi:10.1016/S0014-4835(02)00332-9.

Gut, P., Baeza-Raja, B., Andersson, O., Hasenkamp, L., Hsiao, J., Hesselson, D., et al. (2013). Whole-organism screening for gluconeogenesis identifies activators of fasting metabolism. *Nat. Chem. Biol.* 9, 97–104. doi:10.1038/nchembio.1136.

Harada, T., Harada, C., Kohsaka, S., Wada, E., Yoshida, K., Ohno, S., et al. (2002). Microglia-Müller glia cell interactions control neurotrophic factor production during light-induced retinal degeneration. *J. Neurosci.* 22, 9228–36. doi:10.1523/jneurosci.22-21-09228.2002.

Harada, T., Harada, C., Nakayama, N., Okuyama, S., Yoshida, K., Kohsaka, S., et al. (2000). Modification of glial-neuronal cell interactions prevents photoreceptor apoptosis during light-induced retinal degeneration. *Neuron* 26, 533–41.

Hartong, D. T., Berson, E. L., and Dryja, T. P. (2006). Retinitis pigmentosa.

Lancet 368, 1795–1809. doi:10.1016/S0140-6736(06)69740-7.

Hayden, M. S., and Ghosh, S. (2008). Shared Principles in NF-κB Signaling. *Cell* 132, 344–362. doi:10.1016/j.cell.2008.01.020.

Heintzman, N. D., Stuart, R. K., Hon, G., Fu, Y., Ching, C. W., Hawkins, R. D., et al. (2007). Distinct and predictive chromatin signatures of transcriptional promoters and enhancers in the human genome. *Nat. Genet.* 39, 311–318. doi:10.1038/ng1966.

Heinz, S., Benner, C., Spann, N., Bertolino, E., Lin, Y. C., Laslo, P., et al. (2010). Simple combinations of lineage-determining transcription factors prime cis-regulatory elements required for macrophage and B cell identities. *Mol. Cell* 38, 576–89. doi:10.1016/j.molcel.2010.05.004.

Henn, A. (2009). The suitability of BV2 cells as alternative model system for primary microglia cultures or for animal experiments examining brain inflammation. *ALTEX*, 83–94. doi:10.14573/altex.2009.2.83.

Holtman, I. R., Skola, D., and Glass, C. K. (2017). Transcriptional control of microglia phenotypes in health and disease. *J. Clin. Invest.* 127, 3220–3229. doi:10.1172/JCI90604.

Horie, S., Robbie, S. J., Liu, J., Wu, W.-K., Ali, R. R., Bainbridge, J. W., et al. (2013). CD200R signaling inhibits pro-angiogenic gene expression by macrophages and suppresses choroidal neovascularization. *Sci. Rep.* 3, 3072. doi:10.1038/srep03072.

Huang, L., Xu, W., and Xu, G. (2013). Transplantation of CX3CL1-expressing Mesenchymal Stem Cells Provides Neuroprotective and Immunomodulatory Effects in a Rat Model of Retinal Degeneration. *Ocul. Immunol. Inflamm.* 21, 276–285. doi:10.3109/09273948.2013.791925.

Huang, W., Zhao, S., Ammanamanchi, S., Brattain, M., Venkatasubbarao, K., and Freeman, J. W. (2005). Trichostatin A Induces Transforming Growth Factor β Type II Receptor Promoter Activity and Acetylation of Sp1 by Recruitment of PCAF/p300 to a Sp1·NF-Y Complex. *J. Biol. Chem.* 280, 10047–10054. doi:10.1074/jbc.M408680200.

Huang, Y., Xu, Z., Xiong, S., Qin, G., Sun, F., Yang, J., et al. (2018). Dual extra-retinal origins of microglia in the model of retinal microglia repopulation. *Cell Discov.* 4, 9. doi:10.1038/s41421-018-0011-8.

Hughes, E. G., and Bergles, D. E. (2014). Hidden Progenitors Replace Microglia

in the Adult Brain. *Neuron* 82, 253–255. doi:10.1016/j.neuron.2014.04.010.

Indaram, M., Ma, W., Zhao, L., Fariss, R. N., Rodriguez, I. R., and Wong, W. T. (2015). 7-Ketocholesterol Increases Retinal Microglial Migration, Activation and Angiogenicity: A Potential Pathogenic Mechanism Underlying Age-related Macular Degeneration. *Sci. Rep.* 5, 9144. doi:10.1038/srep09144.

Inman, D. M., and Horner, P. J. (2007). Reactive nonproliferative gliosis predominates in a chronic mouse model of glaucoma. *Glia* 55, 942–953. doi:10.1002/glia.20516.

Jang, S., Kelley, K. W., and Johnson, R. W. (2008). Luteolin reduces IL-6 production in microglia by inhibiting JNK phosphorylation and activation of AP-1. *Proc. Natl. Acad. Sci. U. S. A.* 105, 7534–9. doi:10.1073/pnas.0802865105.

Jin, H., Li, L., Xu, J., Zhen, F., Zhu, L., Liu, P. P., et al. (2012). Runx1 regulates embryonic myeloid fate choice in zebrafish through a negative feedback loop inhibiting Pu.1 expression. *Blood* 119, 5239–49. doi:10.1182/blood-2011-12-398362.

Jurgens, H. A., and Johnson, R. W. (2012). Dysregulated neuronal-microglial cross-talk during aging, stress and inflammation. *Exp. Neurol.* 233, 40–8. doi:10.1016/j.expneurol.2010.11.014.

Kamran, P., Sereti, K.-I., Zhao, P., Ali, S. R., Weissman, I. L., and Ardehali, R. (2013). Parabiosis in mice: a detailed protocol. *J. Vis. Exp.* doi:10.3791/50556.

Kaneko, H., Nishiguchi, K. M., Nakamura, M., Kachi, S., and Terasaki, H. (2008). Characteristics of Bone Marrow–Derived Microglia in the Normal and Injured Retina. *Investig. Opthalmology Vis. Sci.* 49, 4162. doi:10.1167/iovs.08-1738.

Karlstetter, M., Nothdurfter, C., Aslanidis, A., Moeller, K., and Horn, F. (2014a). Translocator protein (18 kDa) (TSPO) is expressed in reactive retinal microglia and modulates microglial inflammation and phagocytosis. *J. Neuroinflammation* 11.

Karlstetter, M., Nothdurfter, C., Aslanidis, A., Moeller, K., Horn, F., Scholz, R., et al. (2014b). Translocator protein (18kDa) (TSPO) is expressed in reactive retinal microglia and modulates microglial inflammation and phagocytosis. *J Neuroinflammation* 11, 3.

Karlstetter, M., Scholz, R., Rutar, M., Wong, W. T., Provis, J. M., and Langmann,

T. (2015). Retinal microglia: Just bystander or target for therapy? *Prog. Retin. Eye Res.* 45, 30–57. doi:10.1016/j.preteyeres.2014.11.004.

Kezic, J., and McMenamin, P. G. (2008). Differential turnover rates of monocyte-derived cells in varied ocular tissue microenvironments. *J. Leukoc. Biol.* 84, 721–729. doi:10.1189/jlb.0308166.

Kierdorf, K., Erny, D., Goldmann, T., Sander, V., Schulz, C., Perdiguero, E. G., et al. (2013). Microglia emerge from erythromyeloid precursors via Pu.1- and Irf8-dependent pathways. *Nat. Neurosci.* 16, 273–280. doi:10.1038/nn.3318.

Kierdorf, K., and Prinz, M. (2013). Factors regulating microglia activation. *Front. Cell. Neurosci.* 7, 44. doi:10.3389/fncel.2013.00044.

Kirsch, M., Lee, M.-Y., Meyer, V., Wiese, A., and Hofmann, H.-D. (2002). Evidence for Multiple, Local Functions of Ciliary Neurotrophic Factor (CNTF) in Retinal Development: Expression of CNTF and Its Receptor and In Vitro Effects on Target Cells. *J. Neurochem.* 68, 979–990. doi:10.1046/j.1471-4159.1997.68030979.x.

Kobayashi, E. H., Suzuki, T., Funayama, R., Nagashima, T., Hayashi, M., Sekine, H., et al. (2016). Nrf2 suppresses macrophage inflammatory response by blocking proinflammatory cytokine transcription. *Nat. Commun.* 7, 11624. doi:10.1038/ncomms11624.

Kolb, H., and Famiglietti, E. V (1974). Rod and cone pathways in the inner plexiform layer of cat retina. *Science* 186, 47–9. doi:10.1126/science.186.4158.47.

Koontz, M. A., and Hendrickson, A. E. (1987). Stratified distribution of synapses in the inner plexiform layer of primate retina. *J. Comp. Neurol.* 263, 581–592. doi:10.1002/cne.902630409.

Kuan, C. S., See Too, W. C., and Few, L. L. (2016). Sp1 and Sp3 Are the Transcription Activators of Human ek1 Promoter in TSA-Treated Human Colon Carcinoma Cells. *PLoS One* 11, e0147886. doi:10.1371/journal.pone.0147886.

Kurihara, T., Westenskow, P. D., Gantner, M. L., Usui, Y., Schultz, A., Bravo, S., et al. (2016). Hypoxia-induced metabolic stress in retinal pigment epithelial cells is sufficient to induce photoreceptor degeneration. *Elife* 5. doi:10.7554/eLife.14319.

Langmann, T. (2007). Microglia activation in retinal degeneration. *J. Leukoc. Biol.*

81, 1345–1351. doi:10.1189/jlb.0207114.

Lanzillotta, A., Porrini, V., Bellucci, A., Benarese, M., Branca, C., Parrella, E., et al. (2015). NF-κB in Innate Neuroprotection and Age-Related Neurodegenerative Diseases. *Front. Neurol.* 6, 98. doi:10.3389/fneur.2015.00098.

Lastres-Becker, I., Innamorato, N. G., Jaworski, T., Rábano, A., Kügler, S., Van Leuven, F., et al. (2014). Fractalkine activates NRF2/NFE2L2 and heme oxygenase 1 to restrain tauopathy-induced microgliosis. *Brain* 137, 78–91. doi:10.1093/brain/awt323.

Li, H., and Papadopoulos, V. (1998). Peripheral-Type Benzodiazepine Receptor Function in Cholesterol Transport. Identification of a Putative Cholesterol Recognition/Interaction Amino Acid Sequence and Consensus Pattern [1]. *Endocrinology* 139, 4991–4997. doi:10.1210/endo.139.12.6390.

Li, M., Ren, H., Sheth, K. N., Shi, F.-D., and Liu, Q. (2017). A TSPO ligand attenuates brain injury after intracerebral hemorrhage. *FASEB J.* 31, 3278–3287. doi:10.1096/fj.201601377RR.

Li, N., Alam, J., Venkatesan, M. I., Eiguren-Fernandez, A., Schmitz, D., Di Stefano, E., et al. (2004). Nrf2 is a key transcription factor that regulates antioxidant defense in macrophages and epithelial cells: protecting against the proinflammatory and oxidizing effects of diesel exhaust chemicals. *J. Immunol.* 173, 3467–81.

Li, Y., Du, X.-F., Liu, C.-S., Wen, Z.-L., and Du, J.-L. (2012). Reciprocal regulation between resting microglial dynamics and neuronal activity in vivo. *Dev. Cell* 23, 1189–202. doi:10.1016/j.devcel.2012.10.027.

Lin, D., Chang, Y. J., Strauss, J. F., and Miller, W. L. (1993). The human peripheral benzodiazepine receptor gene: cloning and characterization of alternative splicing in normal tissues and in a patient with congenital lipoid adrenal hyperplasia. *Genomics* 18, 643–50.

Linnartz, B., and Neumann, H. (2013). Microglial activatory (immunoreceptor tyrosine-based activation motif)- and inhibitory (immunoreceptor tyrosine-based inhibition motif)-signaling receptors for recognition of the neuronal glycocalyx. *Glia* 61, 37–46. doi:10.1002/glia.22359.

Liu, G.-J., Middleton, R. J., Hatty, C. R., Kam, W. W.-Y., Chan, R., Pham, T., et al. (2014). The 18 kDa Translocator Protein, Microglia and

Neuroinflammation. *Brain Pathol.* 24, 631–653. doi:10.1111/bpa.12196.

Liu, G.-J., Middleton, R. J., Kam, W. W.-Y., Chin, D. Y., Hatty, C. R., Chan, R. H. Y., et al. (2017a). Functional gains in energy and cell metabolism after TSPO gene insertion. *Cell Cycle* 16, 436–447. doi:10.1080/15384101.2017.1281477.

Liu, G., Ye, X., Miller, E. J., and Liu, S. F. (2015). NF-κB-to-AP-1 Switch: A Mechanism Regulating Transition From Endothelial Barrier Injury to Repair in Endotoxemic Mice. *Sci. Rep.* 4, 5543. doi:10.1038/srep05543.

Liu, H., and Naismith, J. H. (2008). An efficient one-step site-directed deletion, insertion, single and multiple-site plasmid mutagenesis protocol. *BMC Biotechnol.* 8, 91. doi:10.1186/1472-6750-8-91.

Liu, T., Zhang, L., Joo, D., and Sun, S.-C. (2017b). NF-κB signaling in inflammation. *Signal Transduct. Target. Ther.* 2, 17023. doi:10.1038/sigtrans.2017.23.

Liu, X., Fan, X.-L., Zhao, Y., Luo, G.-R., Li, X.-P., Li, R., et al. (2005). Estrogen provides neuroprotection against activated microglia-induced dopaminergic neuronal injury through both estrogen receptor-α and estrogen receptor-β in microglia. *J. Neurosci. Res.* 81, 653–665. doi:10.1002/jnr.20583.

Lodie, T. A., Savedra, R., Golenbock, D. T., Van Beveren, C. P., Maki, R. A., and Fenton, M. J. (1997). Stimulation of macrophages by lipopolysaccharide alters the phosphorylation state, conformation, and function of PU.1 via activation of casein kinase II. *J. Immunol.* 158, 1848–56.

Ma, W., Zhao, L., Fontainhas, A. M., Fariss, R. N., and Wong, W. T. (2009). Microglia in the Mouse Retina Alter the Structure and Function of Retinal Pigmented Epithelial Cells: A Potential Cellular Interaction Relevant to AMD. *PLoS One* 4, e7945. doi:10.1371/journal.pone.0007945.

Madeira, M. H., Boia, R., Santos, P. F., Ambrósio, A. F., and Santiago, A. R. (2015). Contribution of microglia-mediated neuroinflammation to retinal degenerative diseases. *Mediators Inflamm.* 2015, 673090. doi:10.1155/2015/673090.

Madeira, M. H., Rashid, K., Ambrósio, A. F., Santiago, A. R., and Langmann, T. (2018). Blockade of microglial adenosine A2A receptor impacts inflammatory mechanisms, reduces ARPE-19 cell dysfunction and prevents photoreceptor loss in vitro. *Sci. Rep.* 8, 2272. doi:10.1038/s41598-018-20733-2.

Madrigal, P., and Alasoo, K. (2018). AP-1 Takes Centre Stage in Enhancer Chromatin Dynamics. *Trends Cell Biol.* 28, 509–511. doi:10.1016/j.tcb.2018.04.009.

Martyanova, E., and Tishkina, A. (2015). 3D quantitative analysis of microglial morphology. in *SkoltechOn*.

Masland, R. H. (2001). The fundamental plan of the retina. *Nat. Neurosci.* 4, 877–886. doi:10.1038/nn0901-877.

Masland, R. H. (2012). The neuronal organization of the retina. *Neuron* 76, 266–80. doi:10.1016/j.neuron.2012.10.002.

Matcovitch-Natan, O., Winter, D. R., Giladi, A., Vargas Aguilar, S., Spinrad, A., Sarrazin, S., et al. (2016). Microglia development follows a stepwise program to regulate brain homeostasis. *Science* 353, aad8670. doi:10.1126/science.aad8670.

McEnery, M. W., Snowman, A. M., Trifiletti, R. R., and Snyder, S. H. (1992). Isolation of the mitochondrial benzodiazepine receptor: association with the voltage-dependent anion channel and the adenine nucleotide carrier. *Proc. Natl. Acad. Sci. U. S. A.* 89, 3170–4.

Medzhitov, R., and Horng, T. (2009). Transcriptional control of the inflammatory response. *Nat. Rev. Immunol.* 9, 692–703. doi:10.1038/nri2634.

Messmer, K., and Reynolds, G. P. (1998). Increased peripheral benzodiazepine binding sites in the brain of patients with Huntington's disease. *Neurosci. Lett.* 241, 53–6.

Midzak, A., Zirkin, B., and Papadopoulos, V. (2015). Translocator protein: pharmacology and steroidogenesis. *Biochem. Soc. Trans.* 43, 572–578. doi:10.1042/BST20150061.

Miyajima-Uchida, H., Hayashi, H., Beppu, R., Kuroki, M., Fukami, M., Arakawa, F., et al. (2000). Production and accumulation of thrombospondin-1 in human retinal pigment epithelial cells. *Invest. Ophthalmol. Vis. Sci.* 41, 561–7.

Molday, R. S., and Moritz, O. L. (2015). Photoreceptors at a glance. *J. Cell Sci.* 128, 4039–4045. doi:10.1242/jcs.175687.

Morohaku, K., Pelton, S. H., Daugherty, D. J., Butler, W. R., Deng, W., and Selvaraj, V. (2014). Translocator Protein/Peripheral Benzodiazepine Receptor Is Not Required for Steroid Hormone Biosynthesis. *Endocrinology* 155, 89–97. doi:10.1210/en.2013-1556.

Mukhin, A. G., Papadopoulos, V., Costa, E., and Krueger, K. E. (1989). Mitochondrial benzodiazepine receptors regulate steroid biosynthesis. *Proc. Natl. Acad. Sci. U. S. A.* 86, 9813–6.

Mustafi, D., Engel, A. H., and Palczewski, K. (2009). Structure of cone photoreceptors. *Prog. Retin. Eye Res.* 28, 289–302. doi:10.1016/J.PRETEYERES.2009.05.003.

Nebel, C., Aslanidis, A., Rashid, K., and Langmann, T. (2017). Activated microglia trigger inflammasome activation and lysosomal destabilization in human RPE cells. *Biochem. Biophys. Res. Commun.* 484, 681–686. doi:10.1016/j.bbrc.2017.01.176.

Nerlov, C., and Graf, T. (1998). PU.1 induces myeloid lineage commitment in multipotent hematopoietic progenitors. *Genes Dev.* 12, 2403–12.

Neufeld, A. H. (1999). Microglia in the Optic Nerve Head and the Region of Parapapillary Chorioretinal Atrophy in Glaucoma. *Arch. Ophthalmol.* 117, 1050. doi:10.1001/archopht.117.8.1050.

Neufeld, A. H., Hernandez, M. R., and Gonzalez, M. (1997). Nitric oxide synthase in the human glaucomatous optic nerve head. *Arch. Ophthalmol. (Chicago, Ill. 1960)* 115, 497–503.

Newman, E., and Reichenbach, A. (1996). The Müller cell: a functional element of the retina. *Trends Neurosci.* 19, 307–312. doi:10.1016/0166-2236(96)10040-0.

Nimmerjahn, A., Kirchhoff, F., and Helmchen, F. (2005). Resting microglial cells are highly dynamic surveillants of brain parenchyma in vivo. *Science* 308, 1314–8. doi:10.1126/science.1110647.

Nomaru, H., Sakumi, K., Katogi, A., Ohnishi, Y. N., Kajitani, K., Tsuchimoto, D., et al. (2014). *Fosb* gene products contribute to excitotoxic microglial activation by regulating the expression of complement C5a receptors in microglia. *Glia* 62, 1284–1298. doi:10.1002/glia.22680.

Notter, T., Coughlin, J. M., Sawa, A., and Meyer, U. (2018). Reconceptualization of translocator protein as a biomarker of neuroinflammation in psychiatry. *Mol. Psychiatry* 23, 36–47. doi:10.1038/mp.2017.232.

O'Shea, J. J., and Plenge, R. (2012). JAK and STAT Signaling Molecules in Immunoregulation and Immune-Mediated Disease. *Immunity* 36, 542–550. doi:10.1016/j.immuni.2012.03.014.

Orihuela, R., McPherson, C. A., and Harry, G. J. (2016). Microglial M1/M2 polarization and metabolic states. *Br. J. Pharmacol.* 173, 649–65. doi:10.1111/bph.13139.

Ouchi, Y., Yoshikawa, E., Sekine, Y., Futatsubashi, M., Kanno, T., Ogusu, T., et al. (2005). Microglial activation and dopamine terminal loss in early Parkinson's disease. *Ann. Neurol.* 57, 168–175. doi:10.1002/ana.20338.

Ovcharenko, I., Nobrega, M. A., Loots, G. G., and Stubbs, L. (2004). ECR Browser: a tool for visualizing and accessing data from comparisons of multiple vertebrate genomes. *Nucleic Acids Res.* 32, W280–W286. doi:10.1093/nar/gkh355.

Owen, D. R., Fan, J., Campioli, E., Venugopal, S., Midzak, A., Daly, E., et al. (2017). TSPOmutations in rats and a human polymorphism impair the rate of steroid synthesis. *Biochem. J.* 474, 3985–3999. doi:10.1042/BCJ20170648.

Papadopoulos, V., Amri, H., Li, H., Boujrad, N., Vidic, B., and Garnier, M. (1997). Targeted disruption of the peripheral-type benzodiazepine receptor gene inhibits steroidogenesis in the R2C Leydig tumor cell line. *J. Biol. Chem.* 272, 32129–35. doi:10.1074/JBC.272.51.32129.

Penfold, P. L., Madigan, M. C., Gillies, M. C., and Provis, J. M. (2001). Immunological and aetiological aspects of macular degeneration. *Prog. Retin. Eye Res.* 20, 385–414.

Pfeffer, B. A., Flanders, K. C., Guérin, C. J., Danielpour, D., and Anderson, D. H. (1994). Transforming Growth Factor Beta 2 is the Predominant Isoform in the Neural Retina, Retinal Pigment Epithelium-Choroid and Vitreous of the Monkey Eye. *Exp. Eye Res.* 59, 323–333. doi:10.1006/EXER.1994.1114.

Phanstiel, D. H., Van Bortle, K., Spacek, D., Hess, G. T., Shamim, M. S., Machol, I., et al. (2017). Static and dynamic DNA Loops form AP-1-bound activation hubs during macrophage development. *Mol. Cell* 67, 1037–1048.e6. doi:10.1016/j.molcel.2017.08.006.

Pow, D. V, and Crook, D. K. (1996). Direct immunocytochemical evidence for the transfer of glutamine from glial cells to neurons: use of specific antibodies directed against the d-stereoisomers of glutamate and glutamine. *Neuroscience* 70, 295–302.

Przanowski, P., Dabrowski, M., Ellert-Miklaszewska, A., Kloss, M., Mieczkowski,

J., Kaza, B., et al. (2014). The signal transducers Stat1 and Stat3 and their novel target Jmjd3 drive the expression of inflammatory genes in microglia. *J. Mol. Med.* 92, 239–254. doi:10.1007/s00109-013-1090-5.

Qin, H., Yeh, W.-I., De Sarno, P., Holdbrooks, A. T., Liu, Y., Muldowney, M. T., et al. (2012). Signal transducer and activator of transcription-3/suppressor of cytokine signaling-3 (STAT3/SOCS3) axis in myeloid cells regulates neuroinflammation. *Proc. Natl. Acad. Sci. U. S. A.* 109, 5004–9. doi:10.1073/pnas.1117218109.

Raisner, R., Kharbanda, S., Jin, L., Jeng, E., Chan, E., Merchant, M., et al. (2018). Enhancer activity requires CBP/P300 bromodomain-dependent histone H3K27 acetylation. *Cell Rep.* 24, 1722–1729. doi:10.1016/j.celrep.2018.07.041.

Rajala, R. V. S., and Gardner, T. W. (2016). Burning fat fuels photoreceptors. *Nat. Med.* 22, 342–343. doi:10.1038/nm.4080.

Ramírez, J. M., Triviño, A., Ramírez, A. I., and Salazar, J. J. (1998). "Organization and Function of Astrocytes in Human Retina," in *Understanding Glial Cells* (Boston, MA: Springer US), 47–62. doi:10.1007/978-1-4615-5737-1_3.

Ransohoff, R. M. (2007). Microgliosis: the questions shape the answers. *Nat. Neurosci.* 10, 1507–1509. doi:10.1038/nn1207-1507.

Raschke, W. C., Baird, S., Ralph, P., and Nakoinz, I. (1978). Functional macrophage cell lines transformed by abelson leukemia virus. *Cell* 15, 261–267. doi:10.1016/0092-8674(78)90101-0.

Rashid, K., Geissl, L., Wolf, A., Karlstetter, M., and Langmann, T. (2018a). Transcriptional regulation of Translocator protein (18 kDa) (TSPO) in microglia requires Pu.1, Ap1 and Sp factors. *Biochim. Biophys. Acta - Gene Regul. Mech.* 1861. doi:10.1016/j.bbagrm.2018.10.018.

Rashid, K., Geissl, L., Wolf, A., Karlstetter, M., and Langmann, T. (2018b). Transcriptional regulation of Translocator protein (18 kDa) (TSPO) in microglia requires Pu.1, Ap1 and Sp factors. *Biochim. Biophys. Acta - Gene Regul. Mech.* doi:10.1016/j.bbagrm.2018.10.018.

Rashid, K., Wolf, A., and Langmann, T. (2018c). Microglia activation and immunomodulatory therapies for retinal degenerations. *Front. Cell. Neurosci.* 12, 176. doi:10.3389/fncel.2018.00176.

Ravichandran, K. S. (2003). "Recruitment Signals" from Apoptotic Cells: Invitation

to a Quiet Meal. *Cell* 113, 817–820. doi:10.1016/S0092-8674(03)00471-9.

Rechichi, M., Salvetti, A., Chelli, B., Costa, B., Da Pozzo, E., Spinetti, F., et al. (2008). TSPO over-expression increases motility, transmigration and proliferation properties of C6 rat glioma cells. *Biochim. Biophys. Acta - Mol. Basis Dis.* 1782, 118–125. doi:10.1016/j.bbadis.2007.12.001.

Reichenbach, A., and Robinson, S. R. (1995). “The involvement of Müller cells in the outer retina,” in *Neurobiology and Clinical Aspects of the Outer Retina* (Dordrecht: Springer Netherlands), 395–416. doi:10.1007/978-94-011-0533-0_16.

Reyes, N. J., O’Koren, E. G., and Saban, D. R. (2017). New insights into mononuclear phagocyte biology from the visual system. *Nat. Rev. Immunol.* 17, 322–332. doi:10.1038/nri.2017.13.

Rodriguez, I. R., Clark, M. E., Lee, J. W., and Curcio, C. A. (2014). 7-ketocholesterol accumulates in ocular tissues as a consequence of aging and is present in high levels in drusen. *Exp. Eye Res.* 128, 151–155. doi:10.1016/j.exer.2014.09.009.

Rosner, M., Siegel, N., Fuchs, C., Slabina, N., Dolznig, H., and Hengstschläger, M. (2010). Efficient siRNA-mediated prolonged gene silencing in human amniotic fluid stem cells. *Nat. Protoc.* 5, 1081–1095. doi:10.1038/nprot.2010.74.

Rupprecht, R., Papadopoulos, V., Rammes, G., Baghai, T. C., Fan, J., Akula, N., et al. (2010). Translocator protein (18 kDa) (TSPO) as a therapeutic target for neurological and psychiatric disorders. *Nat. Rev. Drug Discov.* 9, 971–988. doi:10.1038/nrd3295.

Rymo, S. F., Gerhardt, H., Wolfhagen Sand, F., Lang, R., Uv, A., and Betsholtz, C. (2011). A Two-Way Communication between Microglial Cells and Angiogenic Sprouts Regulates Angiogenesis in Aortic Ring Cultures. *PLoS One* 6, e15846. doi:10.1371/journal.pone.0015846.

Saijo, K., Collier, J. G., Li, A. C., Katzenellenbogen, J. A., and Glass, C. K. (2011). An ADIOL-ERβ-CtBP transrepression pathway negatively regulates microglia-mediated inflammation. *Cell* 145, 584–595. doi:10.1016/j.cell.2011.03.050.

Saijo, K., Winner, B., Carson, C. T., Collier, J. G., Boyer, L., Rosenfeld, M. G., et al. (2009). A Nurr1/CoREST pathway in microglia and astrocytes protects

dopaminergic neurons from inflammation-induced death. *Cell* 137, 47–59. doi:10.1016/j.cell.2009.01.038.

Santos, A. M., Calvente, R., Tassi, M., Carrasco, M.-C., Martín-Oliva, D., Marín-Teva, J. L., et al. (2008). Embryonic and postnatal development of microglial cells in the mouse retina. *J. Comp. Neurol.* 506, 224–239. doi:10.1002/cne.21538.

Sappington, R. M., and Calkins, D. J. (2006). Pressure-Induced Regulation of IL-6 in Retinal Glial Cells: Involvement of the Ubiquitin/Proteasome Pathway and NFκB. *Investig. Opthalmology Vis. Sci.* 47, 3860. doi:10.1167/iovs.05-1408.

Satoh, J., Asahina, N., Kitano, S., and Kino, Y. (2014). A Comprehensive Profile of ChIP-Seq-Based PU.1/Spi1 Target Genes in Microglia. *Gene Regul. Syst. Bio.* 8, GRSB.S19711. doi:10.4137/GRSB.S19711.

Schafer, D. P., Lehrman, E. K., Kautzman, A. G., Koyama, R., Mardinly, A. R., Yamasaki, R., et al. (2012). Microglia Sculpt Postnatal Neural Circuits in an Activity and Complement-Dependent Manner. *Neuron* 74, 691–705. doi:10.1016/j.neuron.2012.03.026.

Schnur, N., Seuter, S., Katryniok, C., Rådmark, O., and Steinhilber, D. (2007). The histone deacetylase inhibitor trichostatin A mediates upregulation of 5-lipoxygenase promoter activity by recruitment of Sp1 to distinct GC-boxes. *Biochim. Biophys. Acta - Mol. Cell Biol. Lipids* 1771, 1271–1282. doi:10.1016/j.bbalip.2007.08.003.

Scholz, R., Caramoy, A., Bhuckory, M. B., Rashid, K., Chen, M., Xu, H., et al. (2015a). Targeting translocator protein (18 kDa) (TSPO) dampens pro-inflammatory microglia reactivity in the retina and protects from degeneration. *J. Neuroinflammation* 12, 201. doi:10.1186/s12974-015-0422-5.

Scholz, R., Caramoy, A., Bhuckory, M., Rashid, K., Chen, M., Xu, H., et al. (2015b). Targeting translocator protein (18kDa) (TSPO) dampens pro-inflammatory microglia reactivity in the retina and protects from degeneration. *J. Neuroinflammation* 12, 201.

Scholz, R., Sobotka, M., Caramoy, A., Stempfl, T., Moehle, C., and Langmann, T. (2015c). Minocycline counter-regulates pro-inflammatory microglia responses in the retina and protects from degeneration. *J.*

Neuroinflammation 12, 209. doi:10.1186/s12974-015-0431-4.

Selvaraj, V., and Stocco, D. M. (2015). The changing landscape in translocator protein (TSPO) function. *Trends Endocrinol. Metab.* 26, 341–348. doi:10.1016/j.tem.2015.02.007.

Sen, R., and Baltimore, D. (1986). Multiple nuclear factors interact with the immunoglobulin enhancer sequences. *Cell* 46, 705–716. doi:10.1016/0092-8674(86)90346-6.

Shen, W., Zhu, L., Lee, S.-R., Chung, S. H., and Gillies, M. C. (2013). Involvement of NT3 and P75NTR in photoreceptor degeneration following selective Müller cell ablation. *J. Neuroinflammation* 10, 137. doi:10.1186/1742-2094-10-137.

Silverman, S. M., and Wong, W. T. (2018). Microglia in the Retina: Roles in Development, Maturity, and Disease. *Annu. Rev. Vis. Sci.* 4, 45–77. doi:10.1146/annurev-vision-091517-034425.

Simard, A. R., and Rivest, S. (2004). Bone marrow stem cells have the ability to populate the entire central nervous system into fully differentiated parenchymal microglia. *FASEB J.* 18, 998–1000. doi:10.1096/fj.04-1517fje.

Smale, S. T. (2010). Selective Transcription in Response to an Inflammatory Stimulus. *Cell* 140, 833–844. doi:10.1016/j.cell.2010.01.037.

Smale, S. T., and Natoli, G. (2014). Transcriptional control of inflammatory responses. *Cold Spring Harb. Perspect. Biol.* 6, a016261. doi:10.1101/cshperspect.a016261.

Stefater III, J. A., Lewkowich, I., Rao, S., Mariggi, G., Carpenter, A. C., Burr, A. R., et al. (2011). Regulation of angiogenesis by a non-canonical Wnt–Flt1 pathway in myeloid cells. *Nature* 474, 511–515. doi:10.1038/nature10085.

Stetson, D. B., and Medzhitov, R. (2006). Review Type I Interferons in Host Defense. *Immunity* 25, 373–381. doi:10.1016/j.immuni.2006.08.007.

Strettoi, E., and Masland, R. H. (1995). The organization of the inner nuclear layer of the rabbit retina. *J. Neurosci.* 15, 875–88.

Sung, C.-H., and Chuang, J.-Z. (2010). The cell biology of vision. *J. Cell Biol.* 190, 953–963. doi:10.1083/jcb.201006020.

Tannahill, G. M., Iraci, N., Gaude, E., Frezza, C., and Pluchino, S. (2015). Metabolic reprograming of mononuclear phagocytes in progressive multiple sclerosis. *Front. Immunol.* 6, 106. doi:10.3389/fimmu.2015.00106.

Tezel, G., Yang, X., Yang, J., and Wax, M. B. (2004). Role of tumor necrosis

factor receptor-1 in the death of retinal ganglion cells following optic nerve crush injury in mice. *Brain Res.* 996, 202–212. doi:10.1016/j.brainres.2003.10.029.

Thanos, D., and Maniatis, T. (1995). Virus induction of human IFN beta gene expression requires the assembly of an enhanceosome. *Cell* 83, 1091–100.

Tian, N., and Copenhagen, D. R. (2003). Visual Stimulation Is Required for Refinement of ON and OFF Pathways in Postnatal Retina. *Neuron* 39, 85–96. doi:10.1016/S0896-6273(03)00389-1.

Tseng, W. A., Thein, T., Kinnunen, K., Lashkari, K., Gregory, M. S., D'Amore, P. A., et al. (2013). NLRP3 Inflammasome Activation in Retinal Pigment Epithelial Cells by Lysosomal Destabilization: Implications for Age-Related Macular Degeneration. *Investig. Opthalmology Vis. Sci.* 54, 110. doi:10.1167/iovs.12-10655.

Tu, L. N., Morohaku, K., Manna, P. R., Pelton, S. H., Butler, W. R., Stocco, D. M., et al. (2014). Peripheral benzodiazepine receptor/translocator protein global knock-out mice are viable with no effects on steroid hormone biosynthesis. *J. Biol. Chem.* 289, 27444–54. doi:10.1074/jbc.M114.578286.

Tu, L. N., Zhao, A. H., Stocco, D. M., and Selvaraj, V. (2015). PK11195 effect on steroidogenesis is not mediated through the translocator protein (TSPO). *Endocrinology* 156, 1033–1039. doi:10.1210/en.2014-1707.

Turner, M. ., Cagnin, A., Turkheimer, F. ., Miller, C. C. ., Shaw, C. ., Brooks, D. ., et al. (2004). Evidence of widespread cerebral microglial activation in amyotrophic lateral sclerosis: an [11C](R)-PK11195 positron emission tomography study. *Neurobiol. Dis.* 15, 601–609. doi:10.1016/j.nbd.2003.12.012.

Ugolini, G., Cremisi, F., and Maffei, L. (1995). TrkA, TrkB and p75 mRNA expression is developmentally regulated in the rat retina. *Brain Res.* 704, 121–4.

Varatharaj, A., and Galea, I. (2017). The blood-brain barrier in systemic inflammation. *Brain. Behav. Immun.* 60, 1–12. doi:10.1016/J.BBI.2016.03.010.

Vecino, E., Rodriguez, F. D., Ruzafa, N., Pereiro, X., and Sharma, S. C. (2016). Glia–neuron interactions in the mammalian retina. *Prog. Retin. Eye Res.* 51, 1–40. doi:10.1016/j.preteyeres.2015.06.003.

Veenman, L., and Gavish, M. (2012). The Role of 18 kDa Mitochondrial Translocator Protein (TSPO) in Programmed Cell Death, and Effects of Steroids on TSPO Expression. *Curr. Mol. Med.* 12, 398–412. doi:10.2174/1566524011207040398.

Veenman, L., Shandalov, Y., and Gavish, M. (2008). VDAC activation by the 18 kDa translocator protein (TSPO), implications for apoptosis. *J. Bioenerg. Biomembr.* 40, 199–205. doi:10.1007/s10863-008-9142-1.

Vegeto, E., Belcredito, S., Etteri, S., Ghisletti, S., Brusadelli, A., Meda, C., et al. (2003). Estrogen receptor- mediates the brain antiinflammatory activity of estradiol. *Proc. Natl. Acad. Sci.* 100, 9614–9619. doi:10.1073/pnas.1531957100.

Vidal, L., Díaz, F., Villena, A., Moreno, M., Campos, J. G., and Vargas, I. P. de (2006). Nitric oxide synthase in retina and optic nerve head of rat with increased intraocular pressure and effect of timolol. *Brain Res. Bull.* 70, 406–413. doi:10.1016/J.BRAINRESBULL.2006.07.009.

Visel, A., Blow, M. J., Li, Z., Zhang, T., Akiyama, J. A., Holt, A., et al. (2009). ChIP-seq accurately predicts tissue-specific activity of enhancers. *Nature* 457, 854–858. doi:10.1038/nature07730.

Wang, M., Ma, W., Zhao, L., Fariss, R. N., and Wong, W. T. (2011). Adaptive Müller cell responses to microglial activation mediate neuroprotection and coordinate inflammation in the retina. *J. Neuroinflammation* 8, 173. doi:10.1186/1742-2094-8-173.

Wang, M., Wang, X., Zhao, L., Ma, W., Rodriguez, I. R., Fariss, R. N., et al. (2014). Macroglia-microglia interactions via TSPO signaling regulates microglial activation in the mouse retina. *J. Neurosci.* 34, 3793–806. doi:10.1523/jneurosci.3153-13.2014.

Wang, M., and Wong, W. T. (2014). “Microglia-Müller Cell Interactions in the Retina,” in (Springer, New York, NY), 333–338. doi:10.1007/978-1-4614-3209-8_42.

Wang, X., Zhao, L., Zhang, J., Fariss, R. N., Ma, W., Kretschmer, F., et al. (2016). Requirement for Microglia for the Maintenance of Synaptic Function and Integrity in the Mature Retina. *J. Neurosci.* 36, 2827–2842. doi:10.1523/jneurosci.3575-15.2016.

Wässle, H. (2004). Parallel processing in the mammalian retina. *Nat. Rev.*

Neurosci. 5, 747–757. doi:10.1038/nrn1497.

Weigelt, K., Ernst, W., Walczak, Y., Ebert, S., Loenhardt, T., Klug, M., et al. (2007). Dap12 expression in activated microglia from retinoschisin-deficient retina and its PU.1-dependent promoter regulation. *J. Leukoc. Biol.* 82, 1564–1574. doi:10.1189/jlb.0707447.

Weigelt, K., Lichtinger, M., Rehli, M., and Langmann, T. (2009). Transcriptomic profiling identifies a PU.1 regulatory network in macrophages. *Biochem. Biophys. Res. Commun.* 380, 308–312. doi:10.1016/j.bbrc.2009.01.067.

Wen, R., Song, Y., Liu, Y., Li, Y., Zhao, L., and Laties, A. M. (2008). “CNTF negatively regulates the phototransduction machinery in rod photoreceptors: implication for light-induced photostasis plasticity,” in (Springer, New York, NY), 407–413. doi:10.1007/978-0-387-74904-4_48.

Wenzel, A., Grimm, C., Samardzija, M., and Reme, C. E. (2005). Molecular mechanisms of light-induced photoreceptor apoptosis and neuroprotection for retinal degeneration. *Prog. Retin. Eye Res.* 24, 275–306. doi:10.1016/j.preteyeres.2004.08.002.

Wiedemann, J., Rashid, K., and Langmann, T. (2018). Resveratrol induces dynamic changes to the microglia transcriptome, inhibiting inflammatory pathways and protecting against microglia-mediated photoreceptor apoptosis. *Biochem. Biophys. Res. Commun.* 501, 239–245. doi:10.1016/j.bbrc.2018.04.223.

Wilson, R. B., Kunchithapautham, K., and Rohrer, B. (2007). Paradoxical role of BDNF: BDNF+/- retinas are protected against light damage-mediated stress. *Invest. Ophthalmol. Vis. Sci.* 48, 2877–86. doi:10.1167/iovs.06-1079.

Wolf, Y., Yona, S., Kim, K.-W., and Jung, S. (2013). Microglia, seen from the CX3CR1 angle. *Front. Cell. Neurosci.* 7, 26. doi:10.3389/fncel.2013.00026.

Won, J., Yim, J., and Kim, T. K. (2002). Sp1 and Sp3 recruit histone deacetylase to repress transcription of human telomerase reverse transcriptase (hTERT) promoter in normal human somatic cells. *J. Biol. Chem.* 277, 38230–8. doi:10.1074/jbc.M206064200.

Wong, W. T. (2013). Microglial aging in the healthy CNS: phenotypes, drivers, and rejuvenation. *Front. Cell. Neurosci.* 7, 22. doi:10.3389/fncel.2013.00022.

Wright, A. F., Chakarova, C. F., Abd El-Aziz, M. M., and Bhattacharya, S. S. (2010). Photoreceptor degeneration: genetic and mechanistic dissection of

a complex trait. *Nat. Rev. Genet.* 11, 273–284. doi:10.1038/nrg2717.

Wu, S. M. (2010). Synaptic organization of the vertebrate retina: general principles and species-specific variations: the Friedenwald lecture. *Invest. Ophthalmol. Vis. Sci.* 51, 1263–74. doi:10.1167/iovs.09-4396.

Xu, H., Chen, M., Mayer, E. J., Forrester, J. V., and Dick, A. D. (2007). Turnover of resident retinal microglia in the normal adult mouse. *Glia* 55, 1189–1198. doi:10.1002/glia.20535.

Yan, Z., Gibson, S. A., Buckley, J. A., Qin, H., and Benveniste, E. N. (2018). Role of the JAK/STAT signaling pathway in regulation of innate immunity in neuroinflammatory diseases. *Clin. Immunol.* 189, 4–13. doi:10.1016/j.clim.2016.09.014.

Yang, Y., Jiang, S., Yan, J., Li, Y., Xin, Z., Lin, Y., et al. (2015). An overview of the molecular mechanisms and novel roles of Nrf2 in neurodegenerative disorders. *Cytokine Growth Factor Rev.* 26, 47–57. doi:10.1016/j.cytogfr.2014.09.002.

Yasuno, F., Ota, M., Kosaka, J., Ito, H., Higuchi, M., Doronbekov, T. K., et al. (2008). Increased binding of peripheral benzodiazepine receptor in Alzheimer's disease measured by positron emission tomography with [11C]DAA1106. *Biol. Psychiatry* 64, 835–841. doi:10.1016/j.biopsych.2008.04.021.

Yeliseev, A. A., Krueger, K. E., and Kaplan, S. (1997). A mammalian mitochondrial drug receptor functions as a bacterial "oxygen" sensor. *Proc. Natl. Acad. Sci. U. S. A.* 94, 5101–6.

Yoshimura, A., Naka, T., and Kubo, M. (2007). SOCS proteins, cytokine signalling and immune regulation. *Nat. Rev. Immunol.* 7, 454–465. doi:10.1038/nri2093.

Yu, C.-R., Mahdi, R. R., Oh, H.-M., Amadi-Obi, A., Levy-Clarke, G., Burton, J., et al. (2011). Suppressor of cytokine signaling-1 (SOCS1) inhibits lymphocyte recruitment into the retina and protects SOCS1 transgenic rats and mice from ocular inflammation. *Invest. Ophthalmol. Vis. Sci.* 52, 6978–86. doi:10.1167/iovs.11-7688.

Zabel, M. K., Zhao, L., Zhang, Y., Gonzalez, S. R., Ma, W., Wang, X., et al. (2016). Microglial phagocytosis and activation underlying photoreceptor degeneration is regulated by CX3CL1-CX3CR1 signaling in a mouse model

of retinitis pigmentosa. *Glia* 64, 1479–91. doi:10.1002/glia.23016.

Zamiri, P., Masli, S., Streilein, J. W., and Taylor, A. W. (2006). Pigment epithelial growth factor suppresses inflammation by modulating macrophage activation. *Investig. Opthalmology Vis. Sci.* 47, 3912. doi:10.1167/iovs.05-1267.

Zamiri, P., Sugita, S., and Streilein, J. W. (2007). “Immunosuppressive properties of the pigmented epithelial cells and the subretinal space,” in *Immune Response and the Eye* (Basel: KARGER), 86–93. doi:10.1159/000099259.

Zeng, H., Green, W. R., and Tso, M. O. M. (2008). Microglial Activation in Human Diabetic Retinopathy. *Arch. Ophthalmol.* 126, 227. doi:10.1001/archophthalmol.2007.65.

Zeng, H., Zhu, X., Zhang, C., Yang, L.-P., Wu, L., and Tso, M. O. M. (2005). Identification of sequential events and factors associated with microglial activation, migration, and cytotoxicity in retinal degeneration in rd Mice. *Investig. Opthalmology Vis. Sci.* 46, 2992. doi:10.1167/iovs.05-0118.

Zeng, X.-X., Ng, Y.-K., and Ling, E.-A. (2000). Neuronal and microglial response in the retina of streptozotocin-induced diabetic rats.

Zetterström, R. H., Solomin, L., Jansson, L., Hoffer, B. J., Olson, L., and Perlmann, T. (1997). Dopamine neuron agenesis in Nurr1-deficient mice. *Science* 276, 248–50.

Zhang, Q., Lenardo, M. J., and Baltimore, D. (2017). 30 years of NF-κB: A blossoming of relevance to human pathobiology. *Cell* 168, 37–57. doi:10.1016/j.cell.2016.12.012.

Zhao, L., Zabel, M. K., Wang, X., Ma, W., Shah, P., Fariss, R. N., et al. (2015a). Microglial phagocytosis of living photoreceptors contributes to inherited retinal degeneration. *EMBO Mol. Med.* 7, 1179–97. doi:10.15252/emmm.201505298.

Zhao, X., Sun, G., Ting, S.-M., Song, S., Zhang, J., Edwards, N. J., et al. (2015b). Cleaning up after ICH: the role of Nrf2 in modulating microglia function and hematoma clearance. *J. Neurochem.* 133, 144–52. doi:10.1111/jnc.12974.

Zhu, C., Wang, S., Wang, B., Du, F., Hu, C., Li, H., et al. (2015). 17β-Estradiol up-regulates Nrf2 via PI3K/AKT and estrogen receptor signaling pathways to suppress light-induced degeneration in rat retina. *Neuroscience* 304, 328–339. doi:10.1016/j.neuroscience.2015.07.057.

Zieger, M., Ahnelt, P. K., and Uhrin, P. (2014). CX3CL1 (Fractalkine) protein expression in normal and degenerating mouse retina: In vivo studies. *PLoS One* 9, e106562. doi:10.1371/journal.pone.0106562.

Zusso, M., Methot, L., Lo, R., Greenhalgh, A. D., David, S., and Stifani, S. (2012). Regulation of postnatal forebrain amoeboid microglial cell proliferation and development by the transcription factor Runx1. *J. Neurosci.* 32, 11285–98. doi:10.1523/jneurosci.6182-11.2012.

Acknowledgement

This page only appears on the printed version of the thesis.

Erklärung

Ich versichere, dass ich die von mir vorgelegte Dissertation selbständig angefertigt, die benutzten Quellen und Hilfsmittel vollständig angegeben und die Stellen der Arbeit – einschließlich Tabellen, Karten, und Abbildungen - , die anderen Werken im Wortlaut oder dem Sinn nach entnommen sind, in jedem Einzelfall als Entlehnung kenntlich gemacht habe; dass diese Dissertation noch keiner anderen Fakultät oder Universität zur Prüfung vorgelegen hat; dass sie – abgesehen von unten angegebenen Teilpublikationen – noch nicht veröffentlicht worden ist sowie, dass ich eine solche Veröffentlichung vor Abschluss des Promotionsverfahrens nicht vornehmen werde. Die Bestimmungen dieser Promotionsordnung sind mir bekannt. Die von mir vorgelegte Dissertation ist von Prof. Dr. rer. nat. Thomas Langmann betreut worden.

Publikation:

Rashid, K., Geissl, L., Wolf, A., Karlstetter, M., and Langmann, T. (2018). Transcriptional regulation of Translocator protein (18 kDa) (TSPO) in microglia requires Pu.1, Ap1 and Sp factors. *Biochimica et Biophysica Acta - Gene Regulatory Mechanisms.* https://doi.org/10.1016/j.bbagrm.2018.10.018

Rashid, K., Wolf, A., and Langmann, T. (2018b). Microglia Activation and Immunomodulatory Therapies for Retinal Degenerations. *Frontiers in Cellular Neuroscience* 12, 176. https://doi.org/10.3389/fncel.2018.00176

Ich versichere, dass ich alle Angaben wahrheitsgemäß nach bestem Wissen und Gewissen gemacht habe und verpflichte mich, jedmögliche, die obigen Angaben betreffenden Veränderungen, dem Promotionsausschuss unverzüglich mitzuteilen.

Köln, den 26.02.2019 Khalid Rashid